

NPS 68-90-007

NAVAL POSTGRADUATE SCHOOL

Monterey, California

AD-A240 657



THESIS

THE JAN MAYEN CURRENT
AND THE
DEEP WATERS OF THE GREENLAND BASIN

by

Robert F. Blythe

September, 1990

Thesis Advisor:

Robert H. Bourke

Co-Advisor:

Robert G. Paquette

Approved for public release; distribution is unlimited.

Prepared for:
Director, Arctic Submarine Laboratory
Naval Ocean Systems Center
San Diego, California 92152

91-11226



NAVAL POSTGRADUATE SCHOOL
Monterey, California


Rear Admiral R. W. West, Jr.
Superintendent

Harrison Shull
Provost

This work was prepared in conjunction with research sponsored by the Arctic Submarine Laboratory, Naval Ocean Systems Center, San Diego, California and funded by the Naval Postgraduate School.

Reproduction of all or part of this report is authorized.

Released by:


Dean of Faculty and
Graduate Studies

UNCLASSIFIED

SECURITY CLASSIFICATION OF THIS PAGE

REPORT DOCUMENTATION PAGE				Form Approved OMB No 0704-0188	
1a REPORT SECURITY CLASSIFICATION UNCLASSIFIED			1b RESTRICTIVE MARKINGS		
2a SECURITY CLASSIFICATION AUTHORITY			3 DISTRIBUTION AVAILABILITY OF REPORT Approved for public release; distribution is unlimited.		
2b DECLASSIFICATION/DOWNGRADING SCHEDULE					
4 PERFORMING ORGANIZATION REPORT NUMBER(S) NPS 68-90-007			5 MONITORING ORGANIZATION REPORT NUMBER(S)		
6a NAME OF PERFORMING ORGANIZATION Naval Postgraduate School		6b OFFICE SYMBOL (If applicable) Oc	7a NAME OF MONITORING ORGANIZATION Naval Postgraduate School		
6c ADDRESS (City, State, and ZIP Code) Monterey, CA 93943-5000			7b ADDRESS (City, State, and ZIP Code) Monterey, CA 93943-5000		
8a NAME OF FUNDING SPONSORING ORGANIZATION Arctic Sub Lab, NOSC		8b OFFICE SYMBOL (If applicable)	9 PROCUREMENT INSTRUMENT IDENTIFICATION NUMBER		
8c ADDRESS (City, State, and ZIP Code) San Diego, CA 92152			10 SOURCE OF FUNDING NUMBERS		
			PROGRAM ELEMENT NO	PROJECT NO	TASK NO
			WORK UNIT ACCESSION NO		
11 TITLE (Include Security Classification) THE JAN MAYEN CURRENT AND THE DEEP WATERS OF THE GREENLAND BASIN					
12 PERSONAL AUTHOR(S) Blythe, Robert F.					
13a TYPE OF REPORT Master's Thesis		13b TIME COVERED FROM _____ TO _____		14 DATE OF REPORT (Year, Month, Day) September 1990	
15 PAGE COUNT 162					
16 SUPPLEMENTARY NOTES: The views expressed in this thesis are those of the author and do not reflect the official policy or position of the Department of Defense or the U.S. Government.					
17 COSAT CODES			18 SUBJECT TERMS (Continue on reverse if necessary and identify by block number)		
FIELD	GROUP	SUB-GROUP	None		
19 ABSTRACT (Continue on reverse if necessary and identify by block number) During September 1989 the USNS BARTLETT occupied a dense array of 48 high-quality CTD stations in the Greenland Basin to characterize the Jan Mayen Current (JMC) system as part of the Greenland Sea Project. Hydrographic analyses characterize the JMC by an eastward bowing of East Greenland Current (EGC) water in the form of a surface Polar Water (PW) tongue, a near-surface (appx. 50 m) core of modified Polar Water, and an intermediate (appx. 100 m) core of Atlantic Water displaced appx. 75 km northward of the PW core. In contrast, the Greenland Sea Gyre is very weakly stratified aside from a thin surface gradient. Historical data demonstrate the JMC axis to move appx. 100 km north and south of its 1989 observed position near 74°N and show that upper water column temperatures and salinities were significantly lower in 1989 and 1982 than in 1958. The dynamic height pattern (0-1000 dbar) supplemented with Lagrangian ice drift rates reveal the JMC as partly an anticyclonic meander in the EGC;					
20 DISTRIBUTION AVAILABILITY OF ABSTRACT <input type="checkbox"/> UNCLASSIFIED UNLIMITED <input type="checkbox"/> SAME AS RPT <input type="checkbox"/> DOWNGRADING			21 ABSTRACT SECURITY CLASSIFICATION UNCLASSIFIED		
22a NAME OF RESPONSIBLE INDIVIDUAL R. H. Bourke			22b TELEPHONE (Include Area Code) 408-646-2552		22c OFFICE SYMBOL Oc/Bf

DD Form 1473, JUN 86

Previous editions are obsolete

SECURITY CLASSIFICATION OF THIS PAGE

S/N 0102-LF-014-6603

UNCLASSIFIED

SECURITY CLASSIFICATION OF THIS PAGE

block 19 continued:

the drifters indicate a significant barotropic component. Baroclinic transport estimates yield a 2 Sv initial eastward transport by the JMC. This transport results in an annual freshwater excess of 1.4 m over the survey area which equates to roughly one fourth of the annually available fresh water in the EGC. Deep water analyses show that isopycnal mixing of Eurasian Basin Deep Water and Greenland Sea Deep Water to yield Norwegian Sea Deep Water occurs within the Greenland Basin. Historical data indicate no appreciable inter-annual fluctuation in deep water properties occurs between 1958 and 1989.

Approved for public release; distribution is unlimited.

The Jan Mayen Current
and the
Deep Waters of the Greenland Basin

by

Robert F. Blythe
Lieutenant, United States Navy
B.S., U.S. Naval Academy

Submitted in partial fulfillment
of the requirements for the degree of

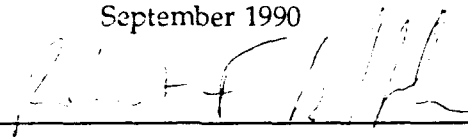
MASTER OF SCIENCE IN PHYSICAL OCEANOGRAPHY AND METEOROLOGY

from the

NAVAL POSTGRADUATE SCHOOL

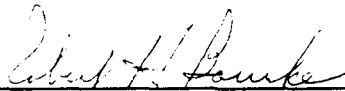
September 1990

Author:

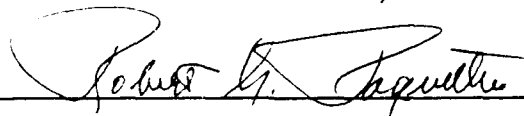


Robert F. Blythe

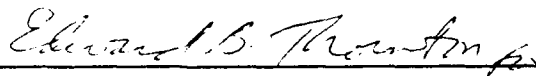
Approved by:



Robert H. Bourke, Thesis Advisor



Robert G. Paquette, Co-Advisor



Curtis A. Collins, Chairman
Department of Oceanography

ABSTRACT

During September 1989 the USNS BARTLETT occupied a dense array of 48 high-quality CTD stations in the Greenland Basin to characterize the Jan Mayen Current (JMC) system as part of the Greenland Sea Project. Hydrographic analyses characterize the JMC by an eastward bowing of East Greenland Current (EGC) waters in the form of a surface Polar Water (PW) tongue, a near-surface (~50 m) core of modified Polar Water, and an intermediate (~100 m) core of Atlantic Water displaced ~75 km northward of the PW core. In contrast, the Greenland Sea Gyre is very weakly stratified aside from a thin surface gradient. Historical data demonstrate the JMC axis to move ~100 km north and south of its 1989 observed position near 74°N and show that upper water column temperatures and salinities were significantly lower in 1989 and 1982 than in 1958, possibly indicating an anomalous excess of PW in 1989 and 1982 compared with 1958. The dynamic height pattern (0-1000 dbar) supplemented with Lagrangian ice drift rates reveal the JMC as partly an anticyclonic meander in the EGC; the drifters indicate a significant barotropic component. Baroclinic transport estimates yield a 2 Sv initial eastward transport by the JMC. This transport results in an annual freshwater excess of 1.4 m over the survey area which equates to roughly one fourth of the annually available fresh water in the EGC. Deep water analyses show that isopycnal mixing of Eurasian Basin Deep Water and Greenland Sea Deep Water to yield Norwegian Sea Deep Water occurs within the Greenland Basin. Historical data indicate no appreciable inter-annual fluctuation in deep water properties occurs between 1958 and 1989.

TABLE OF CONTENTS

I. INTRODUCTION	1
A. OVERVIEW	1
B. THE GREENLAND SEA PROJECT	2
C. GENERAL CIRCULATION	2
D. PURPOSE	5
II. DATA AND METHODS	7
A. DATA COLLECTION	7
1. Cruise Summary	7
2. Instrumentation and Measurements	7
B. DATA PROCESSING	9
C. ADDITIONAL DATA SOURCES	10
III. HYDROGRAPHY	16
A. INTRODUCTION	16
B. SURFACE AND INTERMEDIATE WATER MASSES	17
1. Surface Water Masses	17

2.	Intermediate Water Masses	20
C.	SURFACE WATER SIGNATURE	21
1.	Summer Surface Signature	21
a.	Surface Temperature	21
b.	Surface Salinity	25
2.	Winter Surface Signature	28
D.	INTERMEDIATE WATER SIGNATURE	33
1.	Temperature Maximum	33
2.	Temperature Minimum	36
3.	Salinity maximum	40
4.	Comparison with Historical Intermediate Water Properties	43
E.	VERTICAL STRUCTURE	45
1.	Sections of Temperature and Salinity	47
2.	Vertical Sections of Dissolved Oxygen	53
3.	Comparison with Historical Sections	54
F.	T-S ANALYSIS	57
1.	Overview of BARTLETT 89 Θ -S Characteristics and Historical Comparison	59
2.	T-S Analysis of BARTLETT 89 data	61
G.	SUMMARY	68
IV.	CIRCULATION AND TRANSPORTS	106

A. BAROCLINIC FLOW	106
B. TOTAL FLOW	109
1. Lagrangian Drifters	109
2. A Numerical Model	114
C. TRANSPORTS	116
1. Total Volume Transport	116
2. Transport of Fresh Water and Heat	117
V. DEEP WATER	121
A. INTRODUCTION	121
B. ANALYSIS OF BARTLETT 89 DEEP WATER DATA	124
C. HISTORICAL COMPARISON	131
VI. CONCLUSIONS	133
LIST OF REFERENCES	136
INITIAL DISTRIBUTION LIST	140



Accession For		
NTIS 65481		<input checked="" type="checkbox"/>
DTIC 65481		<input type="checkbox"/>
Unpublished		<input type="checkbox"/>
Journal Article		<input type="checkbox"/>
By		
Distribution		
Availability Codes		
A1, AB, AC, AD, AE, AF, AG, AH, AI, AJ, AK, AL, AM, AN, AO, AP, AQ, AR, AS, AT, AU, AV, AW, AX, AY, AZ, BA, BB, BC, BD, BE, BF, BG, BH, BI, BJ, BK, BL, BM, BN, BO, BP, BQ, BR, BS, BT, BU, BV, BW, BX, BY, BZ, CA, CB, CC, CD, CE, CF, CG, CH, CI, CJ, CK, CL, CM, CN, CO, CP, CQ, CR, CS, CT, CU, CV, CW, CX, CY, CZ, DA, DB, DC, DD, DE, DF, DG, DH, DI, DJ, DK, DL, DM, DN, DO, DP, DQ, DR, DS, DT, DU, DV, DW, DX, DY, DZ, EA, EB, EC, ED, EE, EF, EG, EH, EI, EJ, EK, EL, EM, EN, EO, EP, EQ, ER, ES, ET, EU, EV, EW, EX, EY, EZ, FA, FB, FC, FD, FE, FF, FG, FH, FI, FJ, FK, FL, FM, FN, FO, FP, FQ, FR, FS, FT, FU, FV, FW, FX, FY, FZ, GA, GB, GC, GD, GE, GF, GG, GH, GI, GJ, GK, GL, GM, GN, GO, GP, GQ, GR, GS, GT, GU, GV, GW, GX, GY, GZ, HA, HB, HC, HD, HE, HF, HG, HH, HI, HJ, HK, HL, HM, HN, HO, HP, HQ, HR, HS, HT, HU, HV, HW, HX, HY, HZ, IA, IB, IC, ID, IE, IF, IG, IH, II, IJ, IK, IL, IM, IN, IO, IP, IQ, IR, IS, IT, IU, IV, IW, IX, IY, IZ, JA, JB, JC, JD, JE, JF, JG, JH, JI, JJ, JK, JL, JM, JN, JO, JP, JQ, JR, JS, JT, JU, JV, JW, JX, JY, JZ, KA, KB, KC, KD, KE, KF, KG, KH, KI, KJ, KK, KL, KM, KN, KO, KP, KQ, KR, KS, KT, KU, KV, KW, KX, KY, KZ, LA, LB, LC, LD, LE, LF, LG, LH, LI, LJ, LK, LL, LM, LN, LO, LP, LQ, LR, LS, LT, LU, LV, LW, LX, LY, LZ, MA, MB, MC, MD, ME, MF, MG, MH, MI, MJ, MK, ML, MM, MN, MO, MP, MQ, MR, MS, MT, MU, MV, MW, MX, MY, MZ, NA, NB, NC, ND, NE, NF, NG, NH, NI, NJ, NK, NL, NM, NN, NO, NP, NQ, NR, NS, NT, NU, NV, NW, NX, NY, NZ, OA, OB, OC, OD, OE, OF, OG, OH, OI, OJ, OK, OL, OM, ON, OO, OP, OQ, OR, OS, OT, OU, OV, OW, OX, OY, OZ, PA, PB, PC, PD, PE, PF, PG, PH, PI, PJ, PK, PL, PM, PN, PO, PP, PQ, PR, PS, PT, PU, PV, PW, PX, PY, PZ, QA, QB, QC, QD, QE, QF, QG, QH, QI, QJ, QK, QL, QM, QN, QO, QP, QQ, QR, QS, QT, QU, QV, QW, QX, QY, QZ, RA, RB, RC, RD, RE, RF, RG, RH, RI, RJ, RK, RL, RM, RN, RO, RP, RQ, RR, RS, RT, RU, RV, RW, RX, RY, RZ, SA, SB, SC, SD, SE, SF, SG, SH, SI, SJ, SK, SL, SM, SN, SO, SP, SQ, SR, SS, ST, SU, SV, SW, SX, SY, SZ, TA, TB, TC, TD, TE, TF, TG, TH, TI, TJ, TK, TL, TM, TN, TO, TP, TQ, TR, TS, TT, TU, TV, TW, TX, TY, TZ, UA, UB, UC, UD, UE, UF, UG, UH, UI, UJ, UK, UL, UM, UN, UO, UP, UQ, UR, US, UT, UY, UZ, VA, VB, VC, VD, VE, VF, VG, VH, VI, VJ, VK, VL, VM, VN, VO, VP, VQ, VR, VS, VT, VY, VZ, WA, WB, WC, WD, WE, WF, WG, WH, WI, WJ, WK, WL, WM, WN, WO, WP, WQ, WR, WS, WT, WY, WZ, XA, XB, XC, XD, XE, XF, XG, XH, XI, XJ, XK, XL, XM, XN, XO, XP, XQ, XR, XS, XT, XU, XV, XW, XX, XY, XZ, YA, YB, YC, YD, YE, YF, YG, YH, YI, YJ, YK, YL, YM, YN, YO, YP, YQ, YR, YS, YT, YZ, ZA, ZB, ZC, ZD, ZE, ZF, ZG, ZH, ZI, ZJ, ZK, ZL, ZM, ZN, ZO, ZP, ZQ, ZR, ZS, ZT, ZY, ZZ		

LIST OF TABLES

3.1	Surface and Intermediate Water Masses of the Greenland Basin	19
5.1	Deep Water Masses of the Greenland Basin	125

LIST OF FIGURES

1.1	Greenland Sea Project census station plan	3
2.1	USNS BARTLETT station plan of September 1989	8
2.2	METEOR 61 and HUDSON stations in the Greenland Sea from cruises in winter 1982	12
2.3	JOHAN HJORT/POLJARNIK stations in the Greenland Sea from cruises in summer 1958 of the International Geophysical Year	13
2.4	JOHAN HJORT/POLJARNIK stations in the Greenland Sea from cruises in winter 1958 of the International Geophysical Year	14
3.1	Greenland-Norwegian Sea surface and intermediate water mass circulation schematic	18
3.2	BARTLETT 89 surface temperature	22
3.3	JOHAN HJORT/POLJARNIK 58 summer surface temperature	24
3.4	BARTLETT 89 surface salinity	26
3.5	JOHAN HJORT/POLJARNIK 58 summer surface salinity	27
3.6	METEOR/HUDSON 82 winter surface potential temperature	29
3.7	METEOR/HUDSON 82 winter surface salinity	30
3.8	JOHAN HJORT/POLJARNIK 58 winter surface temperature	31
3.9	JOHAN HJORT/POLJARNIK 58 winter surface salinity	32
3.10	BARTLETT 89 contours of the intermediate temperature maximum	34
3.11	BARTLETT 89 depth of the intermediate temperature maximum	37
3.12	BARTLETT 89 salinity at the intermediate temperature maximum	38
3.13	BARTLETT 89 depth of the subsurface temperature minimum	39
3.14	BARTLETT 89 subsurface temperature minimum	41

3.15	BARTLETT 89 intermediate salinity maximum	42
3.16	BARTLETT 89 100 m temperature	71
3.17	BARTLETT 89 100 m salinity	72
3.18	JOHAN HJORT/POLJARNIK 58 100 m temperature in summer	73
3.19	JOHAN HJORT/POLJARNIK 58 100 m salinity in summer	74
3.20	METEOR/HUDSON 82 100 m potential temperature in winter	75
3.21	METEOR/HUDSON 82 100 m salinity in winter	76
3.22	JOHAN HJORT/POLJARNIK 58 100 m temperature in winter	77
3.23	JOHAN HJORT/POLJARNIK 58 100 m salinity in winter	78
3.24	Location of BARTLETT 89 Transects A through G	46
3.25	BARTLETT 89 temperature Transect A	48
3.26	BARTLETT 89 salinity Transect A	49
3.27	BARTLETT 89 temperature Transect B	51
3.28	BARTLETT 89 salinity Transect B	52
3.29	BARTLETT 89 temperature Transect C	79
3.30	BARTLETT 89 salinity Transect C	80
3.31	BARTLETT 89 temperature Transect D	81
3.32	BARTLETT 89 salinity Transect D	82
3.33	BARTLETT 89 temperature Transect E	83
3.34	BARTLETT 89 salinity Transect E	84
3.35	BARTLETT 89 temperature Transect F	85
3.36	BARTLETT 89 salinity Transect F	86
3.37	BARTLETT 89 temperature Transect G	87

3.38	BARTLETT 89 salinity Transect G	88
3.39	BARTLETT 89 dissolved oxygen Transect A	89
3.40	BARTLETT 89 dissolved oxygen Transect B	90
3.41	BARTLETT 89 dissolved oxygen Transect C	91
3.42	BARTLETT 89 dissolved oxygen Transect D	92
3.43	BARTLETT 89 dissolved oxygen Transect E	93
3.44	BARTLETT 89 dissolved oxygen Transect F	94
3.45	BARTLETT 89 dissolved oxygen Transect G	95
3.46	Location of JOHAN HJORT 58 summer Transects 12 and 14	55
3.47	JOHAN HJORT/POLJARNIK 58 summer temperature Transect 12	96
3.48	JOHAN HJORT/POLJARNIK 58 summer salinity Transect 12	97
3.49	JOHAN HJORT/POLJARNIK 58 summer temperature Transect 14	98
3.50	JOHAN HJORT/POLJARNIK 58 summer salinity Transect 14	99
3.51	Location of METEOR/HUDSON 82 winter Transect 2	56
3.52	METEOR/HUDSON 82 winter temperature Transect 2	100
3.53	METEOR/HUDSON 82 winter salinity Transect 2	101
3.54	Location of JOHAN HJORT/POLJARNIK 58 winter Transects 32 and 34	58
3.55	JOHAN HJORT/POLJARNIK 58 winter temperature Transect 32	102
3.56	JOHAN HJORT/POLJARNIK 58 winter salinity Transect 32	103
3.57	JOHAN HJORT/POLJARNIK 58 winter temperature Transect 34	104
3.58	JOHAN HJORT/POLJARNIK 58 winter salinity Transect 34	105
3.59	Θ -S diagram derived from data at all 48 BARTLETT 89 stations on contours of σ_θ	60

3.60	Θ -S diagram of METEOR/HUDSON 82 data from stations in the Greenland and Boreas basins on contours of σ_θ	62
3.61	Θ -S diagram derived from JOHAN HJORT/POLJARNIK 58 summer data from stations located entirely within the Greenland Basin on contours of σ_θ	63
3.62	Θ -S diagram derived from JOHAN HJORT/POLJARNIK 58 winter data from stations located entirely within the Greenland Basin on contours of σ_θ	64
3.63a	T-S diagram of selected BARTLETT 89 stations on contours of σ_t	65
3.63b	T-S diagram with water masses of the Greenland Basin on contours of σ_t	67
3.64	T-S diagram of the deeper portions of selected BARTLETT 89 station profiles on contours of σ_t	69
4.1	BARTLETT 89 dynamic height at the surface referenced to 1000 dbar	108
4.2	METEOR /HUDSON 82 winter dynamic height at 100 dbar referenced to 1000 dbar	110
4.3	JOHAN HJORT/POLJARNIK 58 summer dynamic height at the surface referenced to 1000 dbar	111
4.4	ARCTEMIZ 89 ice floe drift trajectories late May to early August	112
4.5	Flow streamlines of a general circulation model from the University of Hamburg	115
4.6	Schematic of baroclinic total volume flow rate, volume flow rate of liquid fresh water, and heat advection rate in/out of the BARTLETT 89 survey area	118
5.1	Θ -S diagram of BARTLETT 89 (plus H. MOSBY 89 Station 32) deep bottle data on contours of σ_θ	127
5.2	Θ_2 -S diagram of BARTLETT 89 (plus H. MOSBY 89 Station 32) deep bottle data on contours of σ_2	128
5.3	Θ_3 -S diagram of BARTLETT 89 (plus H. MOSBY 89 Station 32) deep bottle data on contours of σ_3	130

ACKNOWLEDGEMENTS

Funding for this research was provided by the Naval Postgraduate School, Monterey, California.

I wish to thank Dr. Robert H. Bourke and Dr. Robert G. Paquette for their interminable patience and masterful guidance throughout the writing of this work. I greatly appreciate the untold hours dedicated by Dr. Paquette to assist me in techniques of data analysis and enlighten me with his innate talent of scientific reasoning. I cherish the rare opportunity to have been able to participate in actual field research and glean from the vast experience of Dr. Bourke, Dr. Jean-Claude Gascard, and Mr. David Muus. I will fondly remember the companionship of Andy Anderson, Marla Stone, and Julien Gascard during the September 1989 cruise of the USNS BARTLETT to the arctic circle. The success of this expedition is owed to the able crew of the USNS BARTLETT.

I especially wish to thank my lovely wife, Cindy, and children, Barbara and Rodney, for their loving support and inspiration. Cindy, thanks for pulling me through.

I. INTRODUCTION

This study consists of a detailed analysis of hydrographic data collected during the September 1989 cruise of the USNS BARTLETT for the purpose of characterizing the structure and circulation of the Jan Mayen Current and deep water properties in the Greenland Basin. The BARTLETT 89 cruise is a component of the on going Greenland Sea Project described below.

A. OVERVIEW

A large portion of physical oceanographic research is presently focused on polar processes. This interest stems partly from the recent, increased desire to more fully understand the "oceans' role in climate" (*Muench, 1990a*) and partly from the paucity of data occasioned by the near complete inaccessibility of these areas owing to harsh environmental conditions and extended periods of near total darkness. Physical processes in the Nordic Seas are a vital link between climatic changes and the World Ocean since it is here that a large proportion of global bottom waters are formed. In forming these bottom waters vertical circulation mechanisms transmit the climatic signature of the surface waters to the deep ocean. Such spatial and temporal small-scale processes as may be involved in ventilation of the deep oceans are of limited usefulness, however, without the consideration of full context of interrelated physical phenomena in the Nordic Seas which span the gamut of scales.

B. THE GREENLAND SEA PROJECT

The Greenland Sea Project (GSP) is a five year, multi-national effort to probe the physical oceanography of the Nordic Seas. The keystone of the GSP philosophy is to make the utmost attempt to ensure that the data obtained by all investigators are inter-comparable to a high degree of accuracy so that such small amplitude seasonal and inter-annual signals as may be present may be detected. To this end all hydrographic instruments are to be calibrated at the Ocean Data Facility of Scripps Institution of Oceanography. Additionally, investigators have agreed to perform an *in situ* calibration cast at the designated inter-calibration site in the deep Lofoten Basin. The GSP inter-calibration site and a census of hydrographic stations is shown in Figure 1.1. Investigators have agreed to orient their sampling legs to accommodate a maximum number of these stations.

By virtue of its name the GSP predominantly concerns processes in the Greenland Sea but has a small fraction of its observations in the Norwegian Sea. Participating institutions are assigned specific aspects or areas of the general circulation to investigate in detail. Also, to assess inter-annual fluctuations in circulation two intense sampling periods were planned. The first period occurred from 1988 to 1989 and the second is scheduled from 1992 to 1993 with low-level monitoring between these periods.

C. GENERAL CIRCULATION

The following is a brief overview of circulation in the Nordic Seas. The large-scale circulation in the Greenland Sea which occupies the Boreas and Greenland basins is



Figure 1.1 Greenland Sea Project (GSP) census station plan. The bathymetry of the Greenland and Boreas basins is shown at a contour interval of 1000 m. GSP investigators have agreed to accommodate sampling a maximum number of these stations. The *in situ* intercalibration site in the deep Lofoten Basin is encircled.

dominated by a broad cyclonic gyre surrounded in four cardinal directions by major currents or features. Cold, fresh surface polar waters exit the Arctic Ocean within the southward flowing East Greenland Current (EGC) through the west side of the passage between Spitsbergen and Greenland, referred to as Fram Strait. The EGC follows the east Greenland continental slope and forms the western boundary of the Greenland Sea Gyre (GSG). Warm, saline surface Atlantic waters and colder, less saline arctic intermediate waters flow northward in the Norwegian Atlantic Current (NAC) which becomes the West Spitsbergen Current (WSC) off Spitsbergen. This current system remains largely in the Norwegian Sea on the east side of the Mohn Ridge which is a bathymetrically prominent extension of the mid-Atlantic Ridge, thus forming the eastern perimeter of the GSG. Some of these Atlantic waters enter the Arctic Ocean through the east side of Fram Strait and some recirculate southward joining the EGC, isopycnally sinking to intermediate levels in either case. This recirculation gives rise to the East Greenland Polar Front within the EGC and forms the northern boundary of the GSG. The remaining southern limb of the GSG is defined by the Jan Mayen Current (JMC). The JMC consists of surface polar waters and Atlantic intermediate waters bowing eastward from the EGC north of the Jan Mayen Fracture Zone (JMFZ), a major bathymetric feature delineating the southern periphery of the Greenland Basin.

Waters in the Nordic Seas have been observed to be very weakly stratified and measurements have been made indicating flows are significantly barotropic. The deep circulation through the Greenland and Boreas basins is considered to be closely tied to the surface and intermediate flows which demonstrate a response to bathymetric features.

Thus, the deep waters here flow in a cyclonic gyre, effectively an extension of the surface and intermediate circulation described earlier. These cold, moderately saline deep waters, formed through convective, double-diffusive, and other dynamic processes in the GSG and peripheral shelf regions, vary minutely in temperature and salinity, but with sufficiently different values to delineate their *in situ* density levels and identify them with their predominant basins of residence.

D. PURPOSE

This study is concerned with the analysis of high-quality CTD data obtained during the September 1989 cruise of the USNS BARTLETT as part of the first intense GSP sampling period. The GSP-assigned focus was to characterize the Jan Mayen Current, a region which, up to now, has received only cursory treatment in the literature due to a paucity of high-quality hydrographic data. The objectives of this investigation are extracted from the BARTLETT 89 preliminary cruise report of *Bourke et al. (1989)* and are listed below:

- establish northern and southern boundaries for the JMC and describe frontal boundaries
- determine the eastward extent of the JMC
- establish its relation to bathymetry, in particular the JMFZ
- determine the flow rate of the JMC based on geostrophic calculations and ice drift rates
- determine the rate of transport of fresh water into the GSG by the JMC

- determine the deep water characteristics in the Greenland Basin and re-affirm prevalent theories of deep circulation and mixing in the basin.

In the succeeding chapters the BARTLETT 89 data are analyzed to achieve the above objectives. Supplemental data are utilized to augment this analysis. Also, comparison with historical data enables an assessment of seasonal and inter-annual variability in the region.

II. DATA AND METHODS

A. DATA COLLECTION

1. Cruise Summary

A hydrographic survey was conducted on board the USNS BARTLETT (T-AGOR-13) during September 1989. The scientific party embarked at Tromsø, Norway on 6 September with a complement representing the Naval Postgraduate School, Scripps Institution of Oceanography, and the University of Paris and disembarked at Trondheim on 23 September. The 2784 nautical mile survey track consisted of five southwest-northeast trending legs which transect the western and central Greenland Basin. A total of 48 closely-spaced O(30-50 km), high-quality CTD stations were accomplished 43 of which consisted of a single cast to 1000 m depth, 4 of which added a second cast from 1000 to 3000 m or the bottom, and the final station consisted of a single cast to 3500 m (Figure 2.1). Stations with casts below 1000 m are encircled on Figure 2.1. Of the 48 stations, 19 were GSP stations (see Figure 1.1). Navigation was accomplished via the ship's satellite navigation system which provided an average of three fixes per hour of better than 0.5 km accuracy.

2. Instrumentation and Measurements

The BARTLETT 89 data set consists of measurements of conductivity, temperature, pressure, and dissolved oxygen. The primary hydrographic instrument was a four-sensor Neil Brown Mark III CTD which was statically and dynamically calibrated

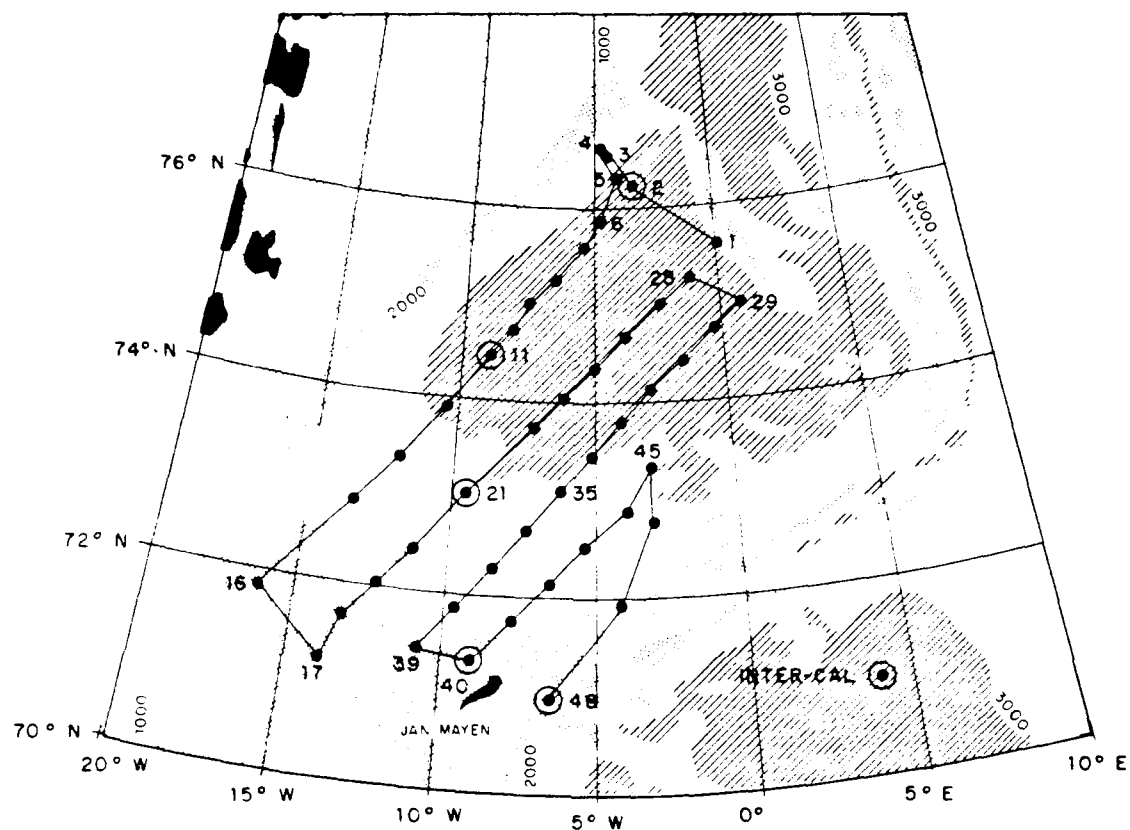


Figure 2.1

USNS BARTLETT station plan of September 1989. A total of 48 high-quality ~1000 m CTD stations were accomplished (solid dots). A second deep cast from ~1000 to 3000 m was accomplished at five of these stations (circled stations). The BARTLETT was unable to sample the inter-cal site, however, this site was sampled as Station 32 during the 1989 cruise of the HAAKON MOSBY. Data from this station is utilized in Chapter V. (courtesy of A. Foldvik, *personal communication*). Bathymetry is shaded at 1000 m intervals.

before and after the cruise at the Ocean Data Facility (ODF) at Scripps Institution of Oceanography (SIO) in keeping with the precepts of the Greenland Sea Project (GSP).

The CTD was fastened to a standard instrument cage provided by SIO which included a 12-place rosette sampler. The unit was lowered at a constant rate of 60 m min^{-1} , varying with ship's roll. The data acquisition program recorded 8616 bytes per cast evenly spaced over the pressure range which was selected prior to lowering. This equates to approximately 9 observations per meter for 1000 m casts and 4.3 observations per meter for 1000-3000 m casts.

For shallow casts, Niskin bottles were closed on the up cast at 100 m intervals with the final two at 75 and 10 m. For deep casts bottles were closed at 200 m intervals with last three at 1100, 700, and 300 m. Low-temperature reversing thermometers were usually fastened to bottles 2, 11, and 12 with 12 being the deepest. Thermometer/bottle firing depths were adjusted to seek isothermal layers. D. Muus of SIO deftly conducted on board salinity bottle analysis utilizing an Autosol calibrated to Wormley standard seawater from batch number 108 which is designated for use by GSP investigators. These measurements formed the basis for the conductivity correction equations developed by the ODF for the final data report. Dissolved oxygen concentrations were determined via the Winkler method and saturation calculations were made at each sample depth.

B. DATA PROCESSING

Upon completion of the cruise the data were transferred from 3.5 inch diskettes to tape for editing on the Naval Postgraduate School (NPS) IBM Mainframe computer. A

data editing program was developed to remove occasional spurious data points and apply the final temperature and conductivity corrections resulting from the ODF analysis.

A non-linear pressure sensitivity of the CTD conductivity cell was detected with the error greater at 3000 m than at 1000 m. The shallow stations could be corrected by one common equation with an acceptable final standard deviation of ± 0.003 PSU; however, the deep stations required individual equations for best results with a final standard deviation of ± 0.0012 PSU. The final accuracy for temperature measurements was 0.002°C and 3 dbar for pressure. Further detail of the data editing process is documented in the BARTLETT 89 data report (*Bourke et al., 1990*).

Densities throughout this study are calculated using the EOS80 formula and appear in sigma notation *e.g.*, $\sigma_t = (\rho - 1000) \text{ kg m}^{-3}$ or $\sigma_p = (\rho_p - 1000) \text{ kg m}^{-3}$.

C. ADDITIONAL DATA SOURCES

This study has been greatly enhanced by the availability of several additional sources of data, three of which were expressly made available for this study through personal communiqué.

Used throughout this study for seasonal and historical comparison are the elegantly prepared atlases of *Dietrich (1969)* and *Koltermann and Lüthje (1989)*. From *Dietrich (1969)* were extracted the results of the summer (September to October) and late winter (March to June) surveys of the JOHAN HJORT and POLJARNIK during the International Geophysical Year (IGY) of 1958. The portions of the JOHAN HJORT/POLJARNIK 58 station plans which correspond to the BARTLETT 89 survey area are shown in

Figures 2.2 and 2.3 for summer and winter, respectively. The IGY data are available from the NODC data base at the NPS and were utilized to construct vertical sections and T-S plots for specific comparison to BARTLETT 89 data. The 1958 salinities were determined via Mohr titration and temperatures were measured utilizing reversing thermometers. Accuracies of these measurements are discussed later as needed. From *Koltermann and Lüthje (1989)* were extracted the results of the winter 1982 surveys of the HUDSON (February to April) and METEOR 61 (May to June). The combined station plans are shown in Figure 2.4. It is recognized that some of the historical winter data is not truly "winter" but certainly representative of conditions prior to intense summer heating. They have been included in these atlases due to the paucity of winter data in these regions.

Three sources of data are mentioned here for completeness, but are introduced in detail as they are utilized in the following chapters. First are the positions (approximately hourly) of three ice floes tracked via ARGOS beacons from May to August 1989 during ARCTEMIZ 89 (*Gascard and Richez, 1989*). These floes fortuitously happened to enter the BARTLETT 89 survey area. These data were made available on tape by *J.-C. Gascard (personal communication)*. Second are the deep cast bottle data from the GSP inter-calibration site, Station 32, of the 1989 cruise of the HAAKON MOSBY. These data, made available by *A. Foldvik (personal communication)*, are greatly appreciated since the BARTLETT was unable to reach this site due to weather and mechanical difficulty. Third are the analysis of results of a general circulation model of the Greenland-Norwegian Sea developed at the University of Hamburg. Analyses specific

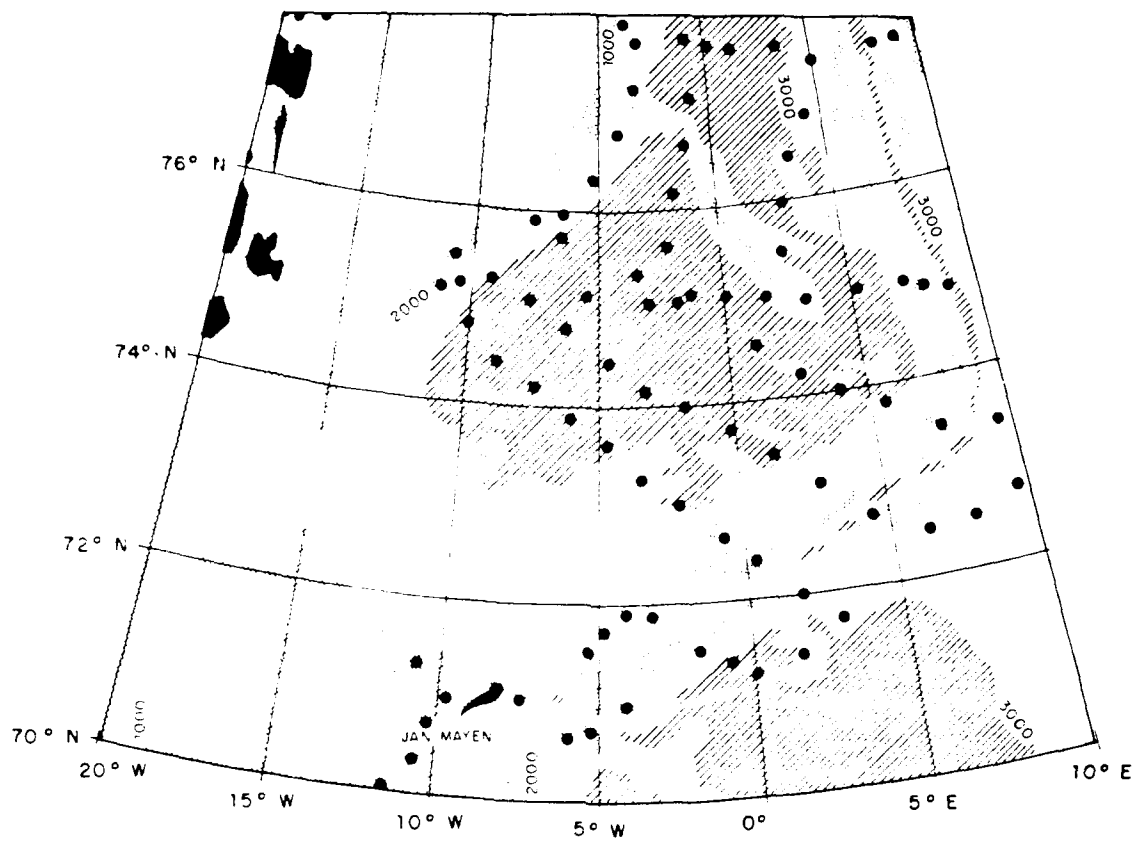


Figure 2.2 METEOR 61 and HUDSON stations in the Greenland Sea from cruises in winter 1982. Note the lack of stations in the southern Greenland Basin (from Koltermann and Lühje, 1989).

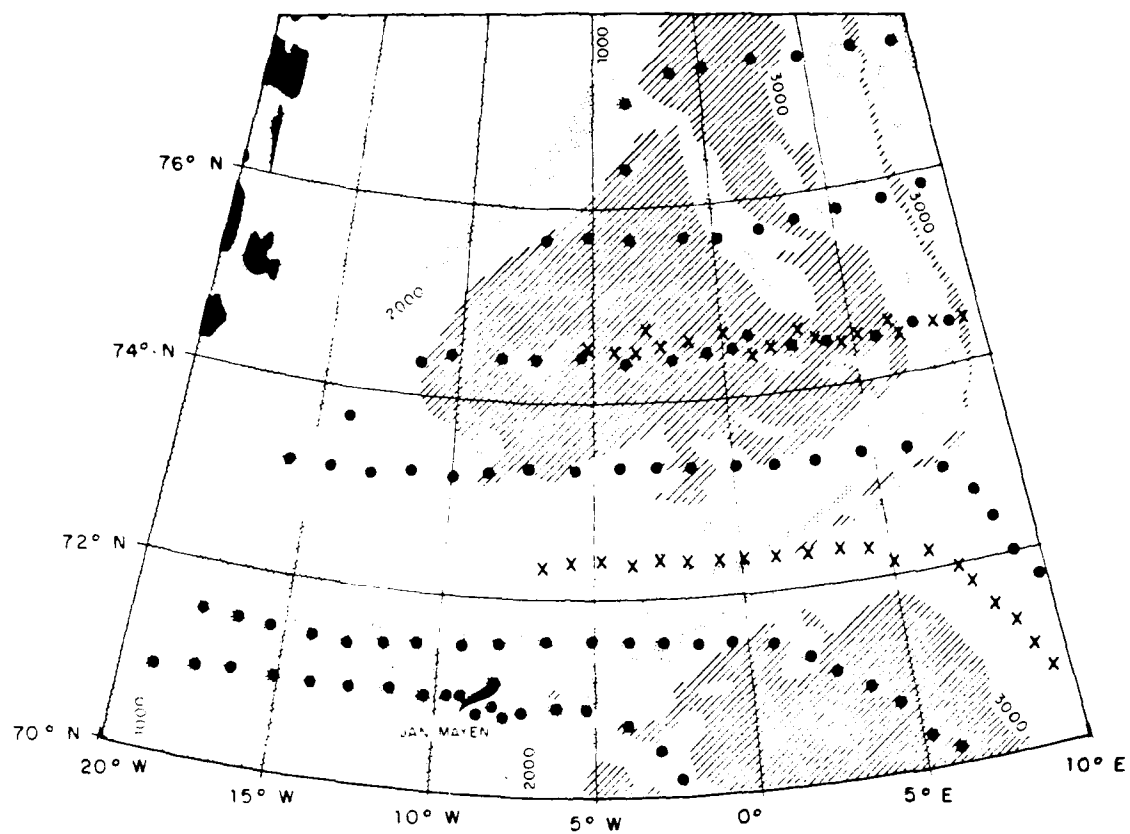


Figure 2.3 JOHAN HJORT (solid dots) and POLJARNIK (x's) stations in the Greenland Sea from cruises in summer 1958 of the International Geophysical Year. Note the legs are separated by up to one degree of latitude (from *Dietrich, 1969*).

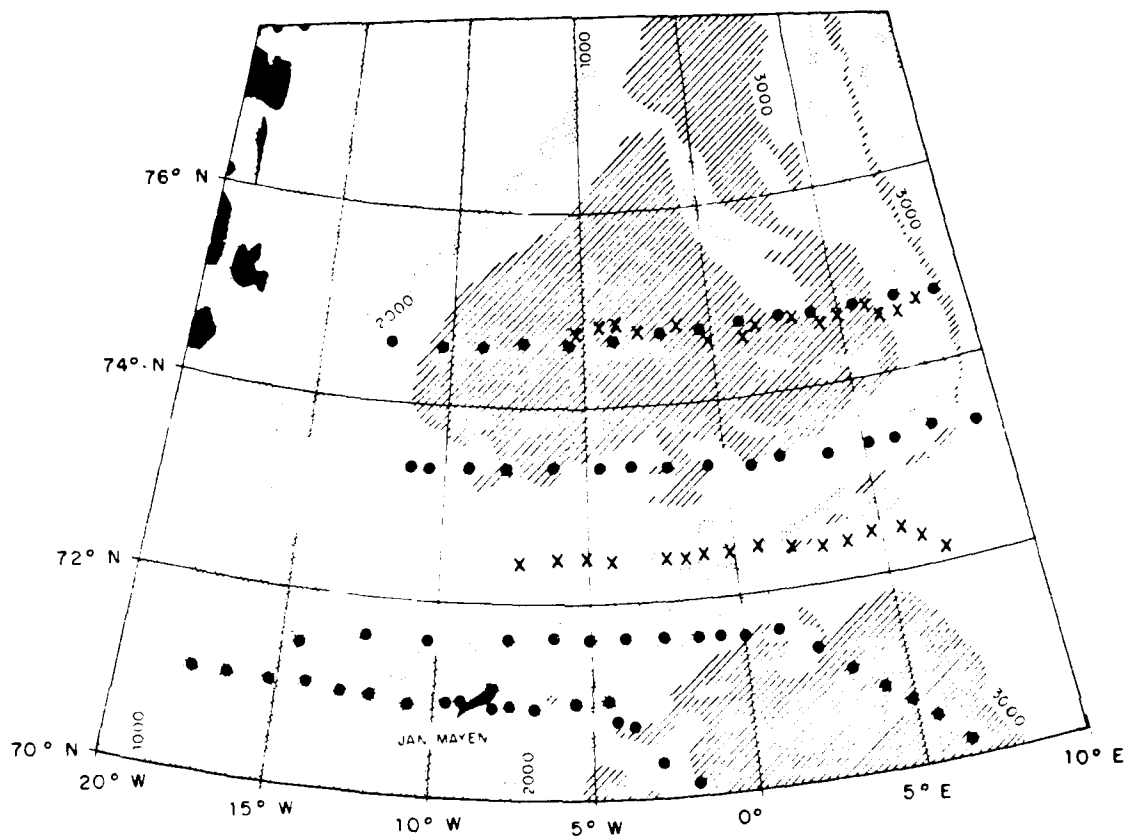


Figure 2.4 JOHAN HJORT (solid dots) and POLJARNIK (x's) stations in the Greenland Sea from cruises in winter 1958 of the International Geophysical Year. Note the absence of stations north of 75°N and that legs are separated by up to one degree of latitude (from *Dietrich, 1969*).

to the BARTLETT 89 survey area were made available by *S. Legutke (personal communication)*.

Bathymetry is compiled from a combination of the DBDB5 digital data base and a bathymetric chart of the Greenland-Norwegian and western Barents seas (*Perry et al., 1984*). The ice edge positions in 1989 are obtained from a combination of DMSP OLS visual and infrared images and the Southern Ice Limit Analysis of the Naval Polar Oceanography Center.

III. HYDROGRAPHY

A. INTRODUCTION

The Jan Mayen Current (JMC) plays a major role in water mass formation and circulation in the Greenland Basin. This current is the medium by which cold, fresh surface waters and warm, saline intermediate waters from the East Greenland Current (EGC) are transported into the Greenland Basin, and more importantly, to the Greenland Sea Gyre (GSG), one of the primary centers of winter deep convection in the World Ocean. One can envision the GSG as the mortar and the JMC as the pestle with which nature delicately attempts to concoct the proper water mass blend to trigger winter convective overturn.

This chapter provides a detailed rendering of the hydrographic structure within the Greenland Basin and the influence of the JMC on this structure. Also included in this discussion are what the hydrographic structure may signal about the circulation in the basin and how this structure varies on a seasonal and inter-annual basis. Evidence will be presented in this and the following chapter that the JMC is partly an anticyclonic meander in the seaward portion of the EGC rather than solely an eastward current forming the southern limb of the GSG indicated by traditional theory.

B. SURFACE AND INTERMEDIATE WATER MASSES

Three broad categories of water masses exist in the Greenland Basin:

- Polar Water (PW) is a cold, fresh surface water usually of Arctic Ocean origin and transported into the region by the EGC. PW is usually found within 100 m of the surface.
- Atlantic Water (AtW) is a warm, saline surface or intermediate water initially transported into the area as a surface water of the Norwegian Atlantic Current (NAC). Surface AtW is usually found in the upper 200 m of the water column, whereas intermediate AtW typically occurs between 100-400 m.
- Arctic Water (ArW) is a generic term for the characteristic surface and intermediate waters formed in the Nordic Seas usually a mixture of the previous two water masses. Surface ArW usually occurs within 100 m of the surface and intermediate ArW breaches the water column between the surface layer and the deep waters at depths exceeding 1000 m.

A complete scheme of specific surface and intermediate water mass variants from the above general categories appears in Figure 3.1 and Table 3.1 adapted from *Hopkins (1988)*. Primary water masses are defined as those which exist outside the JMC whereas secondary water masses are those which compose the JMC. A general description follows of water masses and their relative locations in the Greenland Basin (largely adapted from *Hopkins, 1988*).

1. Surface Water Masses

Three primary surface water masses reside within the Greenland Basin. The first is a cold, fresh surface PW with origins in the Arctic Ocean, which is transported to the Greenland Basin via the EGC (*Bourke et al., 1987*). Within the EGC and the Greenland Basin, this PW is referred to as Greenland Polar Water (GPW). The second

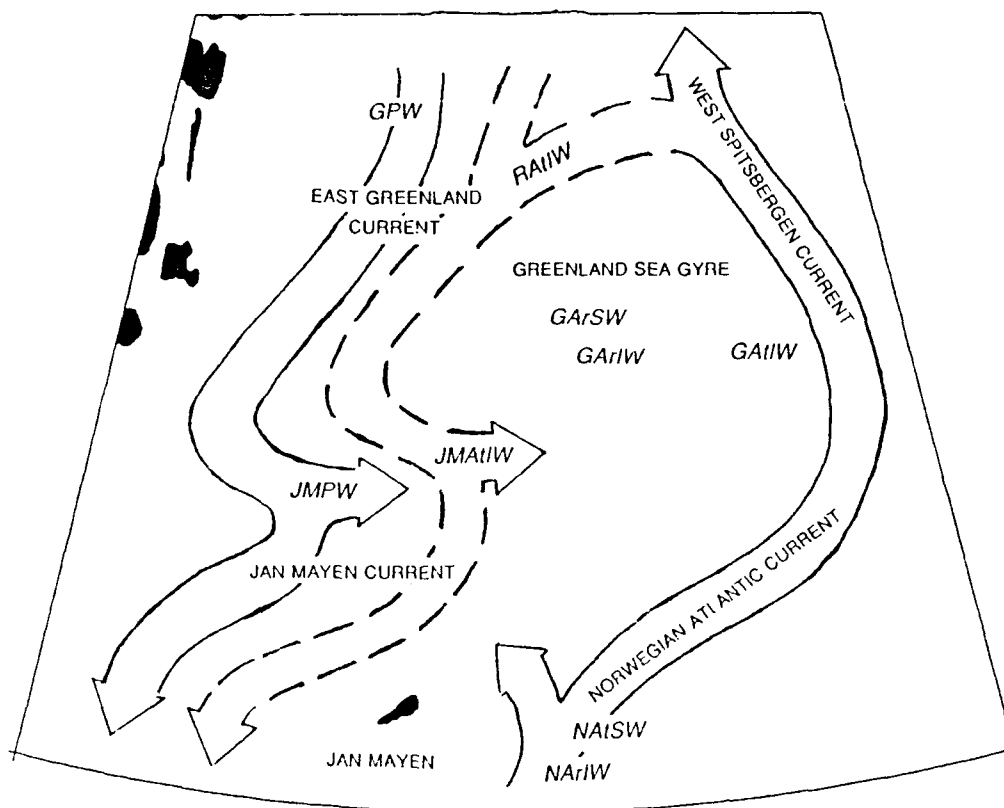


Figure 3.1

Greenland-Norwegian Sea surface and intermediate water mass circulation schematic. In the north, the East Greenland Current (EGC) carries surface Greenland Polar Water (GPW) from the Arctic Ocean into the region; similarly in the south, the Norwegian Atlantic Current (NAC) carries in Norwegian Atlantic Surface Water (NA_tSW) and Norwegian Arctic Intermediate Water (NA_rIW). NA_tSW sinks isopycnally in the West Spitsbergen Current (WSC) to supply intermediate water to the Arctic Ocean via Fram Strait, the EGC as Return Atlantic Intermediate Water (RA_tIW), and directly to the Greenland Sea from the east as Greenland Atlantic Intermediate Water (GA_tIW). The Jan Mayen Current (JMC) consists of waters which bow from the EGC. The cyclonic Greenland Sea Gyre (GSG) consists of a mixture of waters from the surrounding circulations. Refer to Table 3.1 for complete water mass descriptions.

Table 3.1 Surface and Intermediate Water Masses of the Greenland Basin (after Hopkins, 1988). The temperature and salinity ranges of JMPW and JMAIw are broadened from the values given in Hopkins (1988) based on BARTLETT 89 observations; similarly those of RAiW are broadened based on the observations of Bourke *et al.* (1987). Note that JMPW and GARiW are also components of JMAiW.

Surface Waters			
Primary		Secondary	
Greenland Polar Water (GPW)	< 5°C < 34.4	Jan Mayen Polar Water (JMPW)	0 to -1.5°C 34.0 - 34.7
Greenland Arctic Surface Water (GArSW)	freezing to 5°C 34.7 - 34.9		
Norwegian Atlantic Surface Water (NAtSW)	> 2°C > 35.0		
Intermediate Waters			
Return Atlantic Intermediate Water (RAtIW)	0 to 3°C 34.9 - 35.0	Jan Mayen Atlantic Intermediate Water (JMAAtIW)	0 to 1.5°C 34.8 - 35.0
Greenland Arctic Intermediate Water (GArIW)	< 2°C 34.7 - 34.9		
Norwegian Arctic Intermediate Water (NArIW)	0.5°C 34.88		

is a warm, saline surface AtW which is initially transported into the region by the NAC. This Norwegian Atlantic Surface Water (NAtSW) skirts the eastern periphery of the Greenland Basin in the NAC which, further north, becomes the West Spitsbergen Current (WSC). NAtSW sinks along isopycnals as it encounters less dense surface PW in Fram Strait region and becomes intermediate AtW which is supplied to both the Eurasian Basin and EGC. The third primary water mass is a surface ArW characteristic of the GSG which is a mixture of GPW and NAtSW. This surface ArW is termed Greenland Arctic Surface Water (GArSW) within the Greenland Basin and is the only water mass which undergoes significant seasonal changes in temperature. The mixture of GPW and GArSW yields a slightly denser, near-surface, secondary water mass within the JMC termed Jan Mayen Polar Water (JMPW). The temperature ranges of these water masses overlap, thus they are best distinguished by salinity.

2. Intermediate Water Masses

Three primary intermediate water masses are present in the Greenland Basin. The first, Return Atlantic Intermediate Water (RAtIW), is the portion of subducted NAtSW which branches cyclonically from the WSC to join the EGC just south of Fram Strait (*Bourke et al., 1988*). Within the EGC a warm, saline core of RAtIW lies to the east of and beneath the East Greenland Polar Front (EGPF) at depths between 100 to 400 m (*Bourke et al., 1987*). The second primary water mass, Greenland Arctic Intermediate Water (GArIW), characterizes the cold, moderately saline, weakly stratified intermediate layer between GArSW and the deep waters in the GSG. The third, Norwegian Arctic Intermediate Water (NArIW), forms a homogeneous layer about 200 m

thick evidenced by a temperature and salinity minimum between NAtSW and the deep waters in the NAC. This NAtIW layer is thought to be a lateral extension of the intermediate waters of the Icelandic Current.

Jan Mayen Atlantic Intermediate Water (JMAAtIW) is a secondary water mass formed by the dilution of RAtIW by GArIW and JMPW and is the intermediate water of the JMC. Within the JMC a warm, saline core of JMAAtIW is found between 50 and 400 m. Greenland Atlantic Intermediate Water is a warm, saline mixture of NAtSW and GArSW found along the east side of the Greenland Basin. This water mass was not observed in the BARTLETT 89 survey due to station locations, but is included to complete the description of water masses in the basin.

C. SURFACE WATER SIGNATURE

1. Summer Surface Signature

a. Surface Temperature

The BARTLETT 89 surface temperature contour pattern is depicted in Figure 3.2. The sharpest gradient occurs across Stations 2 to 5 within the EGC. Since the above group of stations does not progress westward shallower than the 2000 m isobath nor westward of the 0°C isotherm, only the seaward fringe of the EGC is sampled. The temperature gradient can be expected to increase somewhat more than pictured as the ice edge is encountered farther to the west (*Paquette et al., 1985; Bourke et al., 1987*). These stations are located over the lower East Greenland Continental Slope just south of the deepest point along the west end of the Greenland Fracture Zone (GFZ). This

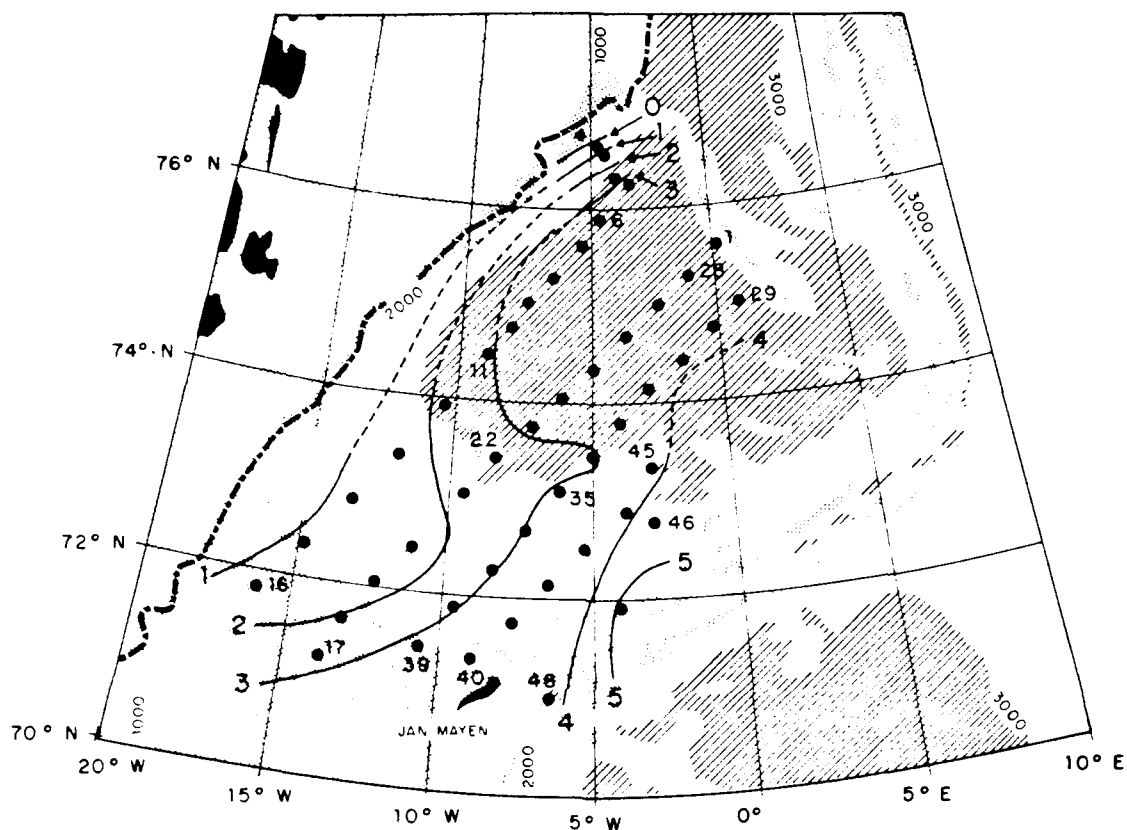


Figure 3.2

BARTLETT 89 surface temperature ($^{\circ}\text{C}$). The temperature gradient is greatest between Stations 3 to 5 in the fringe of the East Greenland Current (EGC). Cold Greenland Polar Water bows eastward from the EGC south of 74°N in the Jan Mayen Current. Warm Norwegian Atlantic Surface Water in the Norwegian Atlantic Current encroaches on the Greenland Basin between Stations 45 to 48. Mean ice edge shown as a heavy dashed line.

depression in the isthmus which connects the GFZ to the continental slope allows the deep waters of the EGC to pass freely to a depth of approximately 2600 m from the Boreas Basin to the Greenland Basin. This depth is also the sill depth confronted by the EGC as it passes southward from Fram Strait.

The surface temperature gradient associated with the EGC continues southward, unhindered, until it crosses the eastward turning 3000 m isobath. This isobath marks the base of the slope of the Jan Mayen Fracture Zone (JMFZ) to the south and Mohn Ridge to the east. At this point the contours of surface temperature progressively broaden and bow eastward until approximately where the 2000 m isobath is crossed (south of 74°N) at which point they turn westward with decreasing separation to rejoin the EGC. This 2000 m isobath corresponds closely with the deepest point between the Jan Mayen Fracture Zone (JMFZ) and the East Greenland Continental Slope which is about 1600 m. This deepest channel is the ultimate passage for any deep waters of the EGC that may flow southward from the Greenland Basin to the Icelandic Plateau.

In figure 3.2 the JMC presents a distinct surface signature as an eastward protrusion of relatively cold GPW from the EGC between 73°N and 74°N as described above. The eastward protrusion of the 3°C isotherm from the EGC by the JMC is seen even in the 4°C isotherm situated over the Mohn Ridge, already on the border of the NAC. North of the JMC is an area of small temperature gradient which is the core of the GSG.

The JOHAN HJORT/POLJARNIK 58 summer surface temperature contour pattern in Figure 3.3 is quite similar to that in summer 1989 including the

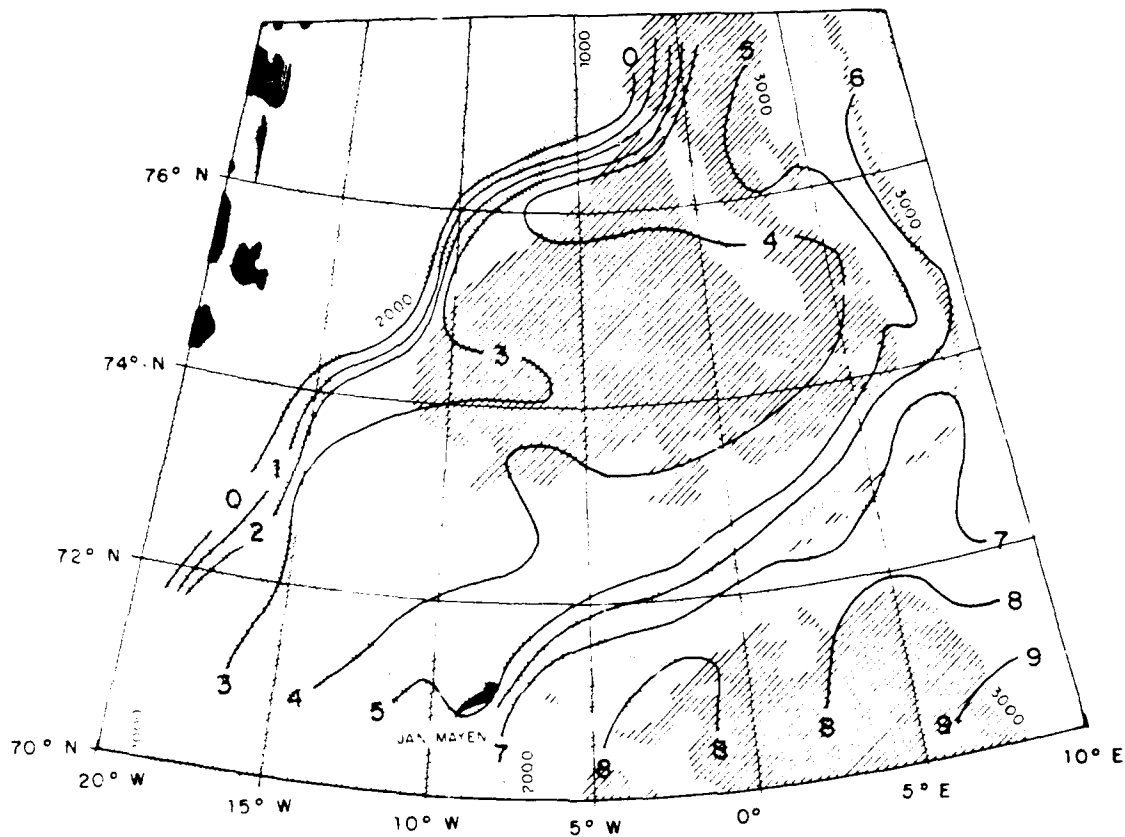


Figure 3.3

JOHAN HJORT/POLJARNIK 58 summer surface temperature (°C). The temperature gradient pattern is similar to BARTLETT 89 along the East Greenland Current. The Jan Mayen Current (JMC) bows eastward just north of 74°N. The largest gradient of the Norwegian Atlantic Current lies along the Mohn Ridge. Overall, temperatures are 1 to 2°C warmer than in 1989. The axis of the JMC is located about 100 km north of its position in 1989 (from *Dietrich, 1969*).

eastward protrusion of the 3°C isotherm, though it occurs about 120 km farther to the north in 1958 than in 1989. However, surface temperatures in the Greenland Basin were generally 1 to 2°C colder in summer 1989 than in summer 1958. This could be due to an increase in the flow of cold GPW from the EGC which would allow less intrusion of warmer NAtSW from the NAC into the Greenland Basin. The same increase in available GPW could render conditions more favorable for winter sea ice formation, thus increasing the quantity of melt water in the summer. Both events could cause the overall decrease in surface temperatures and salinities observed in the basin in 1989.

b. Surface Salinity

The JMC is also well defined by contours of low surface salinity as shown in Figure 3.4. The pattern of the 33.0 isohaline generally coincides with that of the 3°C isotherm (compare with Figure 3.2). As with surface temperature, the BARTLETT 89 surface salinity gradient is sharpest over the East Greenland Continental Slope (in the EGC) just south of the GFZ, broadens while bowing eastward south of 74°N, then tightens while rejoining the EGC prior to passage over the JMFZ sill. The contour pattern in the area of Stations 46 to 48 shows the saline NAtSW of the NAC meeting the fresher GPW of the JMC as with the temperature pattern in Figure 3.2.

The JOHAN HJORT/POLJARNIK 58 summer data in Figure 3.5 also mark the JMC as a tongue of relatively low salinity surface water. Salinity ranges, however, are higher by up to 3 PSU in 1958 over 1989 in both the JMC and GSG. As mentioned above, the increase in surface salinity in 1958 is probably due to a reduced flow of cold, fresh GPW in the EGC compared with 1989.

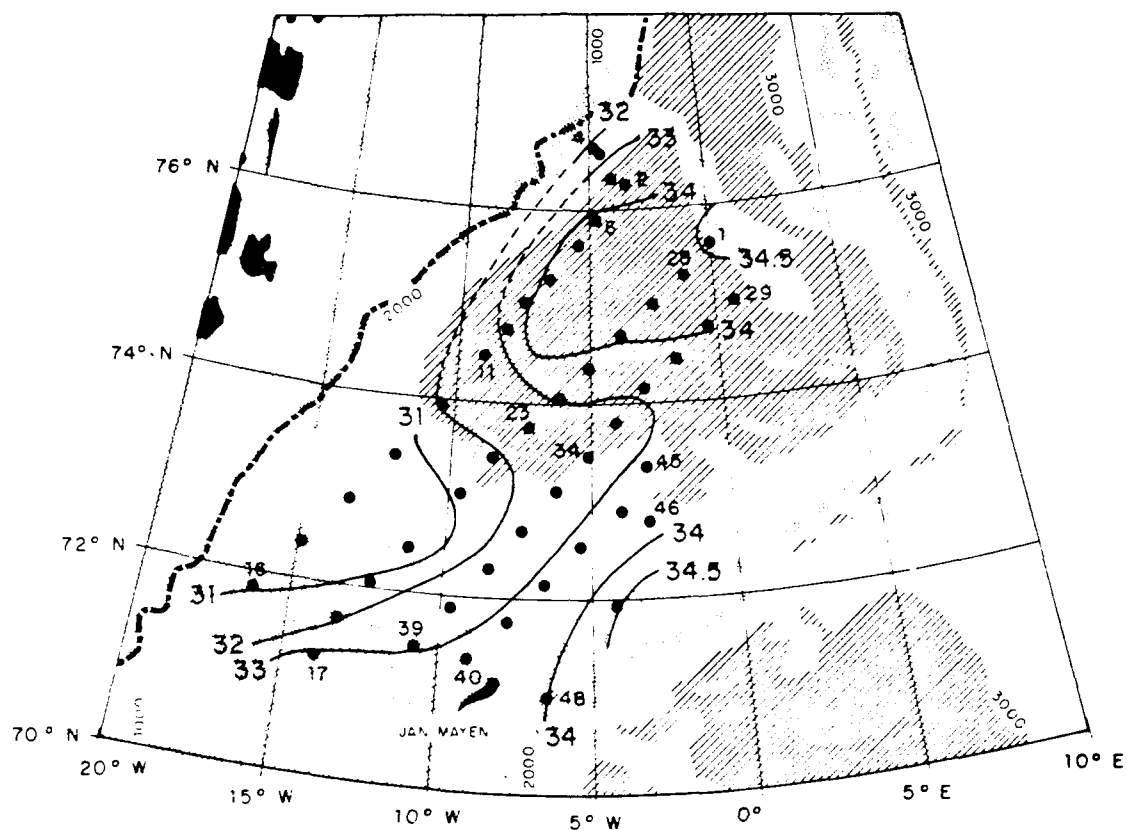


Figure 3.4

BARTLETT 89 surface salinity (PSU). The pattern of gradients is similar to that of the surface temperature. The Jan Mayen Current is seen in eastward bowing of fresh Greenland Polar Water from the East Greenland Current. The tightening gradient over the Mohn Ridge indicates the fringe of the Norwegian Atlantic Current. Mean ice edge shown as a heavy dashed line.

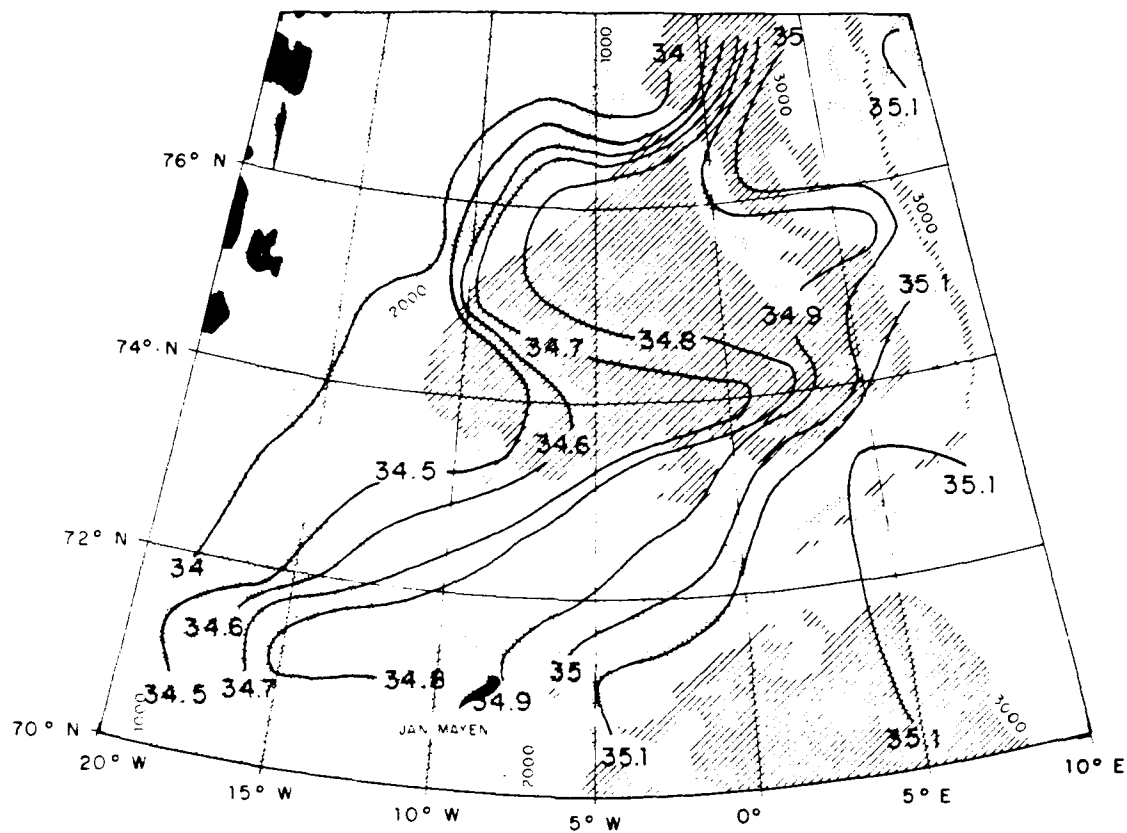


Figure 3.5 JOHAN HJORT/POLJARNIK 58 summer surface salinity (PSU). The gradient pattern is similar to that of BARTLETT 89 though salinities are between 0.4 to 3.5 PSU greater in 1958 than in 1989 (from *Dietrich, 1969*).

2. Winter Surface Signature

The JMC winter signature in surface properties is derived from the METEOR/HUDSON 82 (Figures 3.6 and 3.7) and JOHAN HJORT/POLJARNIK 58 (Figures 3.8 and 3.9) data sets. Immediately apparent in winter is the marked eastward shift in the gradients of surface properties, undoubtedly due to a widening of the East Greenland ice pack (presumed to be bounded by the 0°C isotherm). This eastward projection of the pack seems to coincide with the location of the JMC.

In 1958, apparently due to a lack of GPW as described earlier, the winter temperatures in the region of the JMC were more than 1°C warmer than in 1982. In contrast, temperatures in the GSG were 0.1°C colder with the surface area of the gyre considerably enlarged in 1958 over 1982. It does not appear that overall changes in atmospheric temperatures could have caused this variation. Isolated areas of water colder than 0°C suggest limited sea ice coverage in 1958, whereas in 1982 sea ice coverage is indicated in the form of an "odden" extending over nearly the entire Greenland Basin (*Parkinson et al., 1987, e.g. p.193*). Thus, a dramatic increase in sea ice production coincidental with a period of markedly lower salinity in 1982 compared with 1958 further suggests a greater quantity of GPW was available in 1982. "Odden" is a Norwegian term which describes the periodic eastward protrusions of the east Greenland ice pack in winter in the area of the JMC. The extent and frequency of occurrence of the "odden" varies inter-annually (*Parkinson et al., 1987, e.g. p.195*).

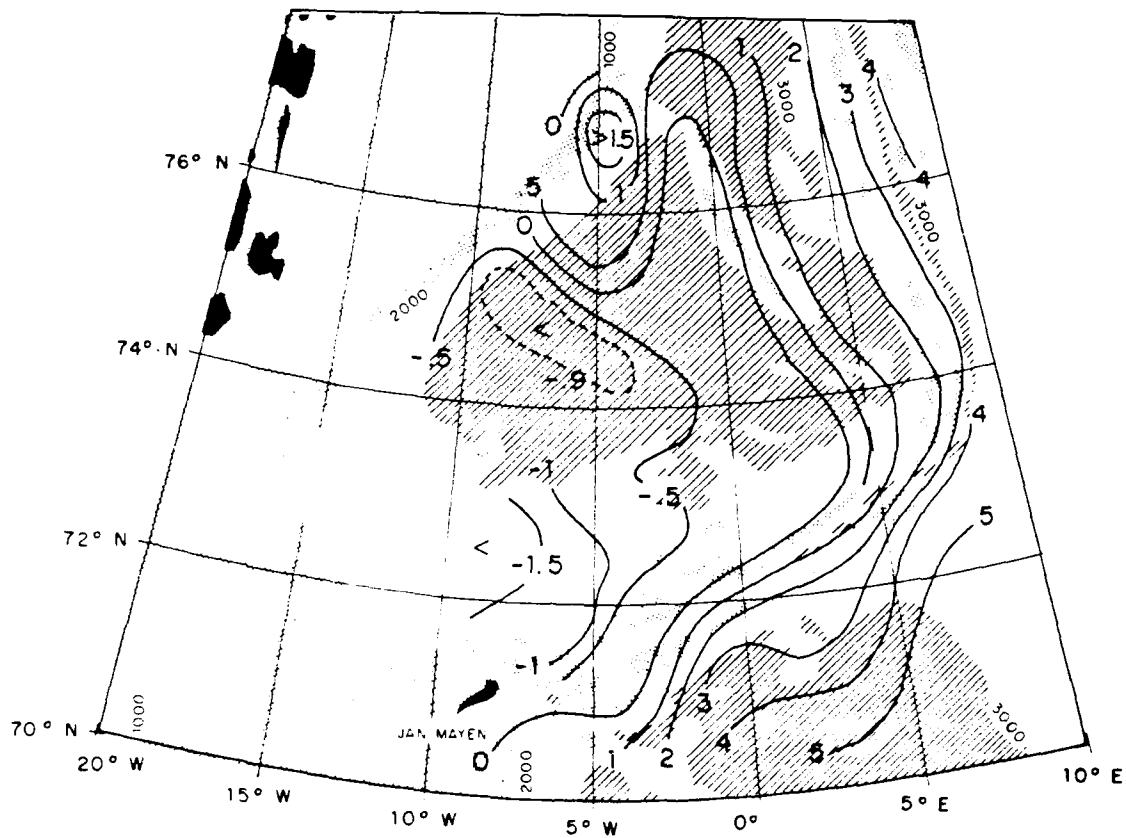


Figure 3.6 METEOR/HUDSON 82 winter surface (5 m) potential temperature ($^{\circ}\text{C}$). The large eastward projection of the 0°C isotherm indicates extensive sea ice coverage over most of the Greenland Basin. A tongue of very cold Greenland Polar Water ($< -1.5^{\circ}\text{C}$) along the Jan Mayen Fracture Zone indicates the presence of the Jan Mayen Current (JMC). The axis of the JMC is located about 120 km south of its position in 1989 (from Koltermann and Lüthje, 1989).

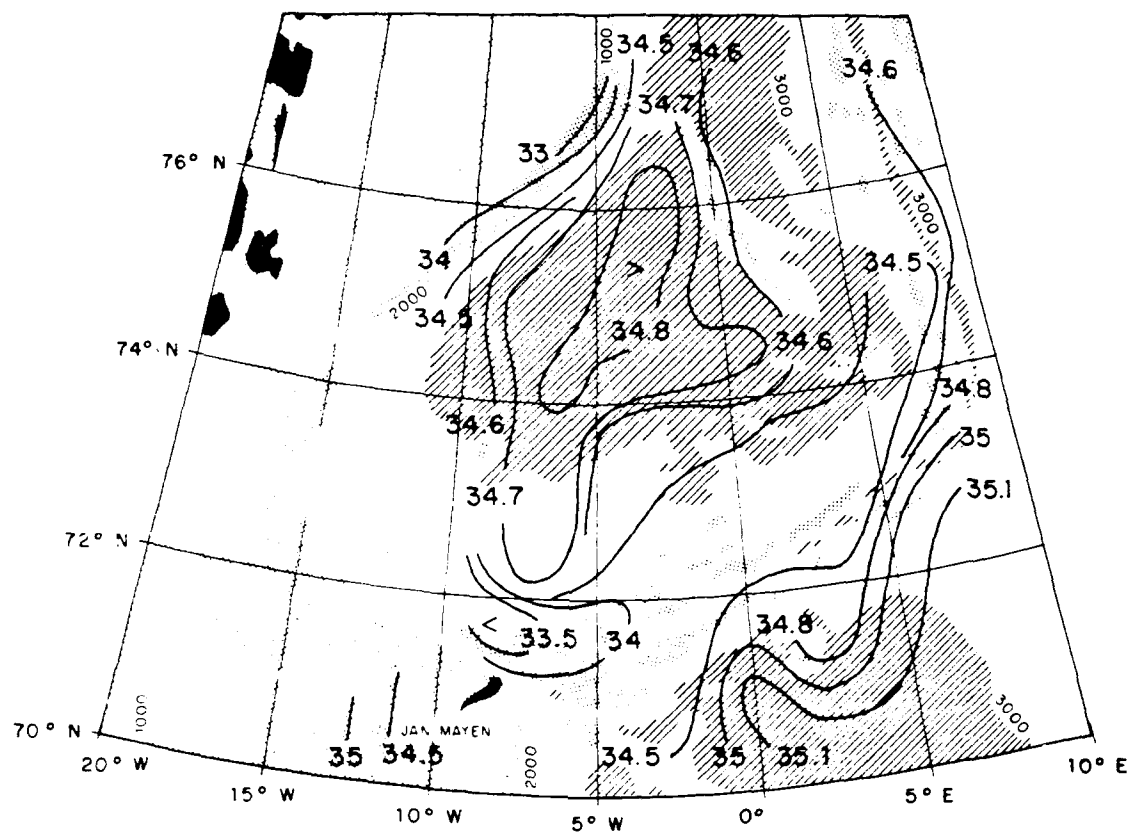


Figure 3.7 METEOR/HUDSON 82 winter surface (5 m) salinity (PSU). The surface salinity pattern is greatly similar to that of BARTLETT 89 although 1982 salinities are slightly higher (perhaps due to sampling at 5 m instead of the surface). A tongue of low-salinity Greenland Polar Water along the Jan Mayen Fracture Zone indicates the presence of the Jan Mayen Current (from Koltermann and Lühje, 1989).

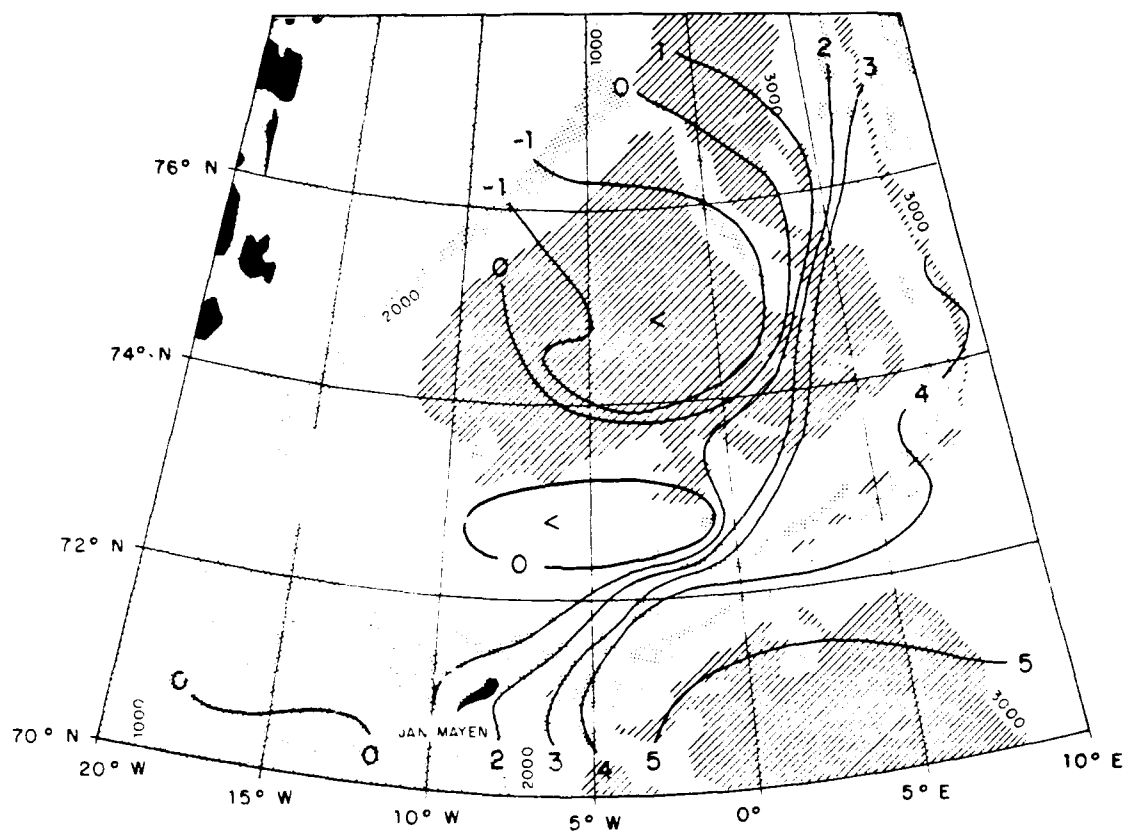


Figure 3.8

JOHAN HJORT/POLJARNIK 58 winter surface temperature (°C). Temperatures are slightly lower by -0.1°C in the Greenland Sea Gyre than in winter 1982, though elsewhere in the Greenland Basin temperatures are higher by $> 1^{\circ}\text{C}$. The location of the 0°C isotherm indicates only limited sea ice coverage (from *Dietrich, 1969*).

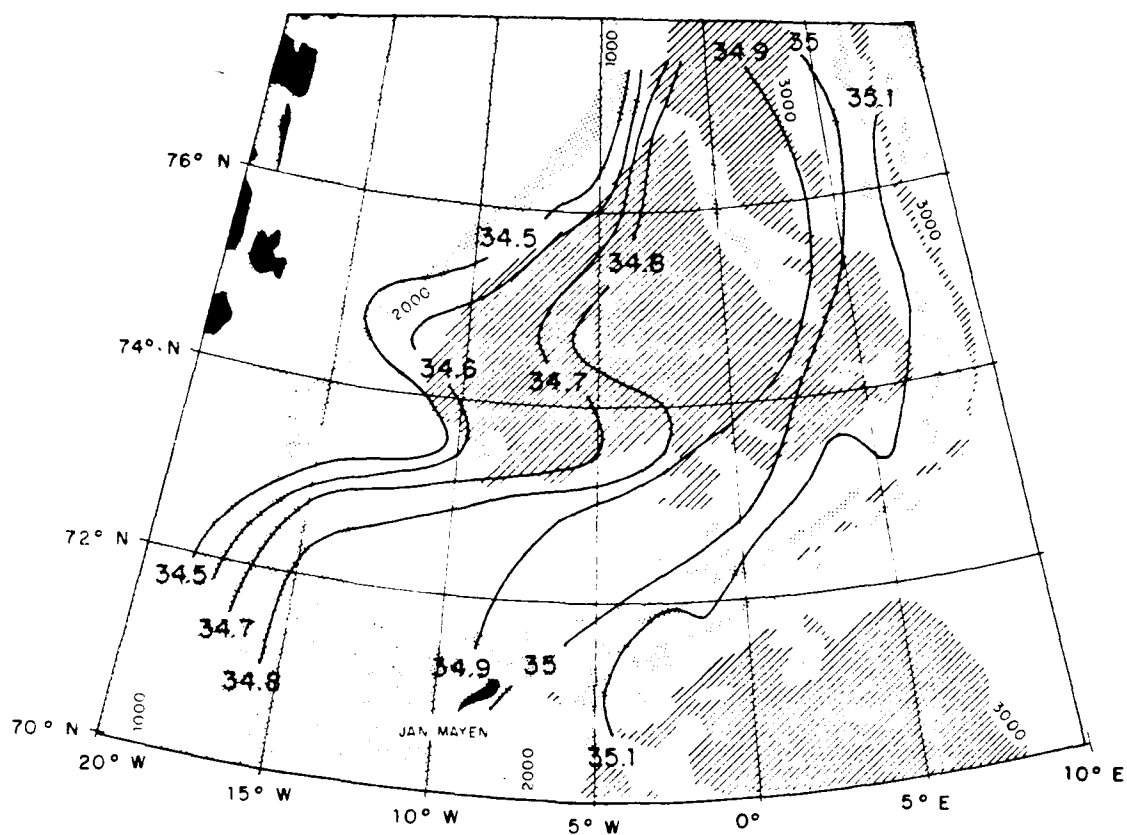


Figure 3.9 JOHAN HJORT/POLJARNIK 58 winter surface salinity (PSU). The surface salinity pattern is similar to both winter 1982 and summer 1989, though actual salinities are markedly higher showing a greatly diminished presence of Greenland Polar Water. The winter axis of the Jan Mayen Current is nearly collocated with that of summer 1958 (from Dietrich, 1969).

These figures also show a north-south translation of the east-west axis of the JMC perturbation between data collection years. In 1982, the perturbation axis seems to hug the JMFZ being located about 120 km *south* of its position in 1989. In 1958 the axis is relatively stationary between seasons, though it is located about 100 km *north* of its position in 1989.

D. INTERMEDIATE WATER SIGNATURE

The analysis of the intermediate water structure of the Greenland Basin involves several modes of data presentation which are useful owing to the dramatic differences in temperature and mild differences in salinity generally found among water masses in the high latitude regime.

1. Temperature Maximum

The contour pattern of the intermediate water temperature maximum (T_{max}) is useful in locating the JMC since there is such sharp contrast between the temperature ranges of colder GArIW and warmer JMArIW. Figure 3.10 shows that a large, eastward meander of warm JMArIW ($> 0^{\circ}\text{C}$) protrudes from the EGC south of 74°N in the BARTLETT 89 data set. The 1989 data also show RArIW to be as warm as 2°C though only the seaward fringe of the EGC was sampled. The historical data of *Bourke et al.* (1987) from the years 1981, 1984, and 1985 indicate RArIW core temperatures in the EGC may exceed 3°C . That this meander in the gradient of the warm intermediate waters is located directly beneath and is similar in shape to the GPW meander in the surface gradient indicates the flow of the water column is coordinated between these two levels.

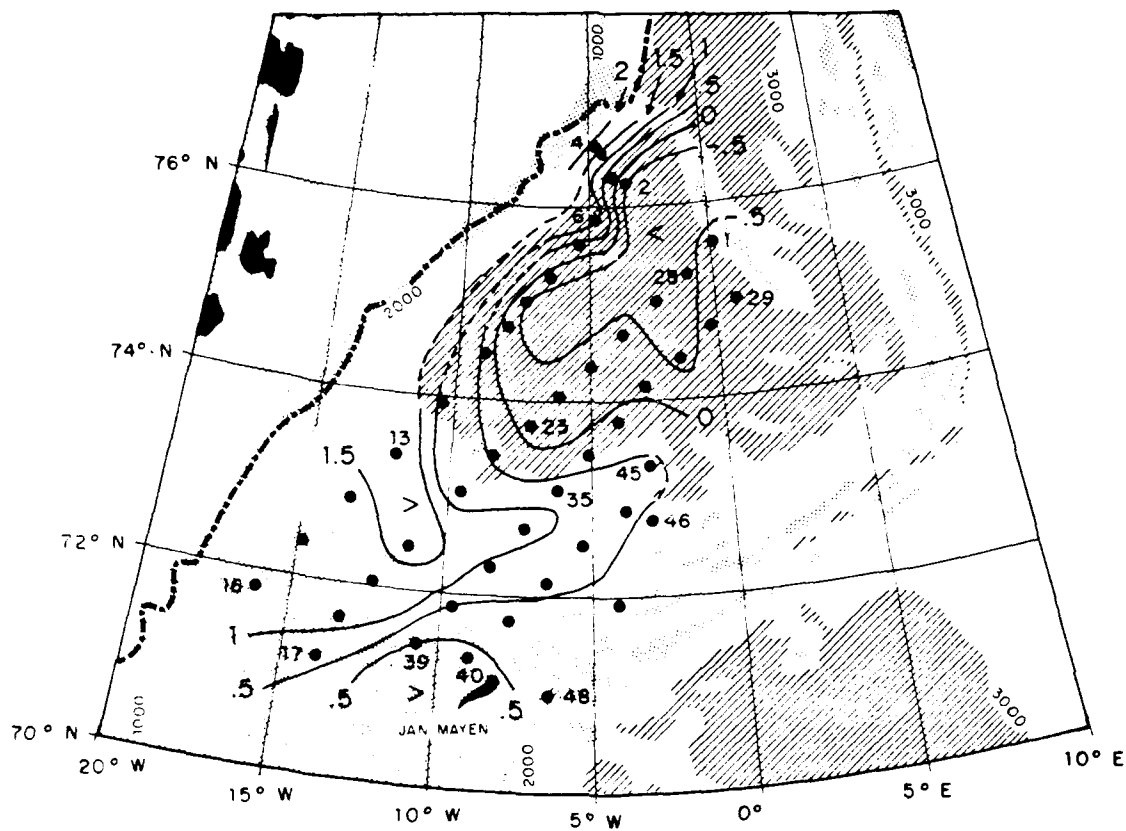


Figure 3.10 BARTLETT 89 contours of the intermediate temperature maximum (T_{max}) ($^{\circ}\text{C}$). The Jan Mayen Current (JMC) is marked by a large eastward meander of Return Atlantic Intermediate Water from the East Greenland Current which becomes Jan Mayen Atlantic Intermediate Water within the JMC proper. The meander seems to occur in response to the underlying bathymetry. The perturbation at Station 6 (radius ~ 50 km) may have been resolved as a large warm-core eddy had sampling progressed farther to the west. Mean ice edge shown as a heavy dashed line.

This inference of the flow together with a distinct and coordinated response to the underlying bathymetry at both levels suggest the flow is significantly barotropic as is expected in the region.

The perturbation of isopleths (radius 50 km) at Station 6 resembles either a small meander in the flow of intermediate water or a large warm-core eddy that might have been resolved had the survey continued farther west. According to *Gascard et al. (1988)* large, barotropic eddies of WSC origin are a major mechanism in the recirculation of AtW from the WSC to the EGC. These eddies, formed along the continental slope between Norway and Spitsbergen, propagate westward topographically conserving potential vorticity by following fracture zones. Such eddies are often observed as semi-permanent features along the East Greenland Continental Slope just south of fractures zones such as the GFZ. Interaction of these large eddies with the marginal ice zone (MIZ) upon reaching the EGC produces various baroclinic mesoscale phenomena. These resultant new eddies with a first baroclinic Rossby radius of deformation (R_d) of order 5 km cannot be resolved given the coarse station spacing of the data sets used herein. *Muench (1989)* states that "wave-like" or "meander-like" features are frequently observed in the MIZ, often in conjunction with eddies.

South of the JMC there is a second warm, intermediate water mass at Stations 39, 40, and 48 distinguished by a T_{max} of greater than 0.5°C . This water mass appears to be an infusion from the southeast of NArIW from the NAC. Such a flow consistently appears in general circulation schematics of the region (see *Jónsson, 1989*).

North of the JMC lies the colder, intermediate water of the GSG. This GArIW is characterized by a much colder T_{max} of less than -0.5°C.

In Figure 3.11 the T_{max} of warm JMA_tIW in the heart of the JMC occurs at a depth of less than 100 m while to the north in the GSG the T_{max} of cold GArIW lies at depths exceeding 150 m. Away from the influence of JMA_tIW in the JMC and NArIW at Stations 39, 40, and 48 the depth of T_{max} exceeds 200 m.

In Figure 3.12 salinities at T_{max} away from the influence of the EGC vary minutely across the Greenland Basin from less than 34.85 in the heart of the JMC to greater than 34.88 north and south of the JMC. This small horizontal variation in salinities is indicative of overall weak density stratification beneath the more intense near-surface salinity (density) gradient. The lower salinity at T_{max} associated with JMA_tIW is due to a depression of the salinity by some vertical mixing with the large volume of less saline GPW immediately above. Thus, the JMC may be traced by a signature of slightly depressed salinities at T_{max}.

2. Temperature Minimum

There is naturally a minimum temperature (T_{min}) in the cold upper PW layer between the surface warmed by insolation and the intermediate waters warmed by AtW influence. In Figure 3.13 in the JMC the presence of the warm, buoyant JMA_tIW causes the overlying surface layer to be thin and thus T_{min} to be shallow (approximately 25 m), whereas in the absence of such warm intermediate waters in the GSG T_{min} occurs at greater depths (75 m or more). Thus, the depth of T_{min} is another means by which to locate the core of the JMC. Salinities at T_{min} vary more than those at T_{max} since T_{min}

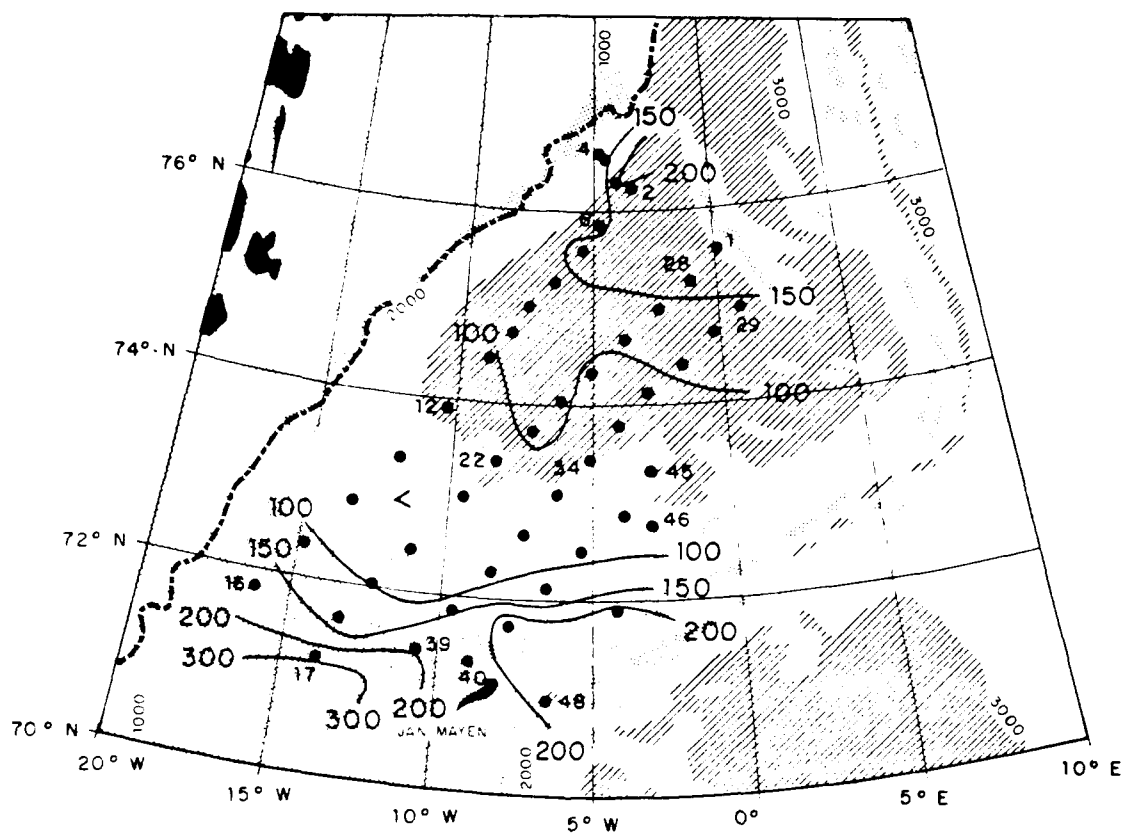


Figure 3.11 BARTLETT 89 depth of the intermediate temperature maximum (Tmax) (m). The depth of Tmax is less than 100 m in the heart of the Jan Mayen Current. Tmax occurs at depths exceeding 150 m in the Greenland Sea Gyre. Mean ice edge shown as a heavy dashed line.

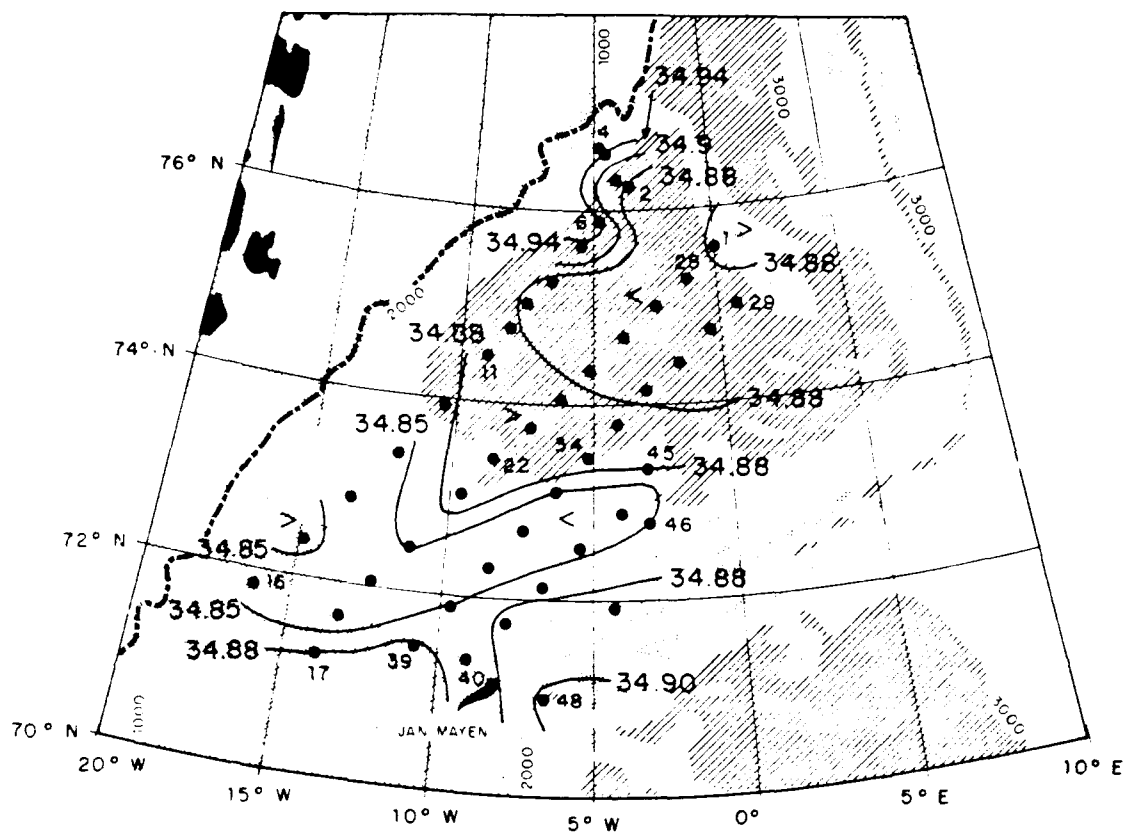


Figure 3.12 BARTLETT 89 salinity at the intermediate temperature maximum (Tmax) (PSU). Salinities are slightly depressed at Tmax in the Jan Mayen Current apparently due to vertical mixing with the overlying volume of Greenland Polar Water. Salinities at Tmax are slightly higher in the Greenland Sea Gyre. Mean ice edge shown as a heavy dashed line.

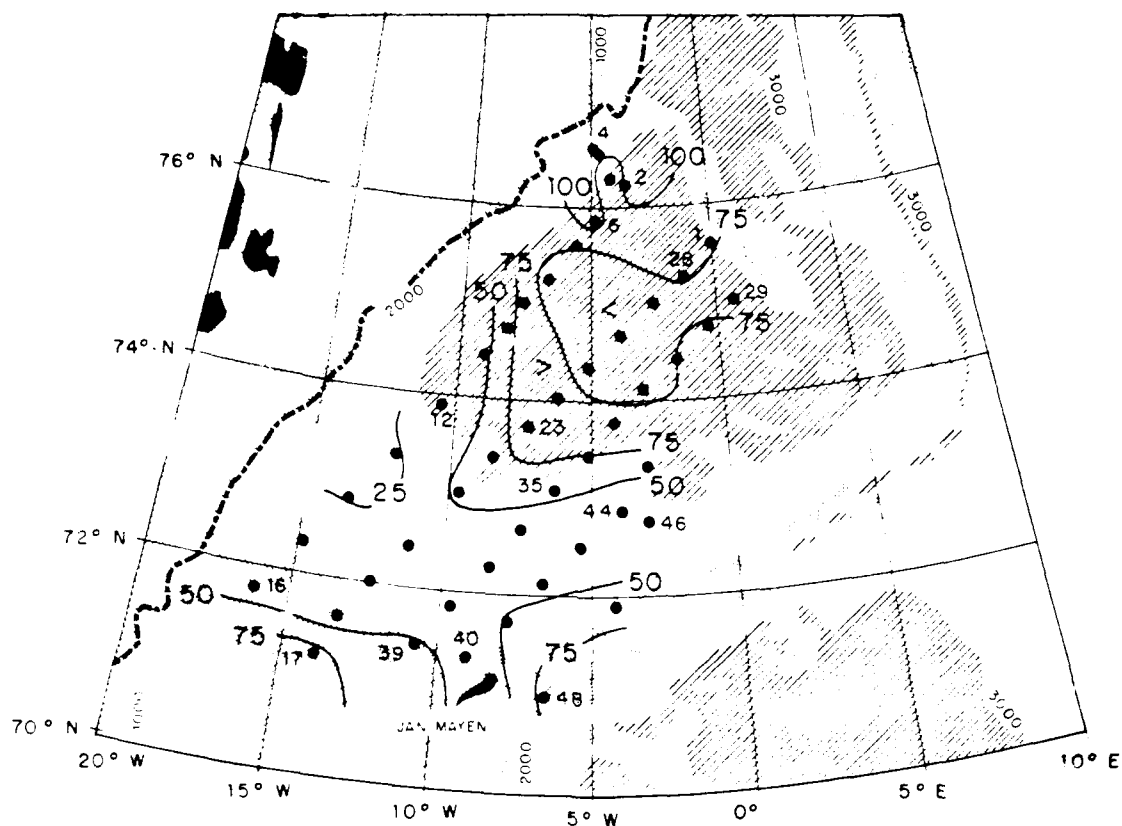


Figure 3.13 BARTLETT 89 depth of the subsurface temperature minimum (T_{min}) (m). A subsurface temperature minimum occurs between the surface, warmed by insolation and the intermediate waters warmed by Atlantic Water influence. In the Jan Mayen Current T_{min} occurs within a shallow subsurface core of modified Greenland Polar Water, or Jan Mayen Polar Water at < 50 m. In the Arctic Water of the Greenland Sea Gyre, T_{min} occurs slightly deeper at < 75 m. Mean ice edge shown as a heavy dashed line.

always occurs at shallower depths where the water column is more heavily stratified, thus salinities at T_{min} range from 34.1 in the JMPW of the JMC to 34.8 in the GArSW of the GSG.

Contours of T_{min} in Figure 3.14 reveal a north-south separation between the warm and cold cores of the JMC of up to 100 km. A solid bar represents the axis of the JMA_{At}IW core derived from contours of T_{max} in Figure 3.10 and the open bar represents the axis of the near-surface JMPW core. The bars do not indicate the direction of flow, but represent the east-west axis of the JMC meander with respect to each of the two core waters for purposes of orientation. A similar portrayal appears in a general circulation schematic by *Koltermann and Lüthje (1989)*. The source waters of these two water masses are initially separated horizontally in the EGC by the EGPF with the GPW core located up to 60 km westward of the RA_{At}IW core (*Bourke et al., 1987*). This gives rise to an apparent turning lag and southward displacement of the JMPW core relative to the JMA_{At}IW core in the JMC.

3. Salinity maximum

A final tracer useful in locating the JMC is the intermediate water salinity maximum (S_{max}). Contours of S_{max} in Figure 3.15 present a pattern quite similar to that of T_{max} including the perturbation previously noted in the EGC at Station 6. The influence of the JMA_{At}IW component of the JMC on the waters below is manifested in an increase in S_{max} (~0.4 PSU greater) and a decrease in the depth of S_{max} (200 m shallower) compared with these values in the GSG. Also noted in contours of S_{max} is

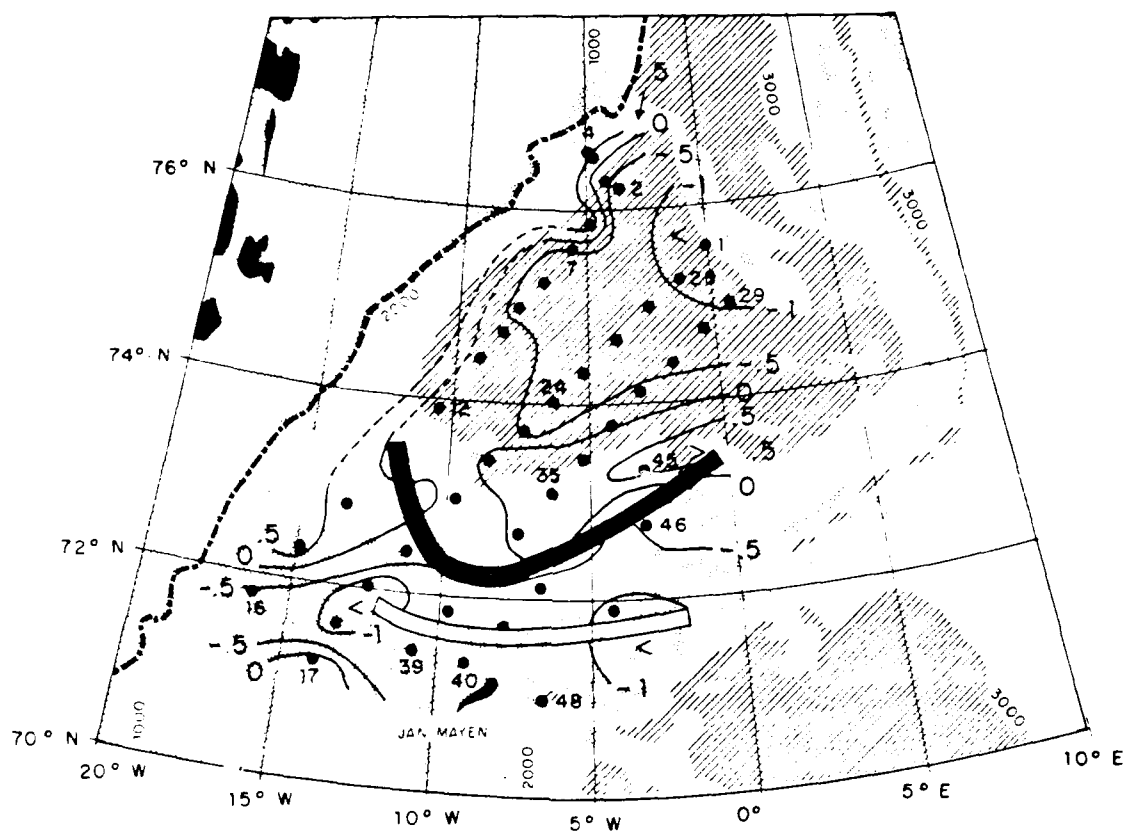


Figure 3.14 BARTLETT 89 subsurface temperature minimum (T_{min}) ($^{\circ}\text{C}$). The orientation of the cold core of the Jan Mayen Current (JMC) is recognized in contours of T_{min} . A separation of up to 100 km exists between the axis of the warm Jan Mayen Atlantic Intermediate Water core of the JMC (solid bar derived from contours of T_{max} in Figure 3.10) and axis of the cold Jan Mayen Polar Water core (open bar). The parent waters are similarly separated by the East Greenland Polar Front in the East Greenland Current. Bars are not intended to indicate the direction of flow. Mean ice edge shown as a heavy dashed line.

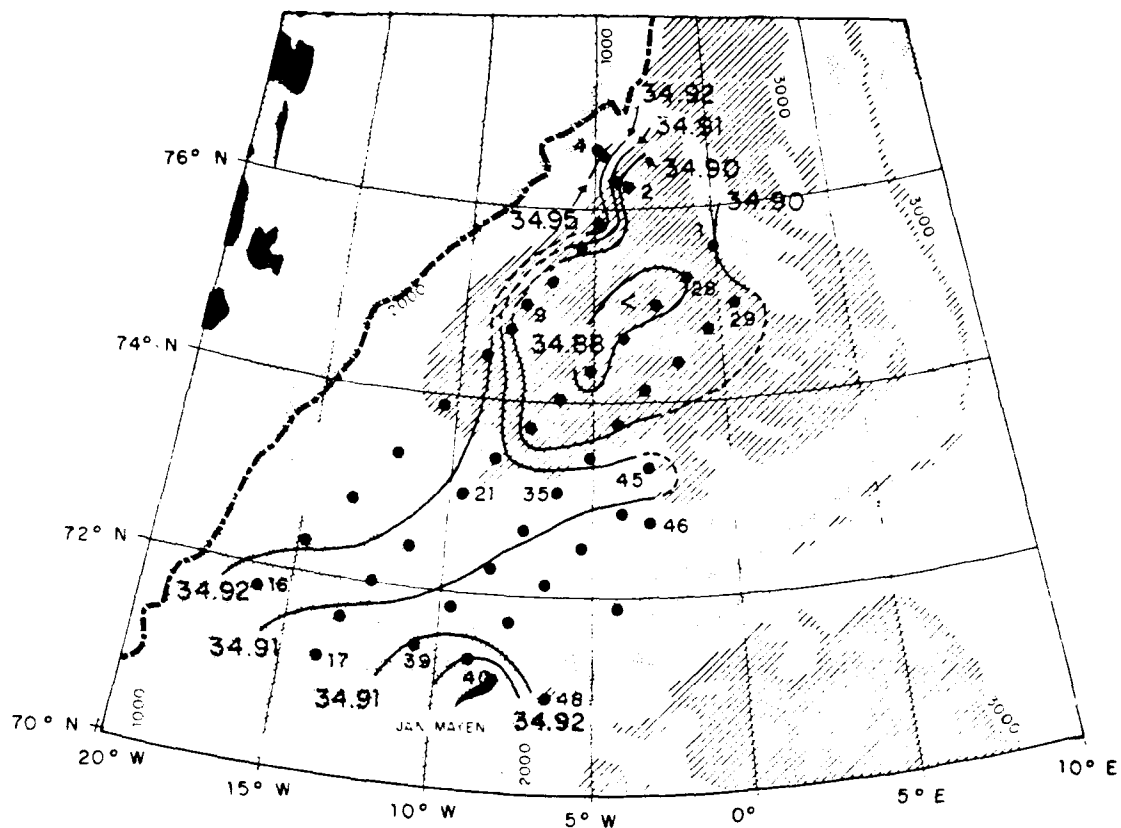


Figure 3.15 BARTLETT 89 intermediate salinity maximum (Smax) (PSU). The Jan Mayen Current is characterized by a salinity maximum which occurs at < 200 m. Smax is slightly less (~0.04 PSU) in the Greenland Sea Gyre and occurs deeper at > 400 m. The pattern of Smax is quite similar to that of Tmax including the perturbation at Station 6. Mean ice edge shown as a heavy dashed line.

the flow of saline NArIW into the Greenland Basin via a branch of the NAC from south and east of Jan Mayen Island at Stations 39, 40, and 48.

The variation in salinity with depth becomes very small at intermediate depths, thus S_{max} varies over a small range from < 34.88 in the GSG to > 34.92 in the JMC. S_{max} in both the JMC and GSG regions occurs consistently near a mean σ_t of 28.02 kg m^{-3} . Depths of S_{max} range from $> 400 \text{ m}$ in the GSG to $< 200 \text{ m}$ in the JMC.

4. Comparison with Historical Intermediate Water Properties

The sparsity of historical data in the JMC region makes a detailed comparison with the above analysis impractical. A general comparison, however, can be made of properties at 100 m, a depth at which contour plots are commonly available and a depth closely corresponding to the average depth of T_{max} within the JMC. It should be noted that though the METEOR/HUDSON 82 data set is contoured in potential temperature, *in situ* temperatures are comparable at 100 dbar to an accuracy of better than 0.01°C .

The historical data sets share three major features in common with the BARTLETT 89 data (see Figures 3.16-23 following this chapter). First, the sharpest gradients occur in the relatively warm, saline intermediate waters of the EGC. Second, there is a large scale meander of warm, saline RAtIW that extends eastward from the EGC, cooling somewhat with little notable dilution, to supply JMatIW to the JMC. Third, the GSG waters are colder and fresher than those of the JMC. Of particular interest in 1982 is the appearance of a warm, saline meander-like feature $\sim 50 \text{ km}$ in radius collocated with the perturbation at BARTLETT 89 Station 6. The feature appears

as a large warm core eddy in the surface temperature pattern (see Figure 3.6). Though a tenuous conclusion from these limited data, the apparent semi-permanent nature of this feature suggests bathymetric triggering which corroborates the observations of *Gascard et al. (1988)* and *Muench (1989)*.

A quantitative comparison of water properties at 100 m shows that throughout the Greenland Basin temperatures and salinities at 100 m are higher (about 1°C and 0.1 PSU) in summer 1958 than in 1989. In winter 1958 salinities are higher (by about 0.1 PSU) than in winter 1982. Temperatures in the JMC are also higher by about 1°C in winter 1958 than in winter 1982, though in the GSG temperatures are similar. Thus, as mentioned earlier in the comparison of winter surface temperatures, inter-annual changes in atmospheric temperatures do not seem a likely cause of the inter-annual differences observed in temperatures at 100 m depth. Though temperatures were seasonally colder (0.5 to 1°C) in winter 1982 compared to summer 1989, salinities at 100 m depth are quite similar.

The reduced temperatures and salinities noted in the 1982 data sets may be related to a long term and wide spread climatic trend reported by *Dickson et al. (1988)*. They refer to a period of reduced salinities in the upper 500 to 800 m of the water column in the northern North Atlantic from 1968 to 1982. They suggest that this low salinity anomaly results either from a significant increase in sea ice production or an anomalous northerly wind both of which occurred in the mid-1960's and both of which could have caused excessive quantities of fresh water to be transmitted from the Arctic Ocean, through the Nordic Seas, and into the North Atlantic sub-polar gyre. The low

salinity anomaly was traced via a time series of observations from north of Iceland, completely around the North Atlantic sub-polar gyre, and back to the Greenland Sea over the fourteen year period. The reduced salinities in the Greenland Basin in 1982 may be the result of the northerly return of the anomalous waters to this region or the manifestation of a similar but shorter term and less wide spread event. *Lazier (1980)* observed the anomaly described by *Dickson et al. (1988)* to persist for a period of 3 to 4 years at weather ship BRAVO in the Labrador Sea (1967-71). A similar phenomenon occurred between 1910-1920 which corresponds to a period of significantly increased sea ice formation. Additionally, *Jónsson (1989)* reports that large inter-annual fluctuations in wind stress occur and can influence water mass structure in the Nordic Seas.

E. VERTICAL STRUCTURE

Thus far, the signature of the JMC has been recognized in horizontal sections of various properties, specifically at surface and intermediate levels. Before discussing the temperature versus salinity (T-S) characteristics at specific stations, a series of vertical sections of temperature, salinity, and dissolved oxygen provide a vertically continuous picture of the hydrography of the JMC via a network of closely spaced stations. Figure 3.24 shows the orientation of these vertical sections. Transects A, B, C, D, and E were constructed from BARTLETT 89 data so as to maintain orientation normal to the axis of the JMC meander (see Figure 3.14 for axis), whereas Transects F and G take slices parallel to this axis (*i.e.* radially to the JMC meander). These sections were

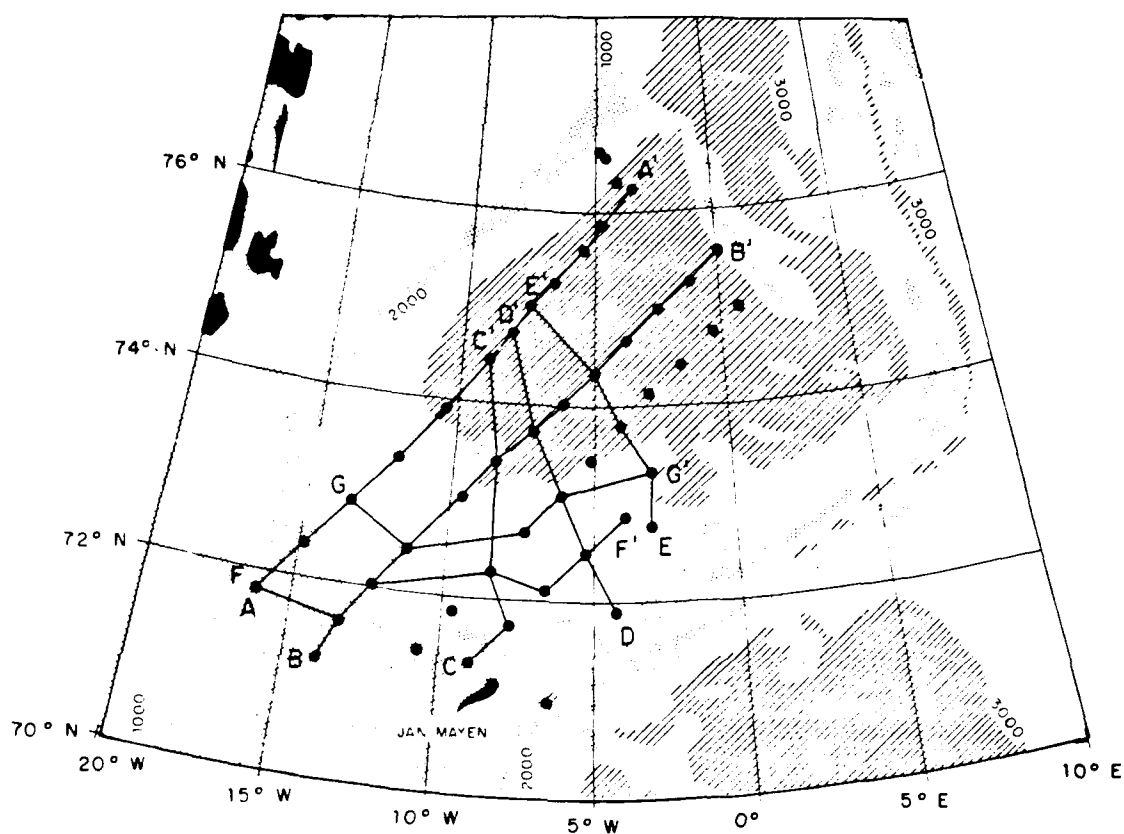


Figure 3.24

Location of BARTLETT 89 Transects A through G. Transects A through E are vertical sections which are oriented normal to the axis of the Jan Mayen Current (JMC) meander. Transects F and G slice the meander parallel to its axis. These two views give a different perspective of the eastward progression of properties and change in vertical structure of the JMC.

initially hand-contoured to verify the accuracy of the computer-contoured versions presented herein. The sections are presented to a depth of 600 m to enable the maximum vertical resolution of upper level features since no significant features occur below this depth.

1. Sections of Temperature and Salinity

Transect A in Figures 3.25 and 3.26 represents the string of stations closest and most nearly parallel to the EGC though still approximately 120 km seaward of the East Greenland Continental Slope. Transect A faces Greenland with the EGC flow right to left and the JMC flow normal to the section. Three basic regimes exist. The first, from Stations 2 to 7, shows the previously mentioned perturbation in the intermediate waters at Station 6. This feature is ~50 km in radius and possesses an RATIW core. The perturbation is not apparent in the surface layers, but is capped by unperturbed ArW. Internally the perturbation causes a depression of the -1°C isotherm to depths below 1000 m.

The second regime, from Stations 7 to 11, involves waters more typical of the GSG. An upward bowing of the -1°C isotherm and essentially a downward bowing of the 34.9 isohaline under the seasonal surface gradient show a very weakly stratified water column, expected in the GSG.

The third regime is the JMC from Stations 11 to 16. Between Stations 11 and 12 RATIW turns eastward followed by GPW either on or near the surface between Stations 13 to 16. The RATIW, now termed JMATIW, is contained within one integral core whereas the GPW, which becomes JMPW, is more filamental in nature illustrated

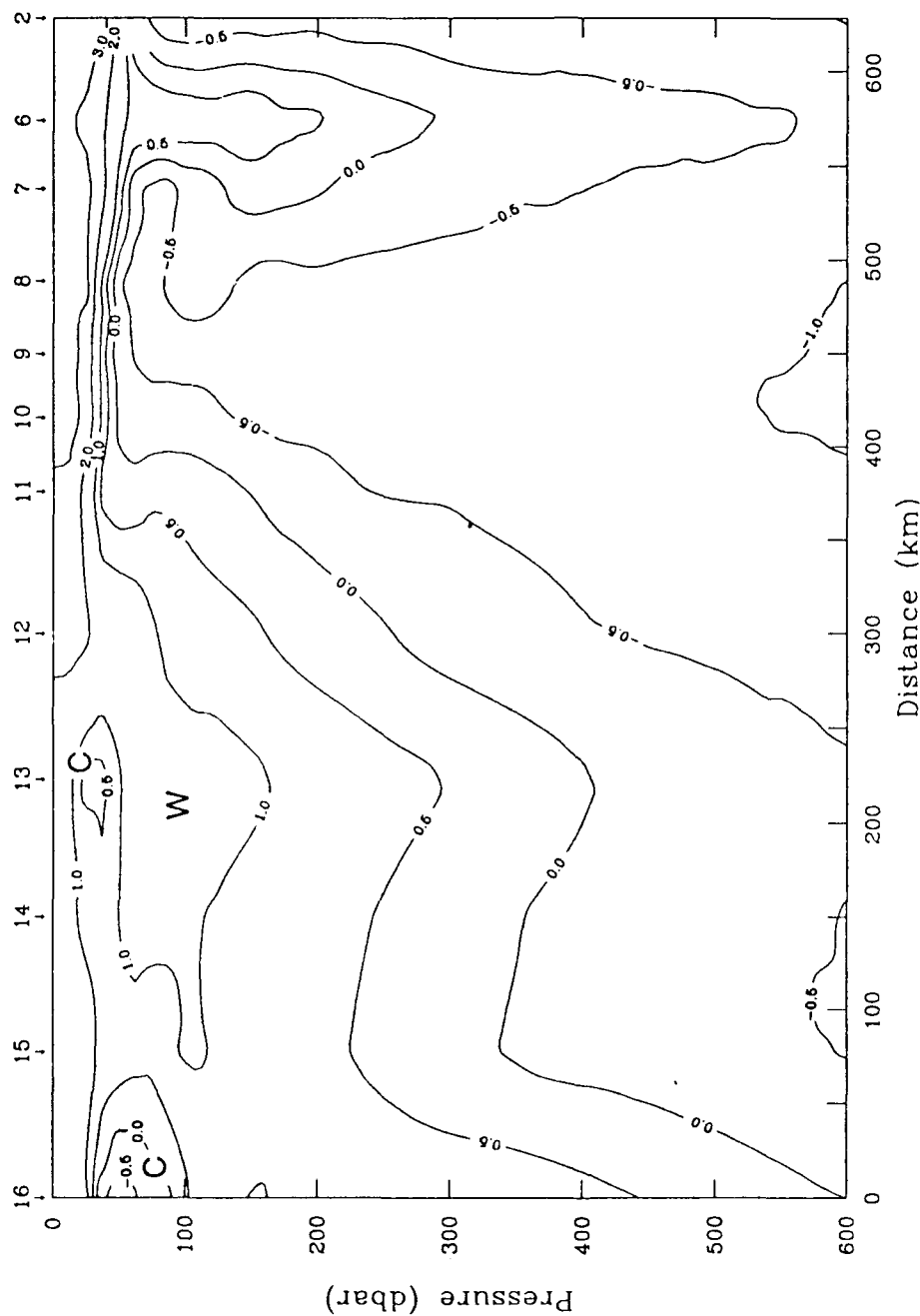


Figure 3.25 BARTLETT 89 temperature Transect A (600 m) (°C). This vertical section of temperature located about 120 km seaward of the continental slope represents the survey leg closest and most nearly parallel to the east Greenland continental slope. The Jan Mayen Current meander (flow in/out of the diagram) from Stations 11 to 16 is manifested in a depression of isotherms centered in the warm core (denoted by a "W") at Station 13 and cold core filaments (each denoted by a "C") between Stations 13 and 16. The less stratified water column between Stations 8 and 10 is characteristic of the Greenland Sea Gyre. The perturbation at Station 6 is seen as a depression of isotherms to depths below 600 m.

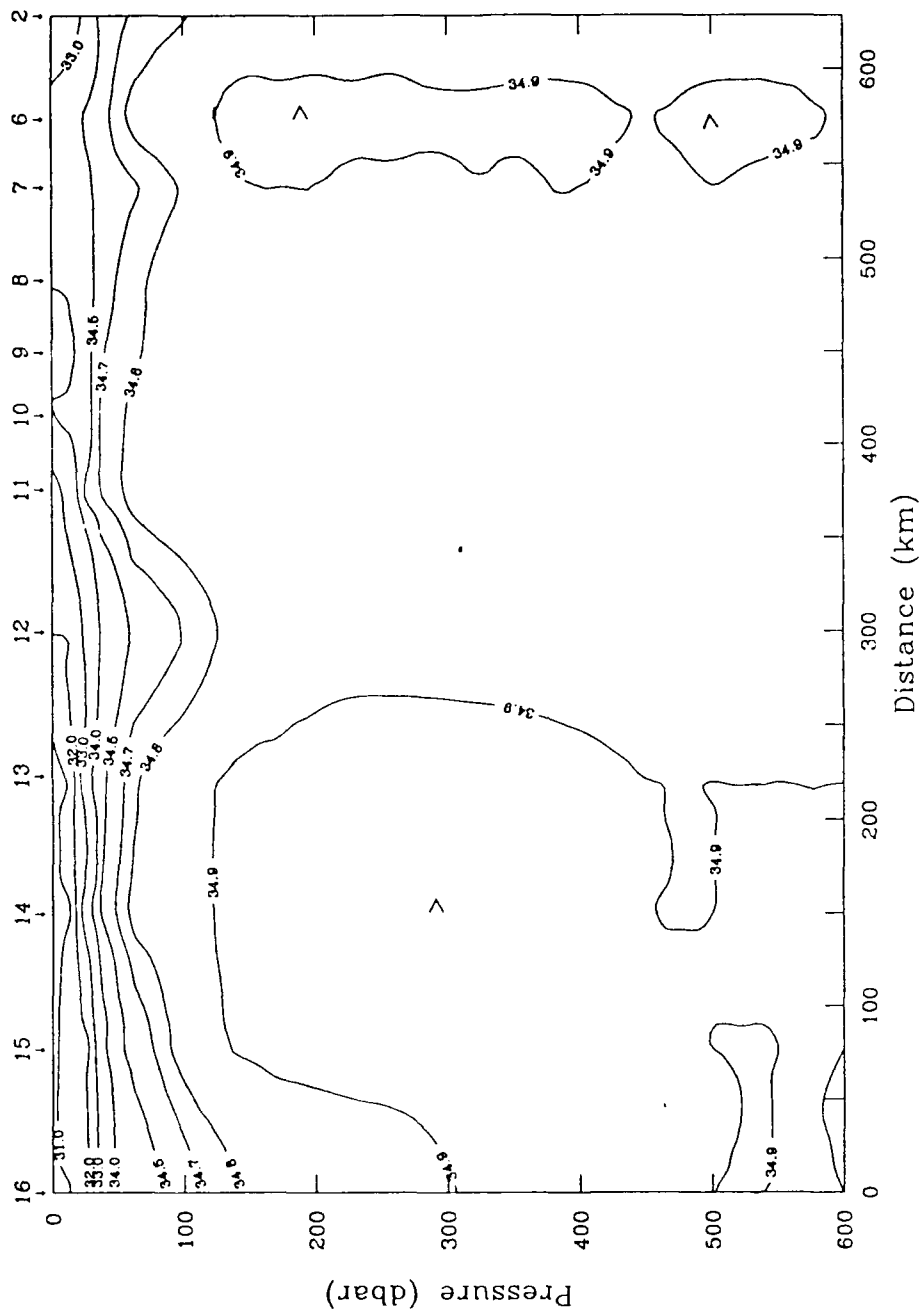


Figure 3.26 BARTLETT 89 salinity Transect A (600 m) (PSU). This vertical section of salinity illustrates the association of the Jan Mayen Current and the perturbation at Station 6 with an intermediate salinity maximum. The waters of the Greenland Sea Gyre between Stations 8 and 12 show less stratification except for the surface gradient.

by individual cells at Stations 13 and 16. Temperatures in the warm JMA₁IW core exceed 1°C with salinities in excess of 34.8. Temperatures in the main filament of JMPW at Station 16 are less than -0.5°C with salinities less than 34.5. The warm and cold cores of the JMC (hereafter denoted by "W" and "C", respectively) are contained within the upper 150 m of the water column, though the presence of JMA₁IW causes a depression of isotherms in the water column below, even to depths exceeding 1000 m. An intermediate salinity maximum (> 34.9) occurs just below the main cores of both JMA₁IW and RA₁IW.

Transect B in Figures 3.27 and 3.28, located about 100 km seaward of Transect A, shows an eastward continuation of the partitioning of properties observed in Transect A. The warm and cold cores of the JMC become more well defined in contours of temperature. The cold core has coalesced into one filament with the innermost waters now colder than -1°C, though its thermal center remains displaced southward of and stepped up from the warm core. Salinities within the cold core remain less than 34.5, while a salinity maximum (> 34.9) persists beneath the warm core. North (to the right) of Station 23 in Transect B the water mass structure is typical of the GSG with moderately stratified GAR₁SW extending from the surface to about 50 m followed by very cold and weakly stratified GAR₁IW through the remainder of the water column. The significant variation in vertical structure between the JMC and GSG reveals two frontal boundaries, one between the surface waters and one between the intermediate waters of the two areas. The fronts are fairly shallow in depth and slope and are manifested in a weak horizontal salinity gradient at the surface and a more pronounced horizontal

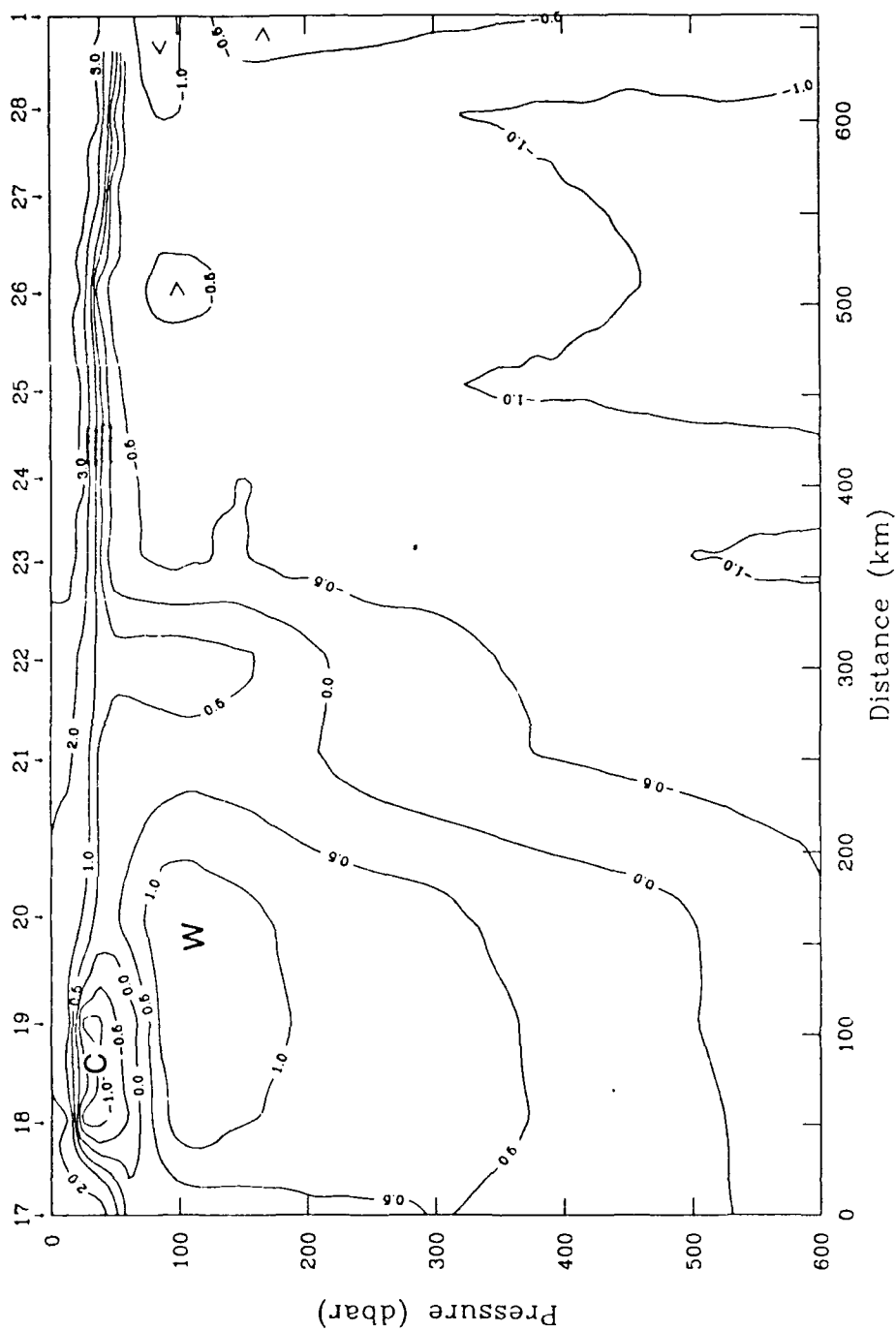


Figure 3.27 BARLETT 89 temperature Transect B (600 m). This section, located about 100 km seaward of Transect A shows an eastward continuation of the water mass partitioning observed in Transect A. The warm, Jan Mayen Atlantic Intermediate Water core and cold, Jan Mayen Polar Water core are both more well defined in contours of temperature. A horizontal temperature gradient in the intermediate waters forms a mild frontal feature between Stations 21 and 24.

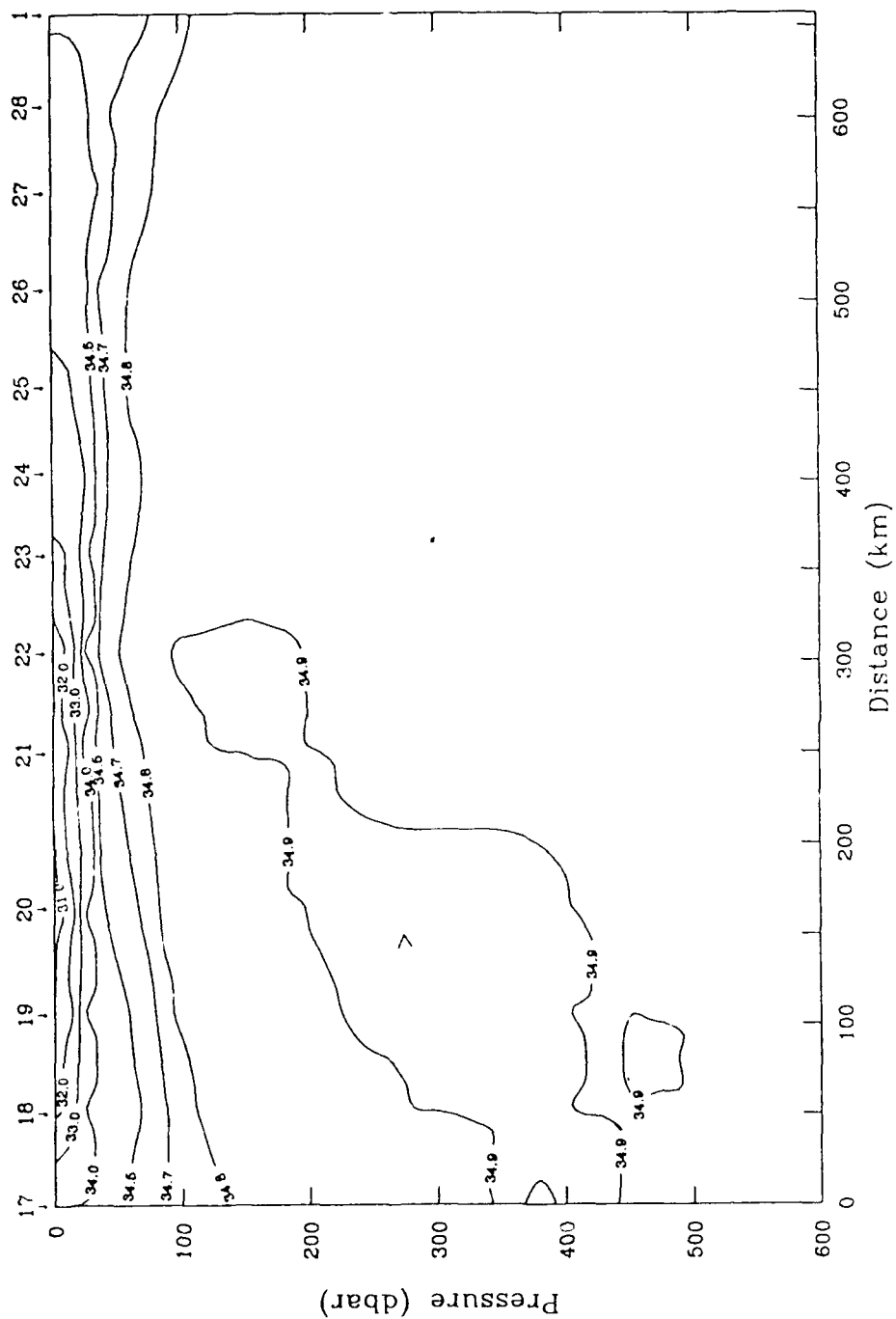


Figure 3.28 BARLETT 89 salinity Transect B (600 m) (PSU). A weak frontal feature exists between Stations 21 and 24 mainly as a horizontal salinity gradient between '1' surface GPW of the Jan Mayen Current and the GArSW of the Greenland Sea Gyre.

temperature gradient in the intermediate waters. In Transect A across Stations 10 to 12 (about 125 km) or in Transect B across Stations 20 to 23 (about 200 km) the salinity changes by up to 2 PSU in the upper 25 m while the temperature change is up to 1.5°C in the layer from 50 to 400 m.

The fronts progressively weaken in subsequent Transects C through E (see Figures 3.29-34 following this chapter). Transects C through E, in keeping orientation normal to the axis of the JMC meander, become increasingly less parallel to the East Greenland Continental Slope (sections are oriented southeast to northwest). In Transect C the presence of NArIW from the NAC is noted at Station 40 by an additional cell of warm intermediate water, also with an underlying salinity maximum. In Transect D an infusion of warmer, more saline NAtSW, from the NAC, occurs at Station 47. The warm core of the JMC is still detectible in Transect E at a great circle distance of approximately 500 km from Transect A. Transects F and G are oriented radially to the meander of the JMC (see Figures 3.35-38 following this chapter). Transect F is located along the southern fringe of the JMC and bisects the cold core of the JMC. Transect G, located about 50 km farther to the north, though still south of the GSG, bisects the warm core of the JMC.

2. Vertical Sections of Dissolved Oxygen

Vertical sections of dissolved oxygen are included to demonstrate a relationship to temperature. Transects A through G present contour patterns which generally mirror their respective temperature sections (see Figures 3.39-45 following this chapter). Subsurface dissolved oxygen concentrations range from < 7.1 ml/l in the

JMAI_W and RA_W warm cores to > 8.0 ml/l in the JMP_W cold core. Concentrations in the GSG average about 7.4 ml/l. At the surface concentrations vary from > 8.0 ml/l in areas of cold GPW to < 7.1 ml/l in areas of warm NA_{SW} influence from the NAC (*e.g.*, Station 47). The observed range of dissolved oxygen concentrations in the BARTLETT 89 data set is quite narrow; similarly the range of percent saturation values (not shown). Such variation as does appear is inversely correlated with temperature and probably is due to the effect of temperature on the solubility of oxygen in the source waters rather than the age of the water as the intermediate waters of the Greenland Basin are probably annually refreshed by both advection of recent surface waters and winter convection of surface waters.

3. Comparison with Historical Sections

Summer Transects 12 and 14 of JOHAN HJORT/POLJARNIK 58 data located on Figure 3.46 are nearly collocated with BARTLETT 89 Transects A and B though station spacing is considerably wider (> 100 km versus < 50 km). The down-bowing of isotherms combined with an intermediate salinity maximum at Stations 679 and 683 locate the core of the JMC (see Figures 3.47-50 following this chapter). Likewise, the doming of isotherms and relatively isohaline conditions at Stations 669, 594, 665, and 598 mark the location of the GSG. GPW and sea ice are lacking in the upper water column. Also, the temperature gradient monotonically decreases with depth showing no closed isotherms of warmer or colder intermediate water parcels as in summer 1989.

METEOR/HUDSON 82 winter Transect 2 located on Figure 3.51 starts just south of Jan Mayen Island and heads northeastward crossing the JMFZ to the east of the

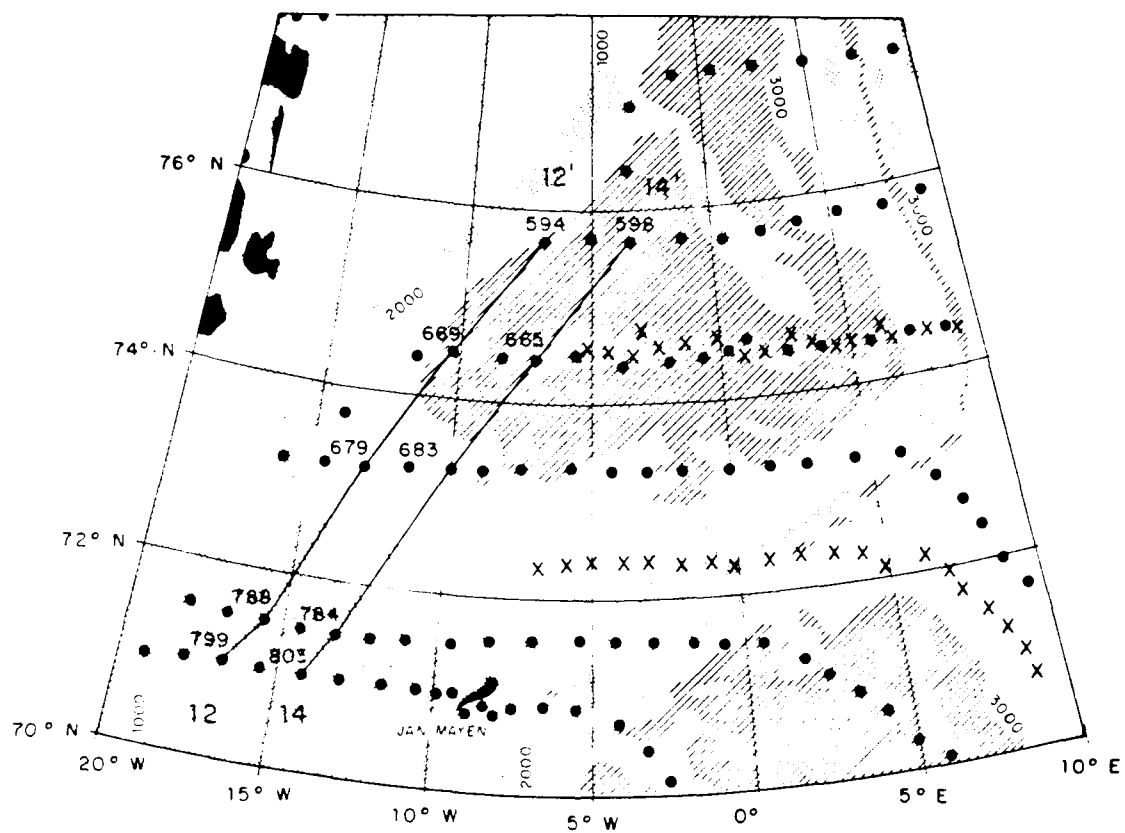


Figure 3.46 Location of JOHAN HJORT 58 summer Transects 12 and 14 (POLJARNIK data not used). These vertical sections are nearly collocated with BARTLETT 89 Transects A and B and are newly compiled from NODC data.

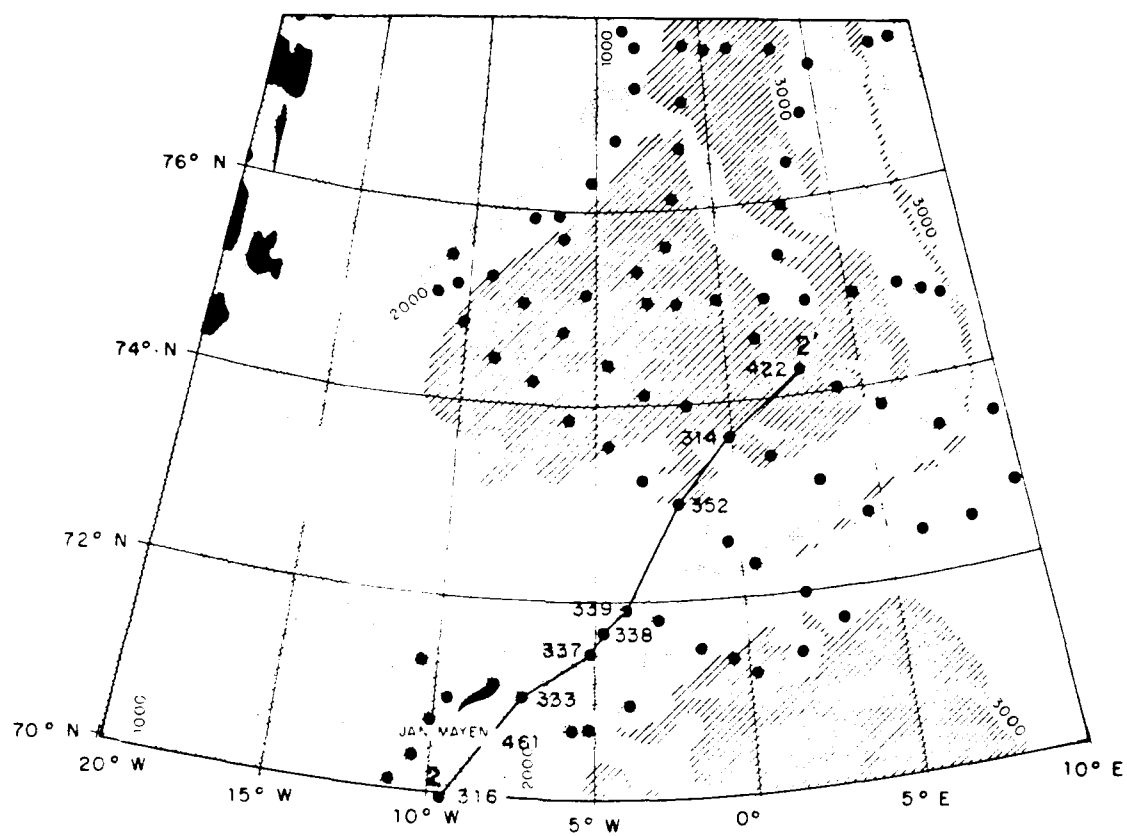


Figure 3.51 Location of METEOR/HUDSON 82 winter Transect 2. This vertical section is best oriented to view the Jan Mayen Current given its position in 1982 (from Koltermann and Lüthje, 1989).

island. The vertical water mass structure in the vicinity of the JMFZ is quite similar to that of the BARTLETT 89 data, though temperatures are markedly colder because the observations were made in wintertime (see Figures 3.52 and 53 following this chapter). The salinity maximum, however, is much deeper in 1982 (> 1000 m) than in 1989. A layer of NAtIW extends northward over the JMFZ from the south and a hint of surface warmth at Station 461 indicates NAtSW influence from the NAC.

Transects 32 and 34 compiled from JOHAN HJORT/POLJARNIK 58 winter data located on Figure 3.54 are nearly collocated with the southern portions of BARTLETT 89 Transects A and B. The arrangements of isotherms and isohalines are quite similar to those of BARTLETT 89 sections including distinct filaments of RAtIW between 100 and 200 m at Stations 343, 350, and 336 (see Figures 3.55-58 following this chapter). Transect 34 shows doming of isotherms toward the GSG at Station 354. Nearly isohaline conditions are predominant at depth with salinities slightly higher under the JMC than in the GSG. Neither salinity nor temperature sections show any evidence of sea ice or presence of GPW. Temperatures and salinities were higher in 1958 than in 1982.

F. T-S ANALYSIS

Plots of temperature versus salinity (T-S) on contours of the density anomaly (σ_t) provide a means for detailed comparison of water mass characteristics and density structure. This discussion begins with a series of figures that show the seasonal and inter-annual progression of properties developed in previous sections. Potential temperatures

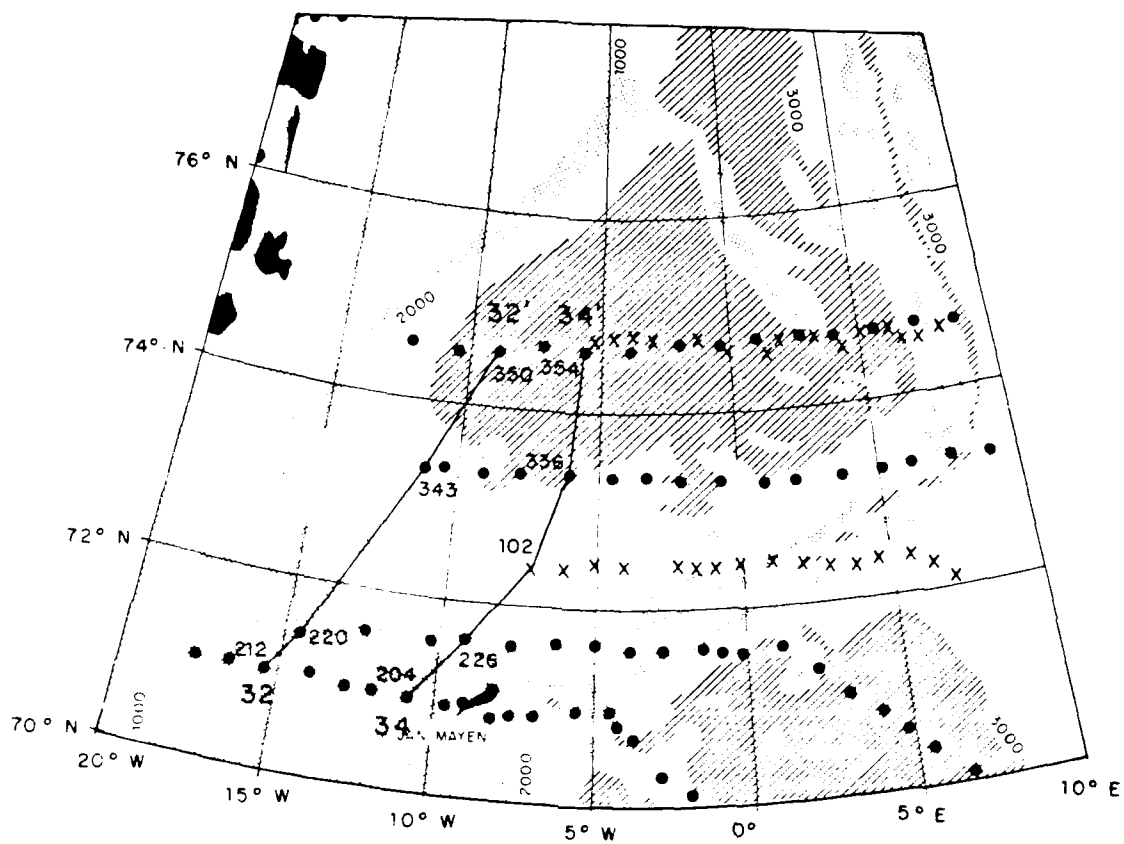


Figure 3.54 Location of JOHAN HJORT/POLJARNIK 58 winter Transects 32 and 34. These vertical sections are intended to be as nearly collocated with BARTLETT 89 sections as possible and are newly compiled from NODC data.

(Θ) and thus σ_θ are used in these plots to enable comparison with METEOR/HUDSON 82 data which is only available in this form. Refer to Table 3.1 and Figure 3.1 in Section B of this chapter for water mass descriptions as needed.

1. Overview of BARTLETT 89 Θ -S Characteristics and Historical Comparison

Figure 3.59 is a Θ -S plot of all BARTLETT 89 stations showing the full range of potential temperatures and salinities observed across the Greenland Basin from the surface to 1000 m depth. Data points (represented as dots) are extracted from the edited CTD record according to a standard decimation schedule. The solid curve represents the typical progression of properties with depth in the GSG. The dashed curves are typical of stations within the JMC and indicate that, unlike the GSG, a variety of profiles may exist depending on the properties of the warm and cold cores at each location *i.e.*, their distance from the origin of the JMC near the EGPF and continental shelf breaks. Each curve leaves the surface through a relatively strong (negative) temperature and (positive) salinity gradient to the first temperature minimum (T_{min}) still located within the surface layer at depths of 25-75 m. T_{min} corresponds to the temperature extreme of either surface ArW or PW depending on the profile. Subsequent to T_{min} the temperature and salinity gradients of both curves are positive until the intermediate temperature maximum (T_{max}) is reached at depths of 100-150 m. T_{max} corresponds to the temperature extreme of either intermediate ArW or AtW depending on the profile. Thereafter, the salinity gradient is minimal and the vertical temperature gradient is dominant.

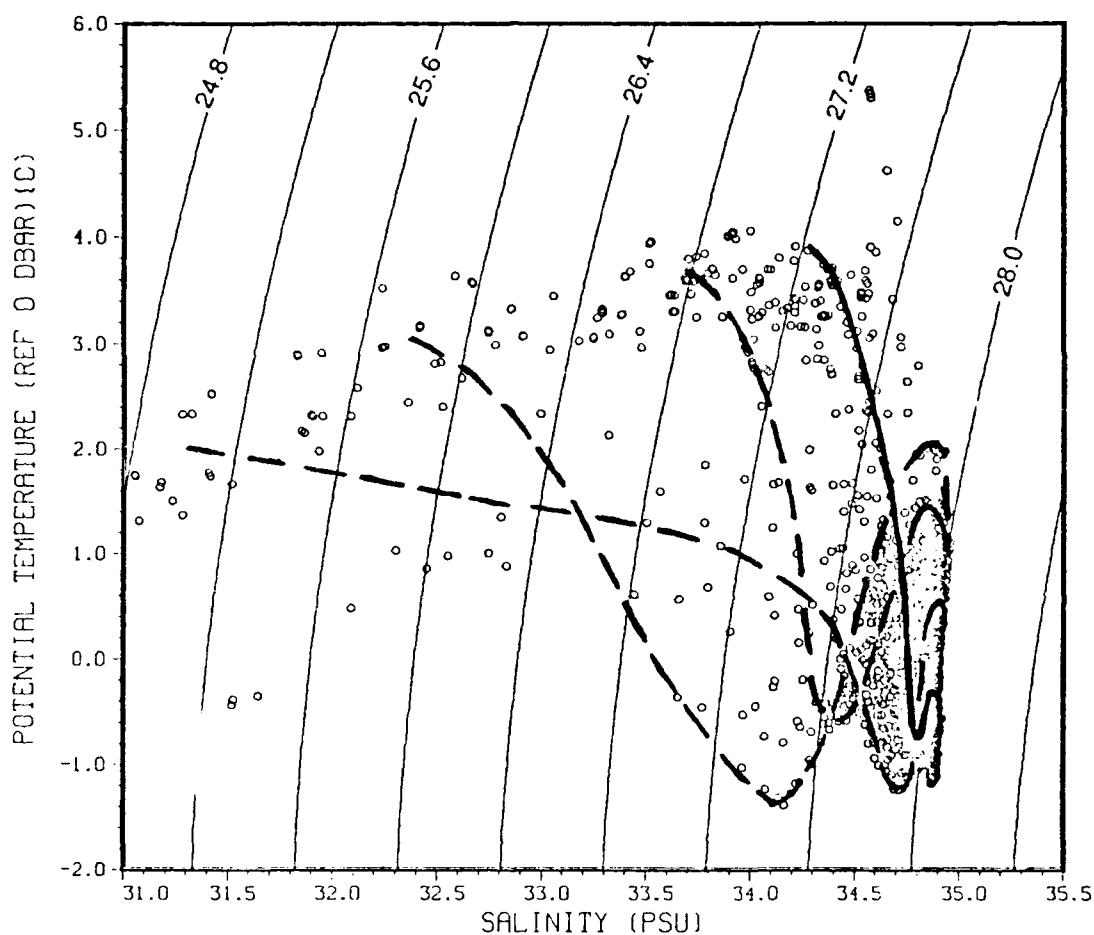


Figure 3.59

Θ -S diagram derived from data at all 48 BARTLETT 89 stations on contours of σ_θ . The solid curve represents a typical station curve in the Greenland Sea Gyre (GSG). The dashed curves are representative of station curves associated with the Jan Mayen Current (JMC) which vary depending on their location with respect to its warm and cold cores. Each curve passes through the surface pycnocline to the subsurface temperature minimum (T_{min}). The water column is considerably less stratified as each curve proceeds to the intermediate temperature maximum (T_{max}). The remainder of the water column is very weakly stratified in salinity. The vertical temperature gradient of the lower water column, however, varies considerably between the JMC and the GSG.

Figure 3.60 is a Θ -S plot of data from METEOR/HUDSON 82 stations predominantly within the Greenland Basin, though a number are located in the Boreas Basin (see Figure 2.2). It is evident from the data point groupings at $-1.8^{\circ}\text{C}/34.1$ and $-1.8^{\circ}\text{C}/34.7$ that despite winter temperatures in 1982 being colder by at least 0.5°C than in 1989, PW and ArW in the surface layer in 1982 possess nearly identical salinities to those in summer 1989. The presence of warm, saline ($> 3^{\circ}\text{C}$ and > 35.0) surface water in 1982 is probably due to stations in the sample being located within the WSC.

Figures 3.61 and 3.62 present Θ -S properties of JOHAN HJORT/POLJARNIK 58 summer and winter data (respectively) acquired at stations located within the area of the BARTLETT 89 survey. Immediately evident is the overall weaker salinity stratification due to a lack of low salinity surface water compared with 1982 and 1989. Also, the NAC/WSC has intruded into the area of the BARTLETT 89 station array, as indicated by the presence of warm water with salinities > 35.0 .

An analysis of the waters at 1000 m depth (figure not shown) concludes that no appreciable difference in temperatures or salinities at this depth occurs among all four data sets. Thus, the low salinity anomaly of the upper water column (*Dickson et al., 1988*) does not appear to have affected the mid-water column.

2. T-S Analysis of BARTLETT 89 data

Figure 3.63a is a T-S plot of a small group of stations selected to represent each water mass while avoiding clutter from excessive data points. Extremely high temperatures and low salinities have also been eliminated to avoid clutter from near-surface data points (< 25 m). Data point groupings denoted by letters "A" through "H"

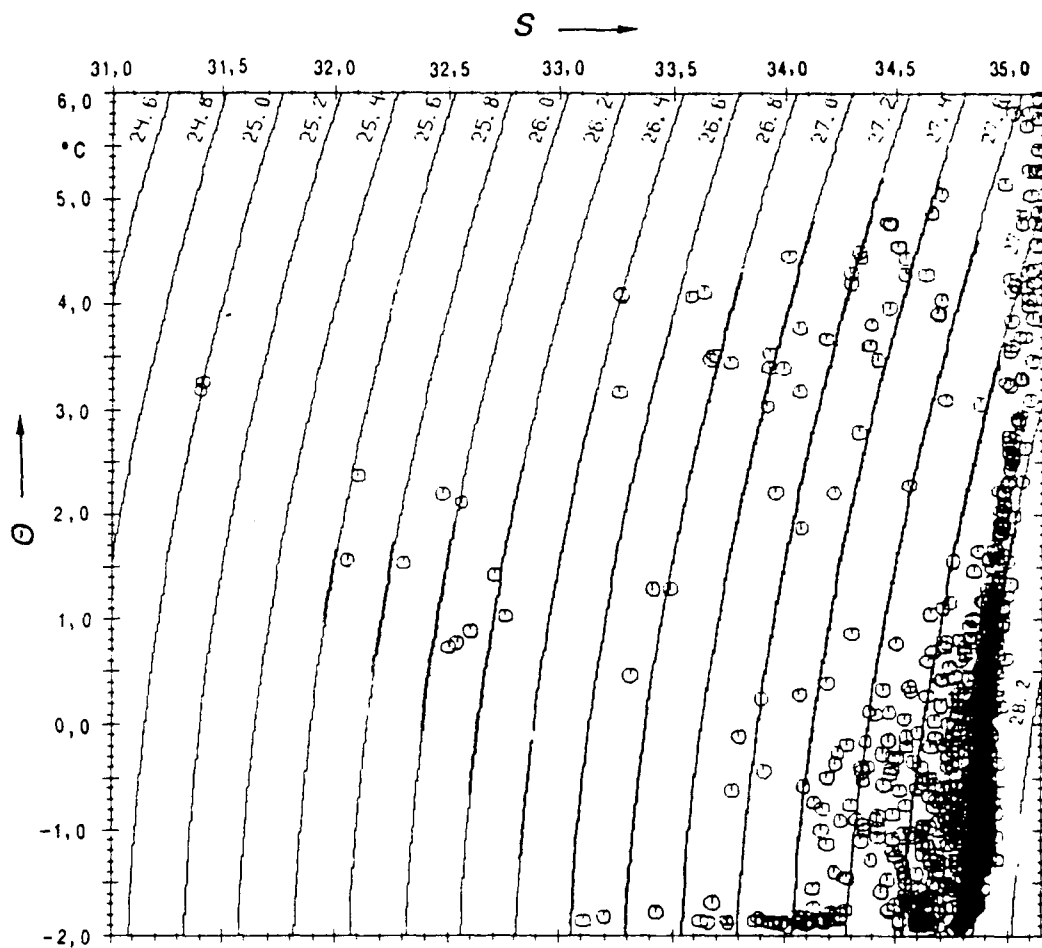


Figure 3.60 Θ -S diagram of METEOR/HUDSON 82 data from stations in the Greenland and Boreas basins on contours of σ_θ . The salinity stratification of the upper water column due to a notable presence of cold, fresh Greenland Polar Water bears resemblance to the BARTLETT 89 diagram. Warm surface waters of salinity > 35 indicate the presence of Norwegian Atlantic Surface Water at stations in the Boreas Basin near the West Spitsbergen Current (from Koltermann and Lühje, 1989).

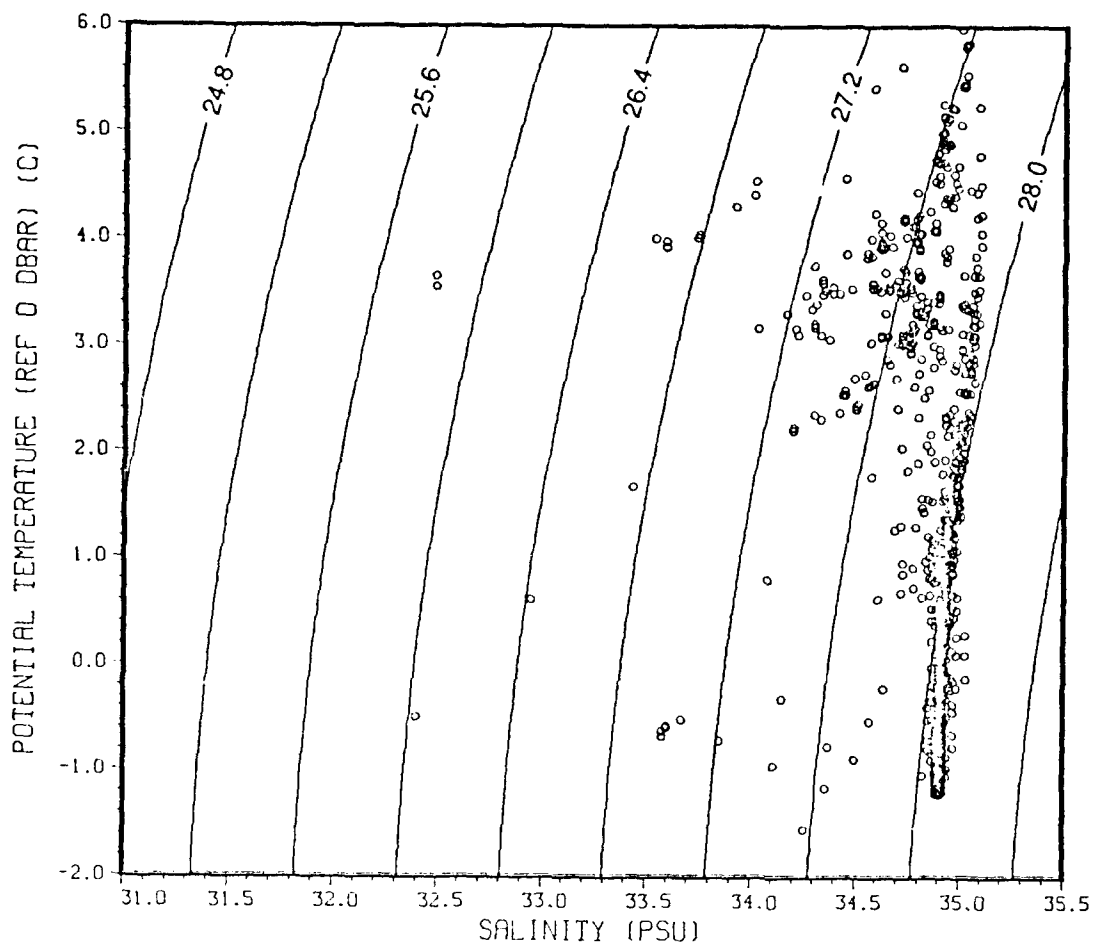


Figure 3.61 Θ -S diagram derived from JOHAN HJORT/POLJARNIK 58 summer data from stations located entirely within the Greenland Basin on contours of σ_t . Very little low-density Greenland Polar Water is present and beneath the surface gradient, the major portion of the water column is very weakly stratified. Warm, saline Norwegian Atlantic Surface Water has intruded into the Greenland Basin from the Norwegian Atlantic and West Spitsbergen currents.

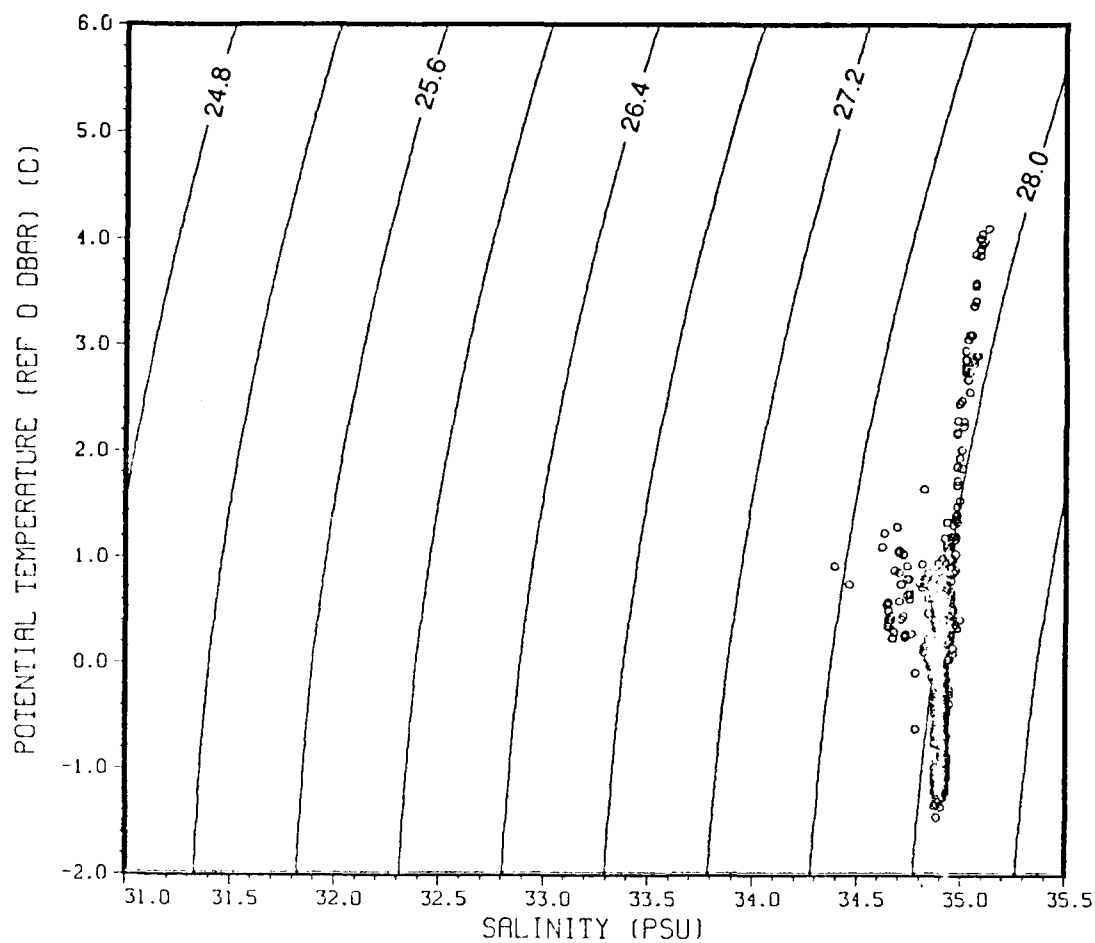


Figure 3.62

Θ -S diagram derived from JOHAN HJORT/POLJARNIK 58 winter data from stations located entirely within the Greenland Basin on contours of σ_θ . The water column is weakly stratified with a near complete absence of Greenland Polar Water as in summer 1958. Norwegian Atlantic Surface Water from the Norwegian Atlantic and West Spitsbergen currents is present in the Greenland Basin.

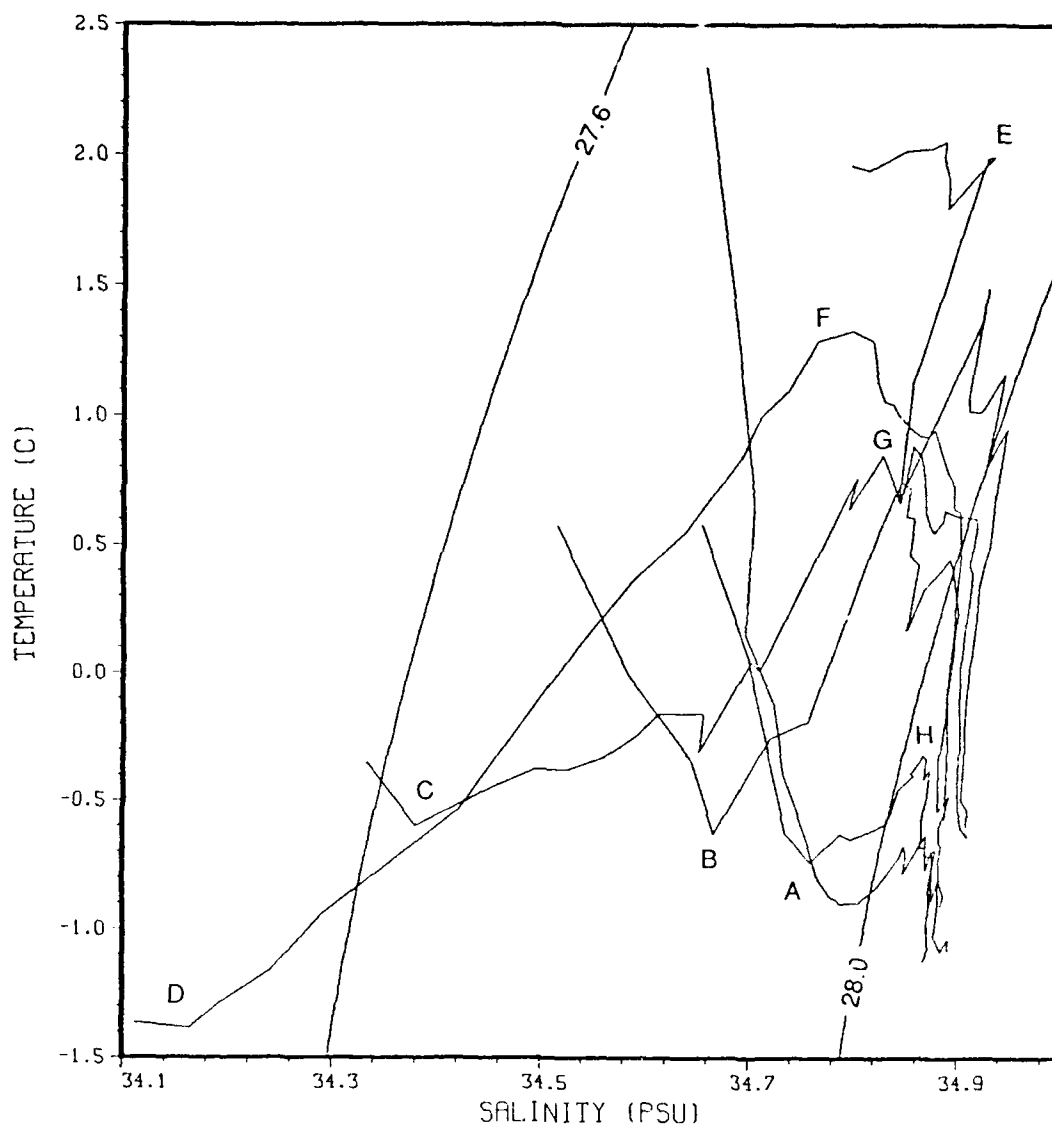


Figure 3.63a T-S diagram of selected BARTLETT 89 stations on contours of σ_t (0-1000 m). These station curves have been selected to represent the gamut of conditions observed in September 1989. Used in conjunction with Figure 3.63b, letters "A" through "H" are associated with the temperature extremes or core waters of water masses in the Greenland Basin.

correspond to observed temperature extremes or core waters within each water mass. The temperature and salinity limits of water masses described in Section B of this chapter are shown in companion Figure 3.63b with the exception of NAtSW which is too saline to appear.

Beginning with the surface waters of the GSG, A shows the core properties of the GArSW layer (properties at T_{min}). Between the surface and T_{min} at A the salinity gradient is weak and a strong seasonal temperature gradient predominates represented by a $\Delta\sigma_t$ of about 0.8 kg m^{-3} (see Figure 3.59). In contrast, the surface gradient of the JMC leading to T_{min} at B, C, and D is due to both temperature and salinity stratification and represents a $\Delta\sigma_t$ of up to 3.0 kg m^{-3} (see Figure 3.59). Locations B, C, and D represent a different variant of JMPW illustrating the filamental nature of this layer as discussed in previous sections.

The intermediate portion of the water column in the GSG is represented by the T-S properties of GArIW at H. With reference to T_{min} salinity stratification continues to weaken compared with the surface layer and the temperature gradient markedly diminishes. The maximum change in σ_t from A to H is of order 0.1 kg m^{-3} . The intermediate water masses of the JMC again provide sharp contrast to those of the GSG. Locations F and G show the core properties (properties at T_{max}) of JMAtIW. Significant temperature and salinity gradients persist into the intermediate waters as indicated by the paths of T-S curves between JMPW (T_{min} at B, C, and D) and JMAtIW (T_{max} at F and G) where $\Delta\sigma_t$ can be as great as 0.4 kg m^{-3} . Curves passing through E represent

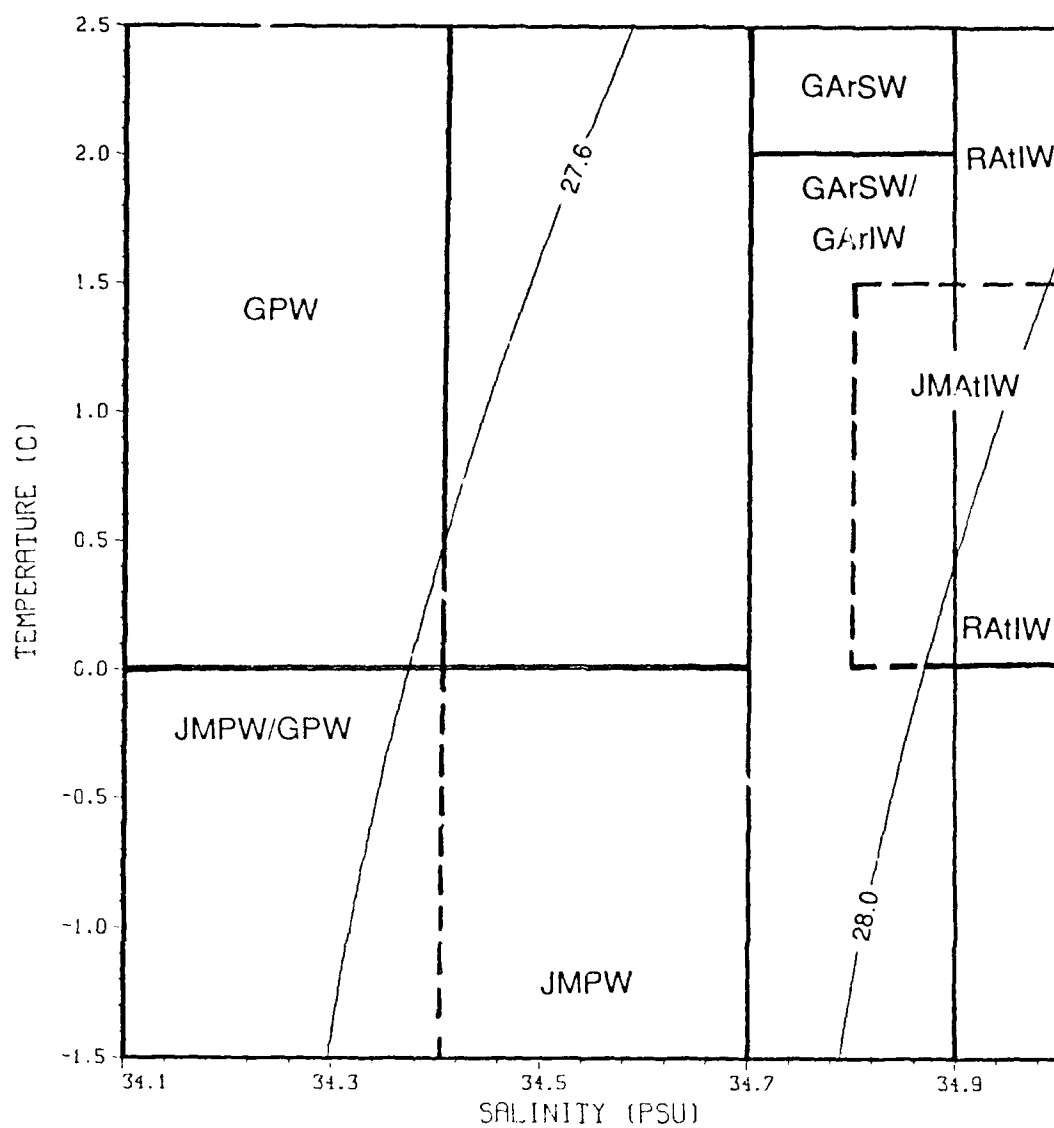


Figure 3.63b T-S diagram with water masses of the Greenland Basin on contours of σ_t . This diagram is for use in conjunction with Figure 3.63a. Refer to Table 3.1 for explanation of water abbreviations.

properties of RAAtIW at stations in the EGC seaward of the EGPF and thus do not show any PW properties at the surface (recall PW is located shelfward of the EGPF).

After passing through E, F, G, and H all T-S curves demonstrate a marked decrease in the vertical salinity gradient. Figure 3.64 is an enlargement of the T-S curves in Figure 3.63a corresponding to properties in the lower 800 m of each station profile. The curves at stations in the JMC are substantially warmer and more saline (by about 0.5°C and 0.1 PSU) compared with those in the GSG. Also, from 200 to 1000 m depth σ_t varies up to 0.6 kg m⁻³ in the JMC compared to 0.3 kg m⁻³ over this depth range in the GSG. The differences in the vertical density gradients between the JMC and the GSG are largely a function of temperature in this depth range.

G. SUMMARY

The JMC presents a signature marked by moderate salinity stratification and strong temperature stratification throughout the upper 1000 m of the water column. This contrasts sharply with the structure of the GSG which is very weakly stratified aside from a thin surface gradient. At the surface, the JMC is recognized by a tongue of GPW which extends eastward from the EGC. PW continues to be associated with the JMC in the subsurface layer, though it appears as filaments of JMPW. The most notable feature of the BARTLETT 89 data set, however, is the eastward protrusion of JMAAtIW, displaced ~100 km northward of the JMPW tongue. The patterns of surface and intermediate properties indicate the JMC may be an anticyclonic meander in the seaward portion of the EGC rather than solely a continuous eastward (cyclonic) flow constituting the

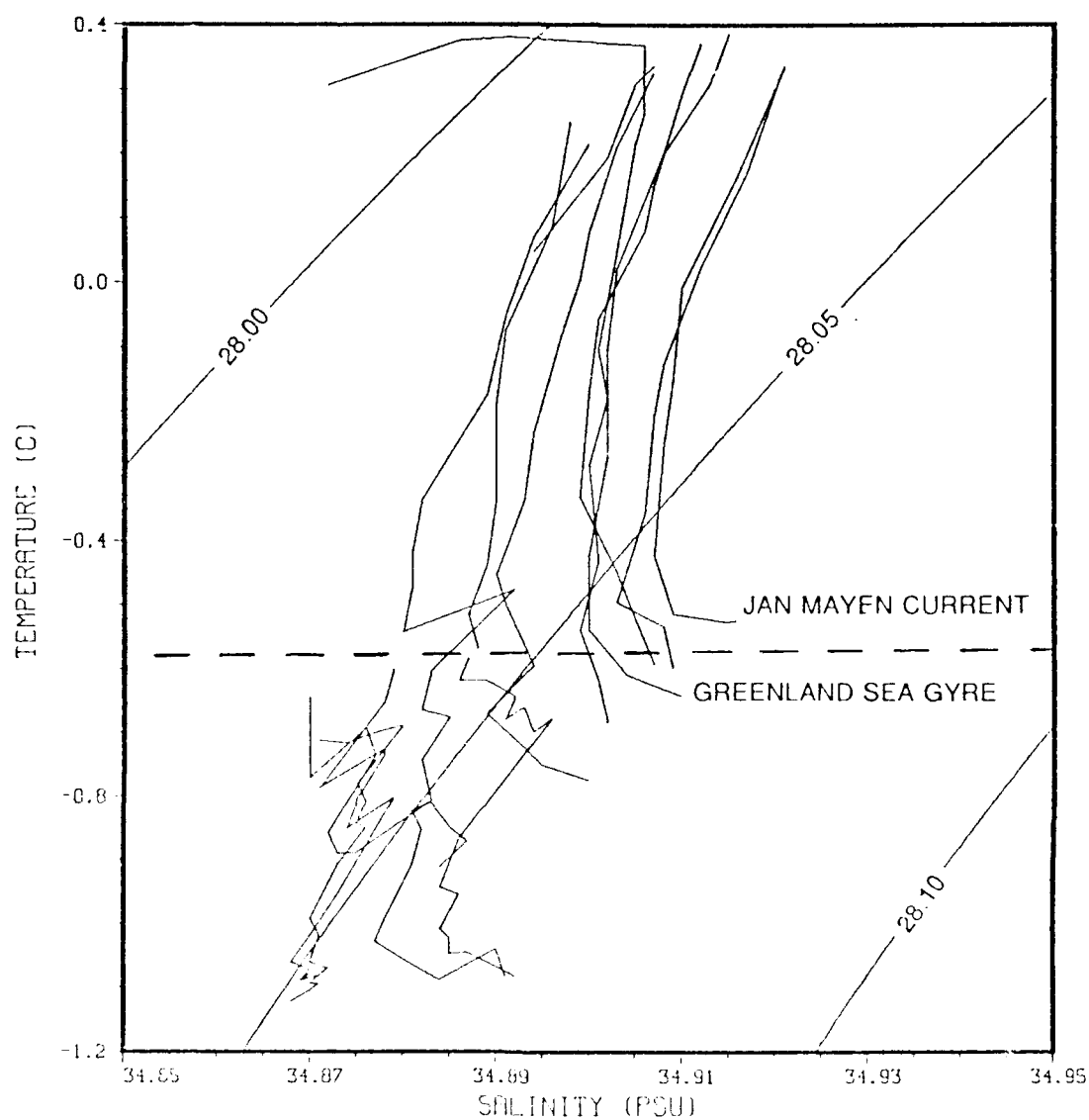


Figure 3.64 T-S diagram of the deeper portions (200-1000 m) of selected BARTLETT 89 station profiles on contours of σ_t . Curves in this depth regime in the Jan Mayen Current (JMC) are substantially warmer and more saline (by -0.5°C and -0.1 PSU) than those in the Greenland Sea Gyre (GSG). In the lower water column differences in the vertical density gradient between the JMC and GSG seem to be due largely to differences in the vertical temperature gradient between these regions.

southern limb of the GSG. These patterns also indicate that flow may be barotropic since all show a correlation to the bathymetry of the JMFZ. Evidence to support these contentions is found in the trajectories of Lagrangian drifters (*Gascard and Richez, 1989*) and the results of a general circulation model by *Legutke (1989)* which appear in the following chapter on circulation.

Clearly evident from a comparison of BARTLETT 89 data with historical data is that the inter-annual variation of properties in the upper water column of the Greenland Basin is at least as pronounced as the seasonal signal. The axis of the JMC meander is not stationary and appears to move $O(100 \text{ km})$ north and south of its 1989 position. Also, there are temperature and salinity variations in the upper water column between the data sets. These fluctuations are likely due to variations in the quantity of GPW available to the Greenland Basin.

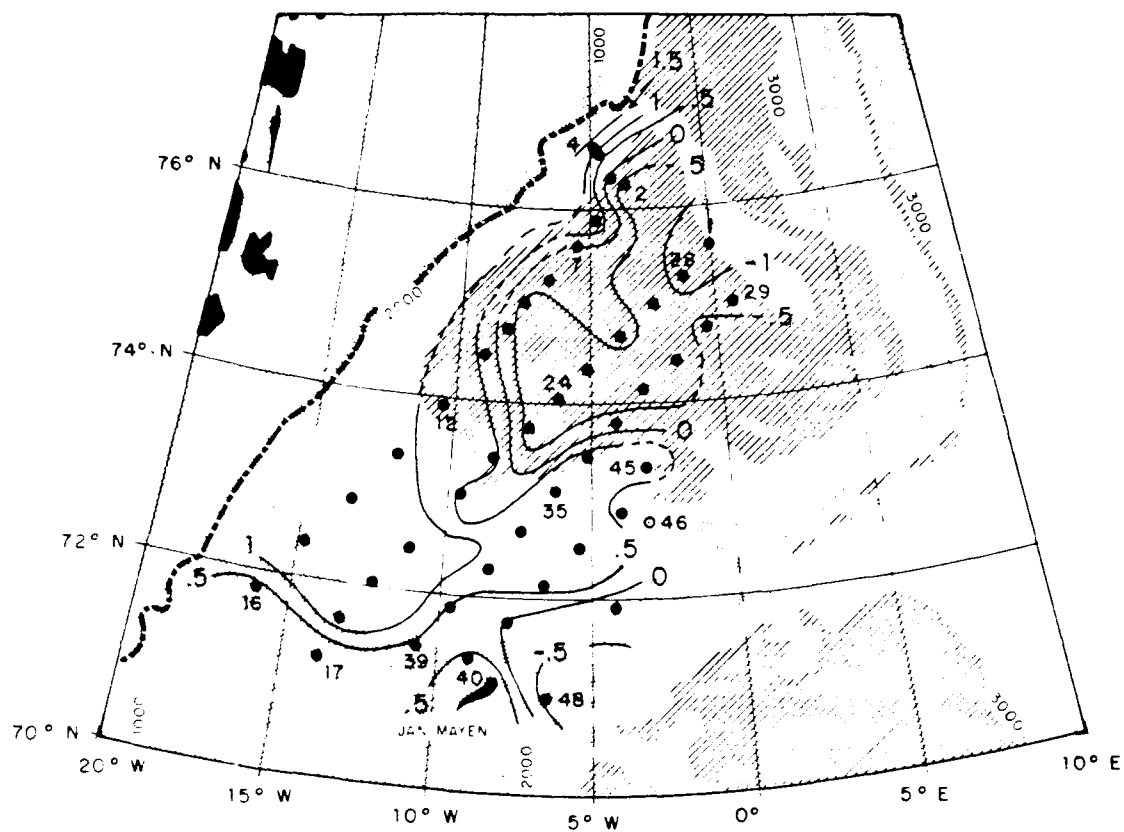


Figure 3.16 BARTLETT 89 100 m temperature (°C). Temperatures at 100 m are used for comparison with the historical data sets. The temperature pattern is quite similar to that of the intermediate temperature minimum. Mean ice edge shown as a heavy dashed line.

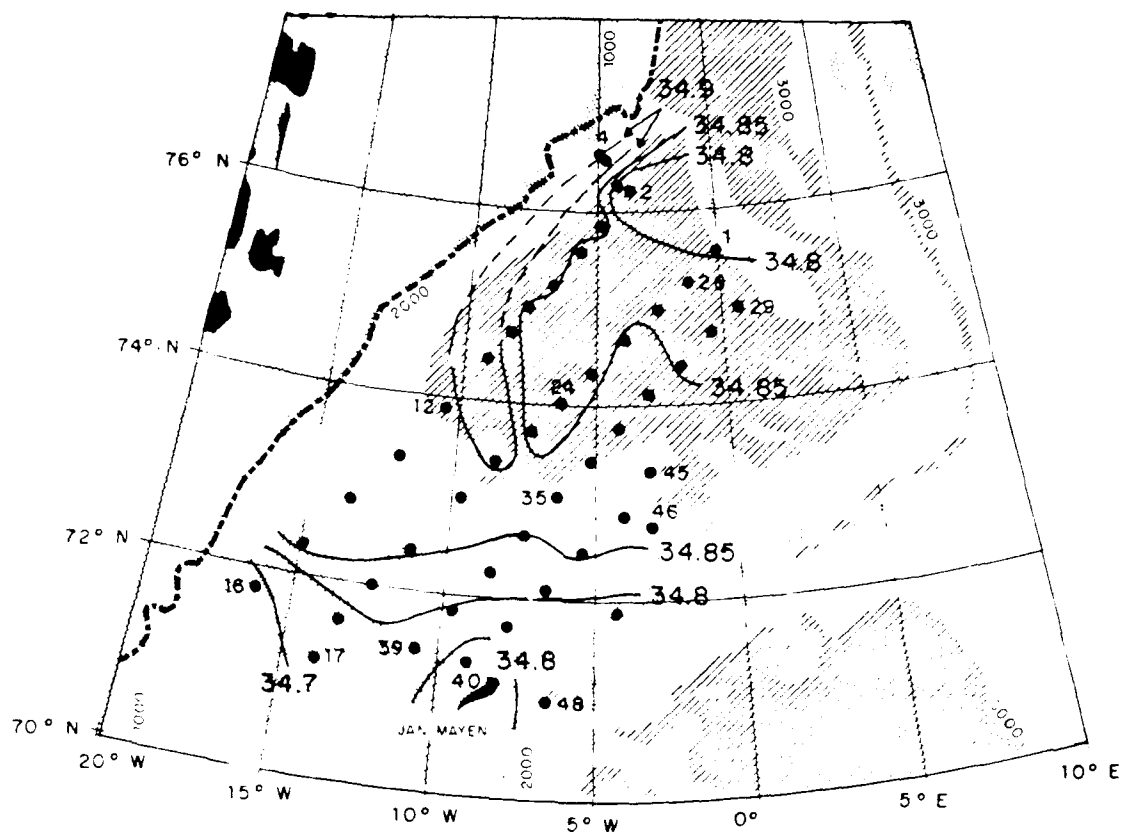


Figure 3.17 BARTLETT 89 100 m salinity (PSU). Salinities are slightly higher at this level in the Jan Mayen Current than in the Greenland Sea Gyre by about 0.05 PSU. The highest salinities are associated with the East Greenland Current. Mean ice edge shown as a heavy dashed line.

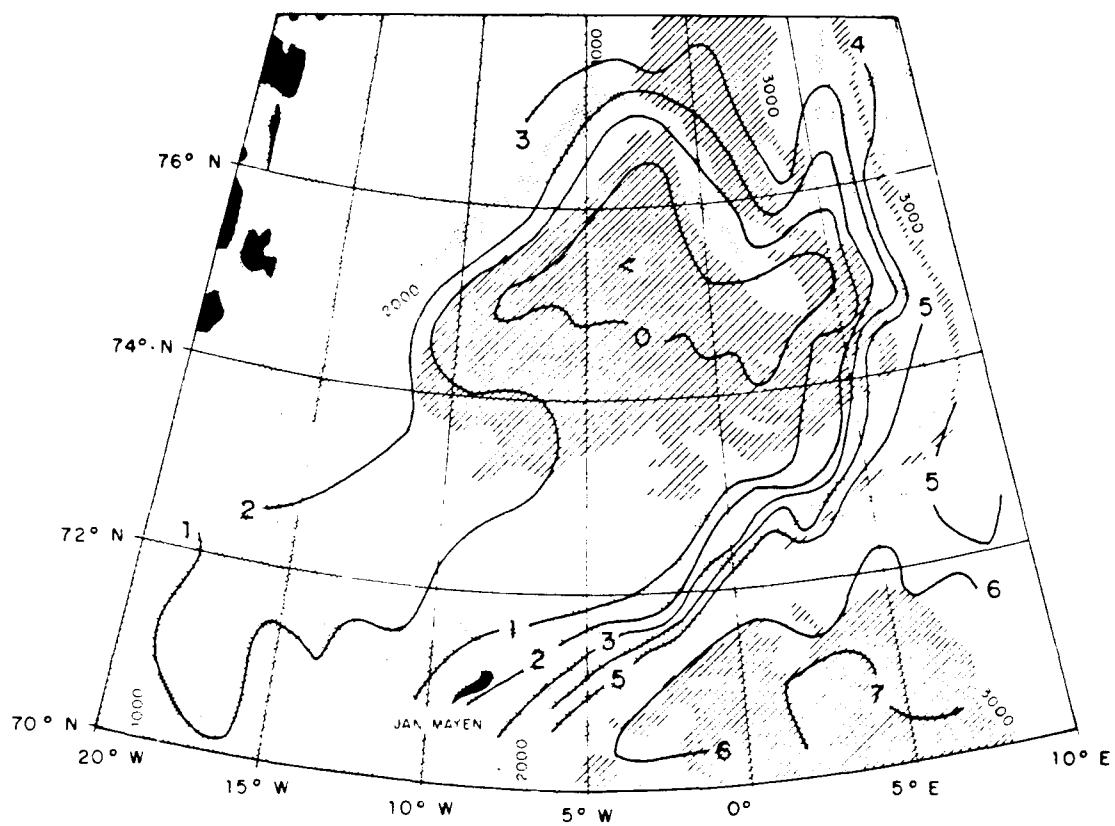


Figure 3.18 JOHAN HJORT/POLJARNIK 58 100 m temperatures in summer ($^{\circ}\text{C}$). The temperature pattern is similar to that in summer 1989, however, actual temperatures are higher by about 1°C (from *Dietrich, 1969*).

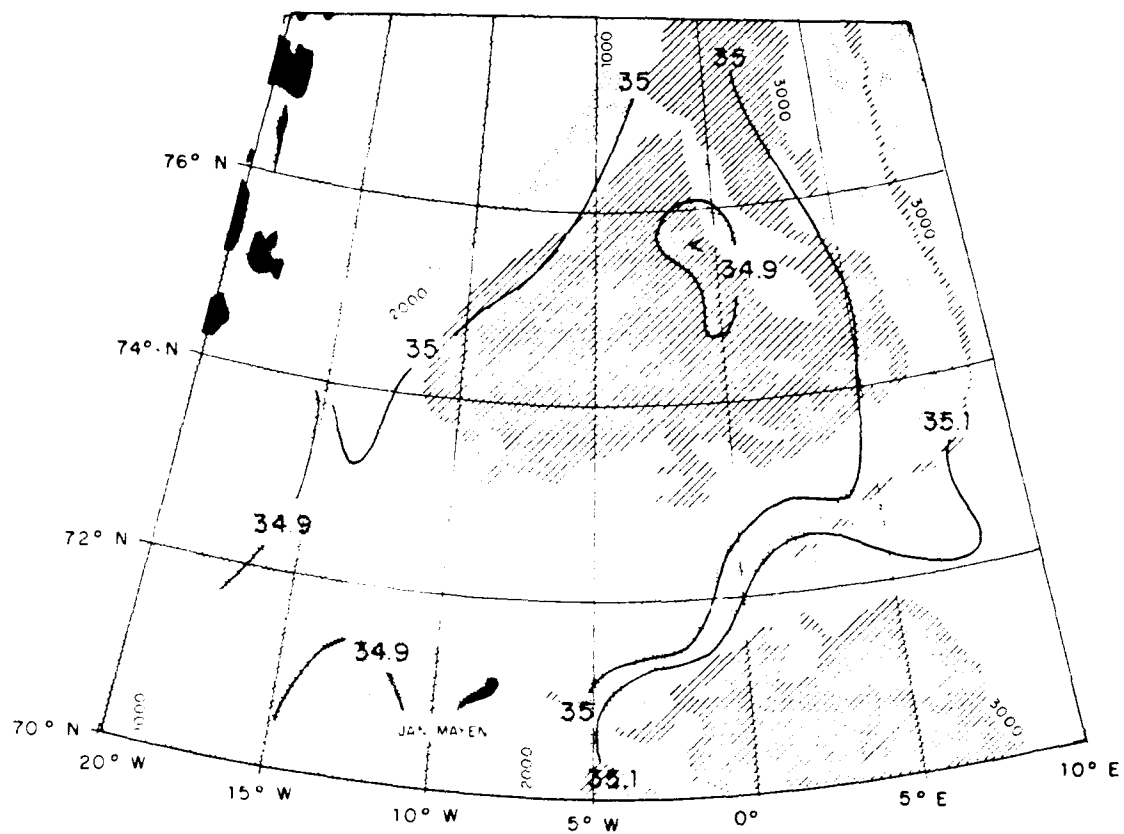


Figure 3.19 JOHAN HJORT/POLJARNIK 58 100 m salinities in summer (PSU). The salinity pattern is similar to that in summer 1989, though actual salinities are higher by about 0.1 PSU. Observed salinities did not reach 35.0 at any depth in 1989 (from *Dietrich, 1969*).

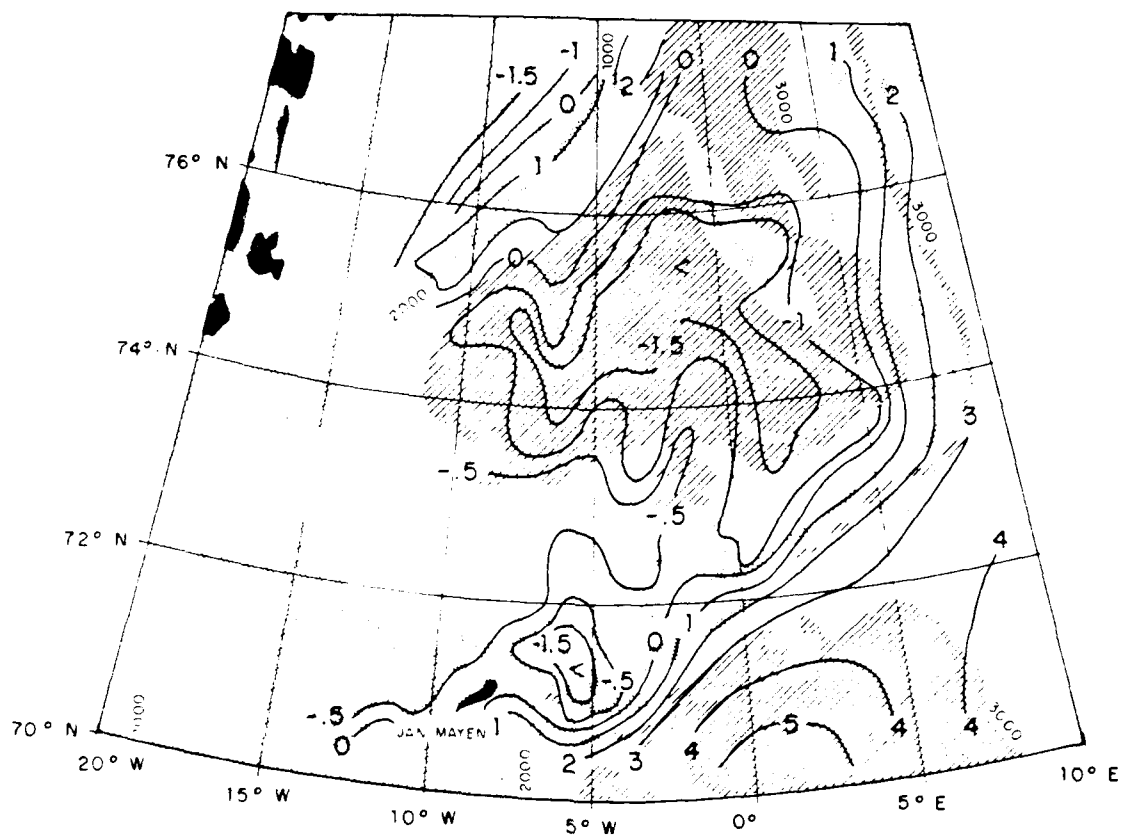


Figure 3.20 METEOR/HUDSON 82 100 m potential temperatures in winter (°C). The 100 m temperature pattern is similar to those of the summer data sets though seasonally colder. A large meander in the isotherms south of the Greenland Fracture Zone corresponds to closed isotherms around a warm water mass in the winter 1982 surface temperature pattern. That this feature is collocated with the smaller perturbation at BARTLETT Station 6 suggests they are bathymetrically triggered (from Koltermann and Lüthje, 1989).

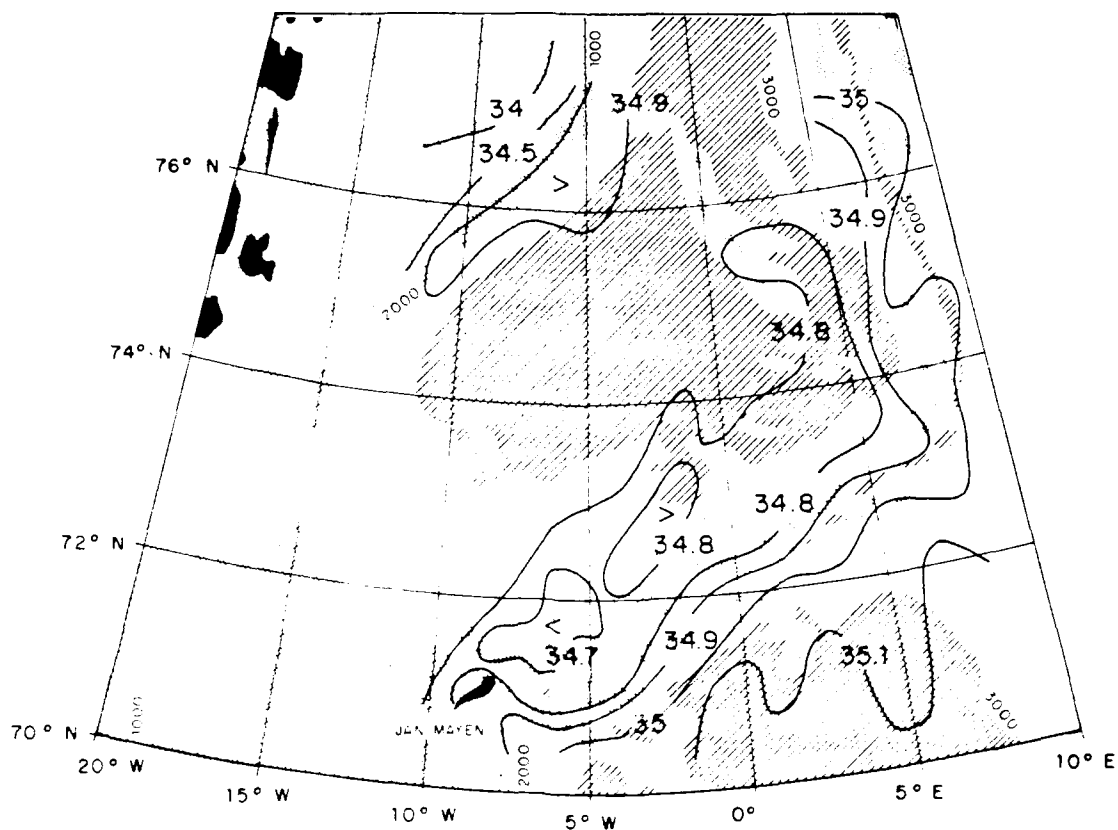


Figure 3.21 METEOR/HUDSON 82 100 m salinity (PSU). The 100 m salinity pattern is quite similar to those of the summer data sets. The actual range of salinities is close to that in summer 1989; likewise salinities are about 0.1 PSU lower than in summer 1958 (from *Koltermann and Lüthje, 1989*).

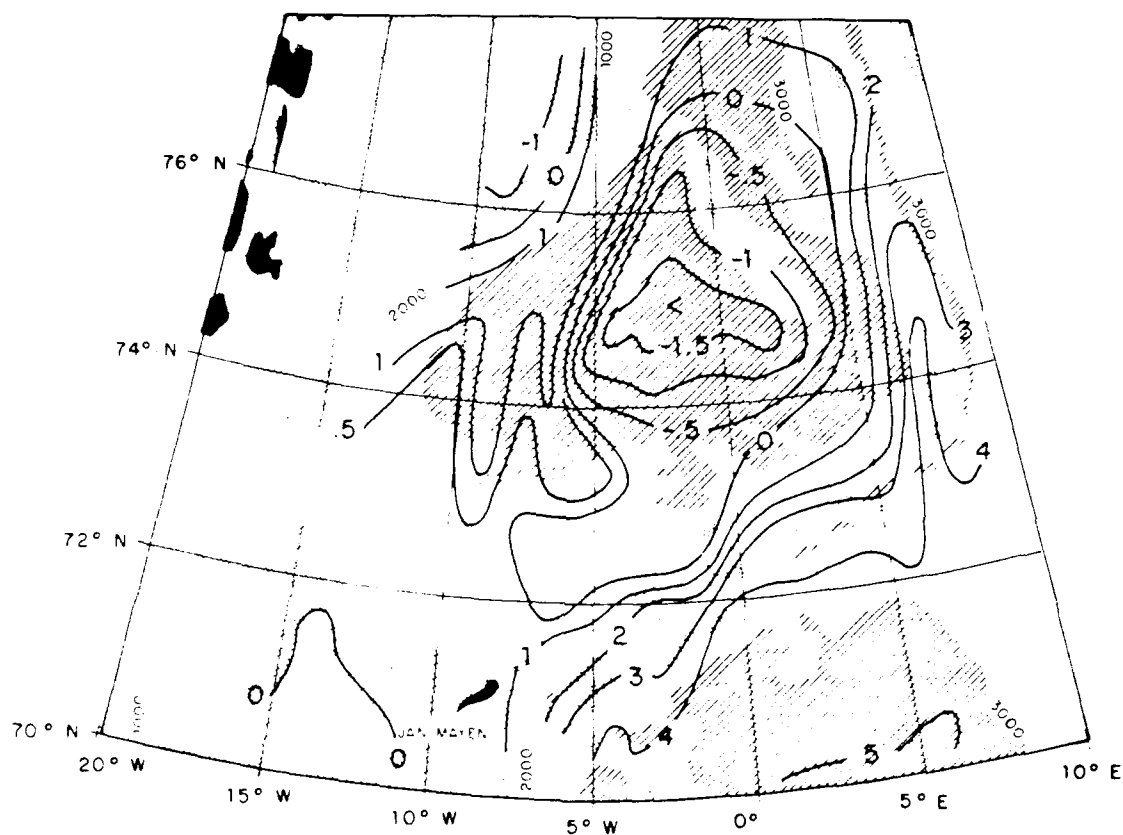


Figure 3.22 JOHAN HJORT/POLJARNIK 58 100 m temperatures in winter ($^{\circ}\text{C}$). Temperatures at 100 m in the Greenland Sea Gyre are similar between the winters of 1958 and 1982, however, in the Jan Mayen Current temperatures are about 1°C warmer in winter 1958 (from *Dietrich, 1969*).

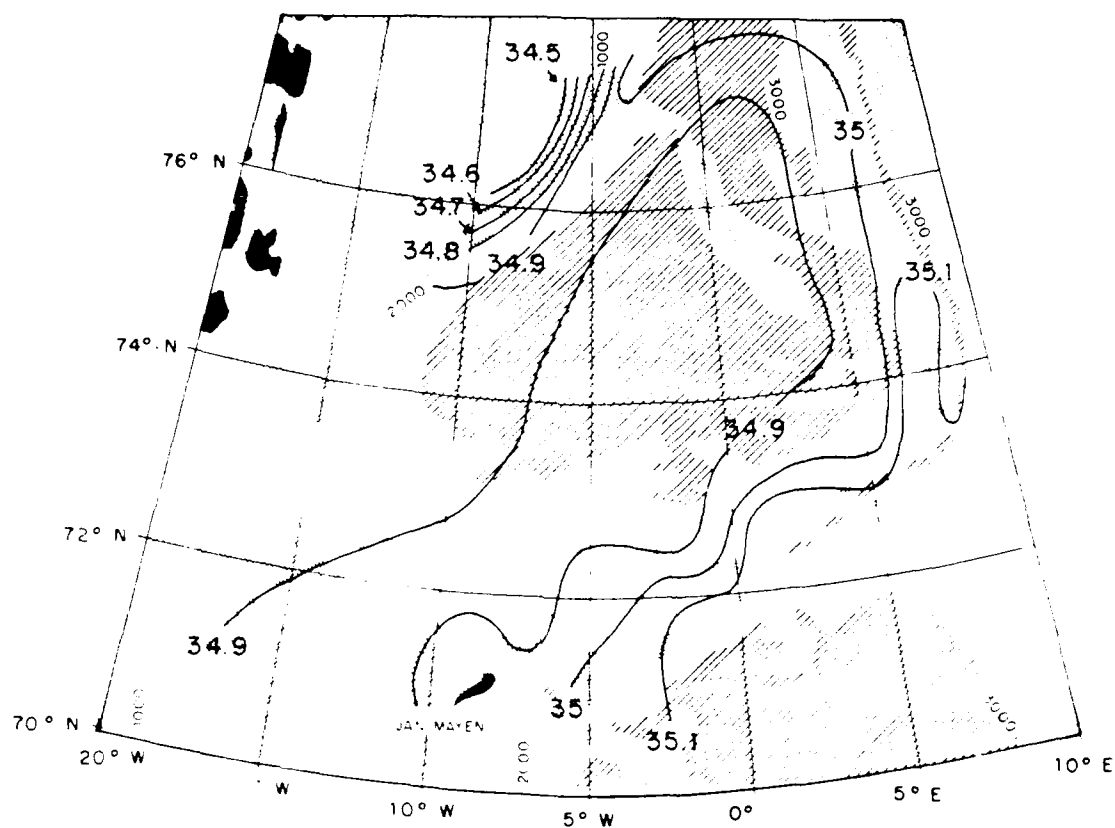


Figure 3.23 JOHAN HJORT/POLJARNIK 58 100 m salinity (PSU). Salinities across the Greenland Basin are up to 0.1 PSU higher in winter 1958 than in either winter 1982 or summer 1989 (from *Dietrich, 1969*).

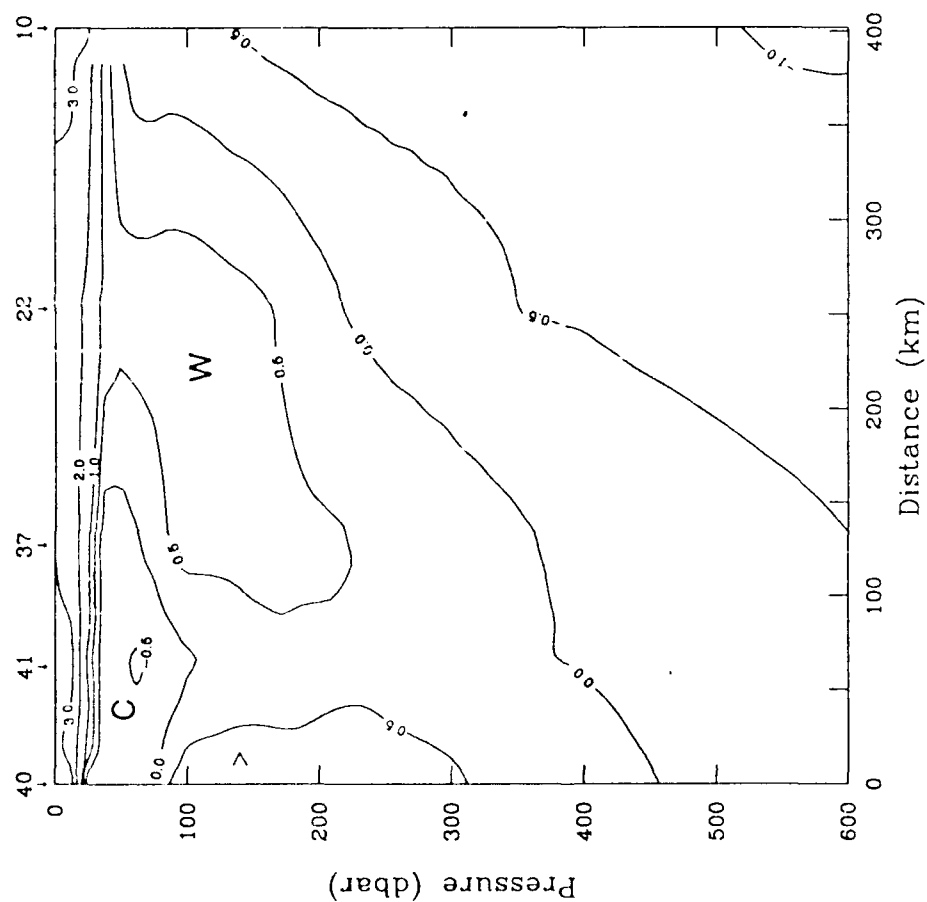


Figure 3.29 BARTLETT 89 temperature Transect C (600 m) (°C). The cold core remains offset southward of the warm core. A second intermediate warm water mass is noted at Station 40, presumably an infusion of Norwegian Arctic Intermediate Water from the Norwegian Atlantic Current. In keeping normal to the Jan Mayen Current axis this and subsequent sections are oriented increasingly more southeast-to-northwest and less parallel to the continental slope.

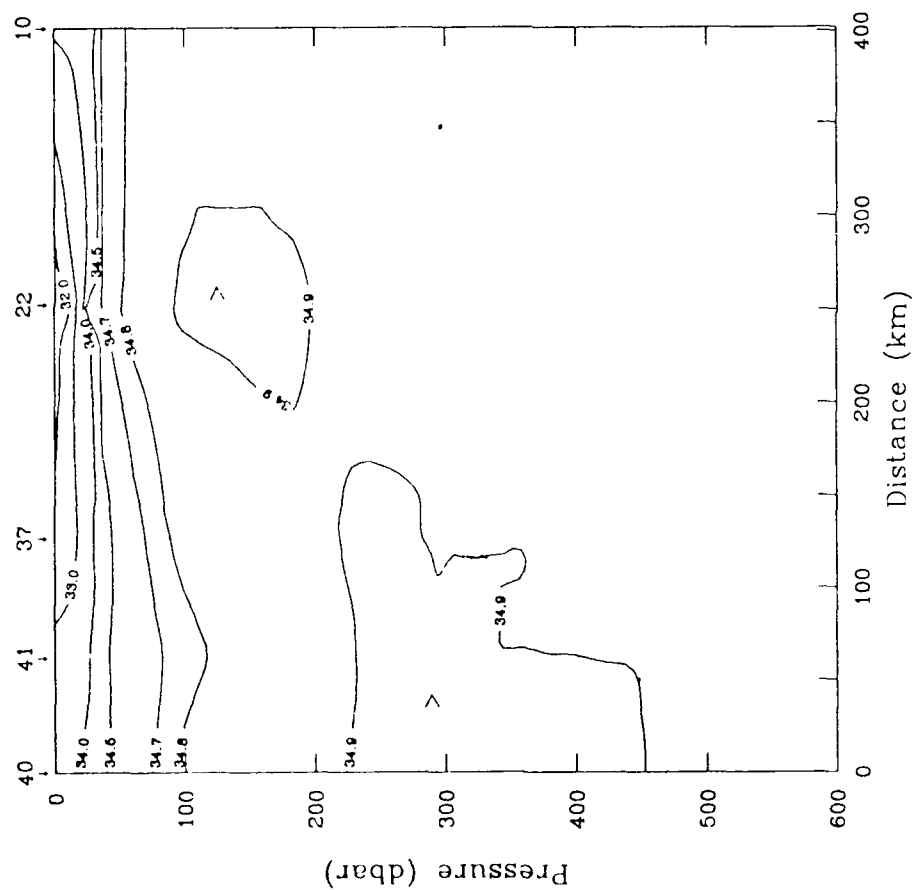


Figure 3.30 BARTLETT 89 salinity Transect C (600 m) (PSU). A salinity maximum continues in association with the warm Jan Mayen and Norwegian Atlantic intermediate waters.

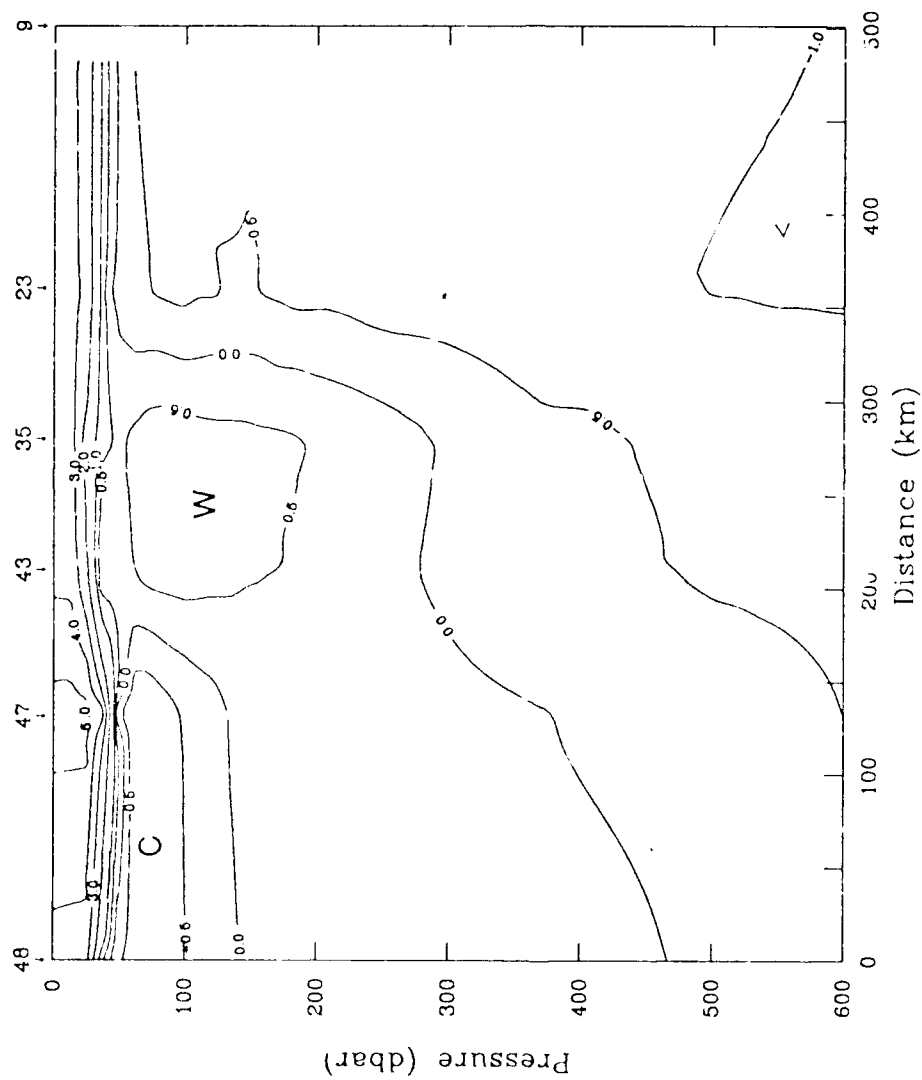


Figure 3.31 BARTLETT 89 temperature Transect D (600 m) ($^{\circ}\text{C}$). The warm core of the Jan Mayen Current is beginning to diminish in size, while the cold core has enlarged and cooled somewhat. An infusion of warm, Norwegian Atlantic Surface Water from the Norwegian Atlantic Current is shown at station 47.

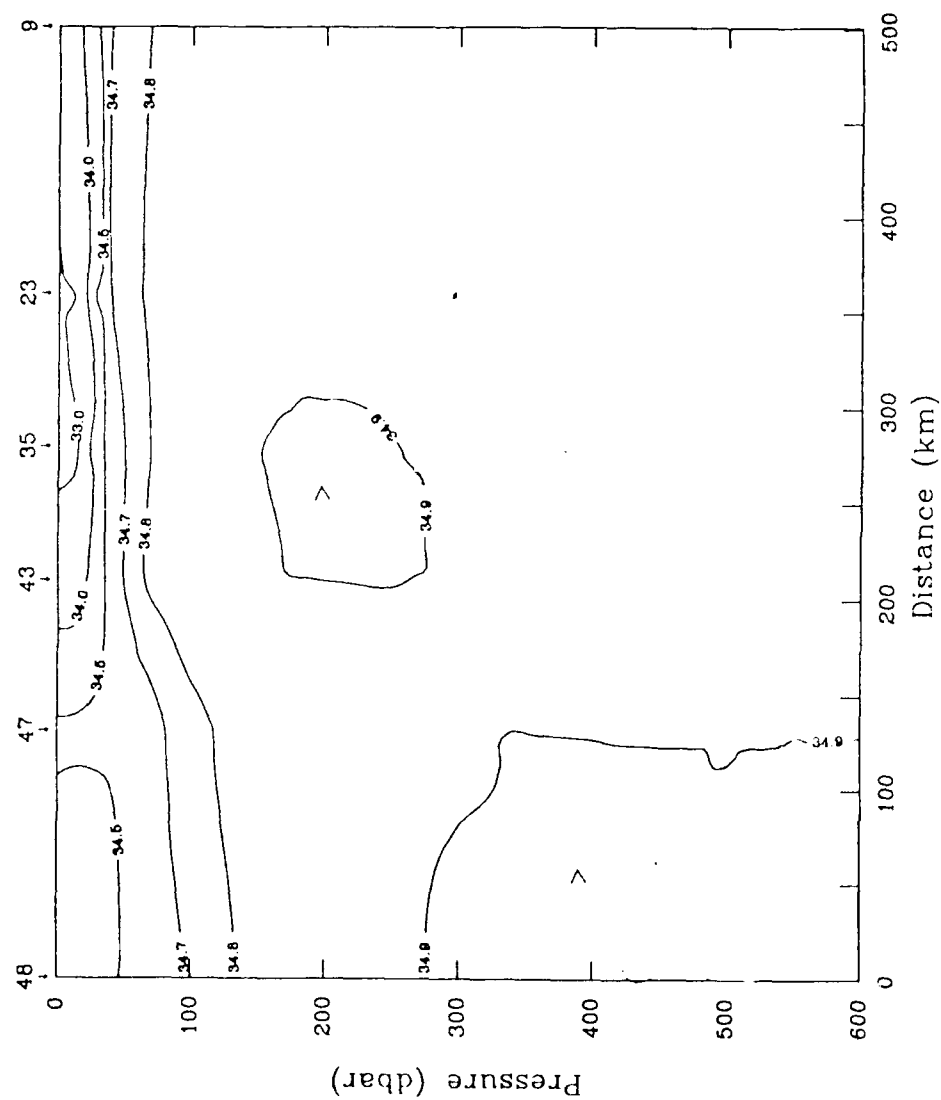


Figure 3.32 BARTLETT 89 salinity Transect D (600 m) (PSU). A salinity maximum continues in association with the warm core. A relatively saline influx of Norwegian Atlantic Surface Water is noted between Station 47 and 48.

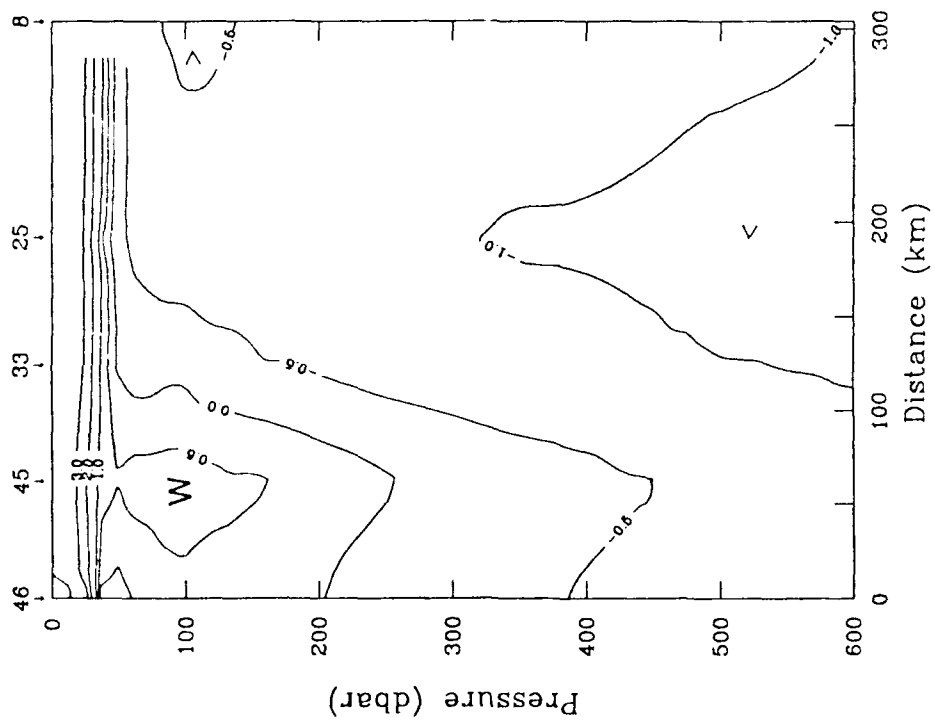


Figure 3.33 BARTLETT 89 temperature Transect E (600 m) ($^{\circ}\text{C}$). At a great circle distance of about 500 km from the East Greenland Current, the warm core of the Jan Mayen Current is considerably reduced in cross-sectional area.

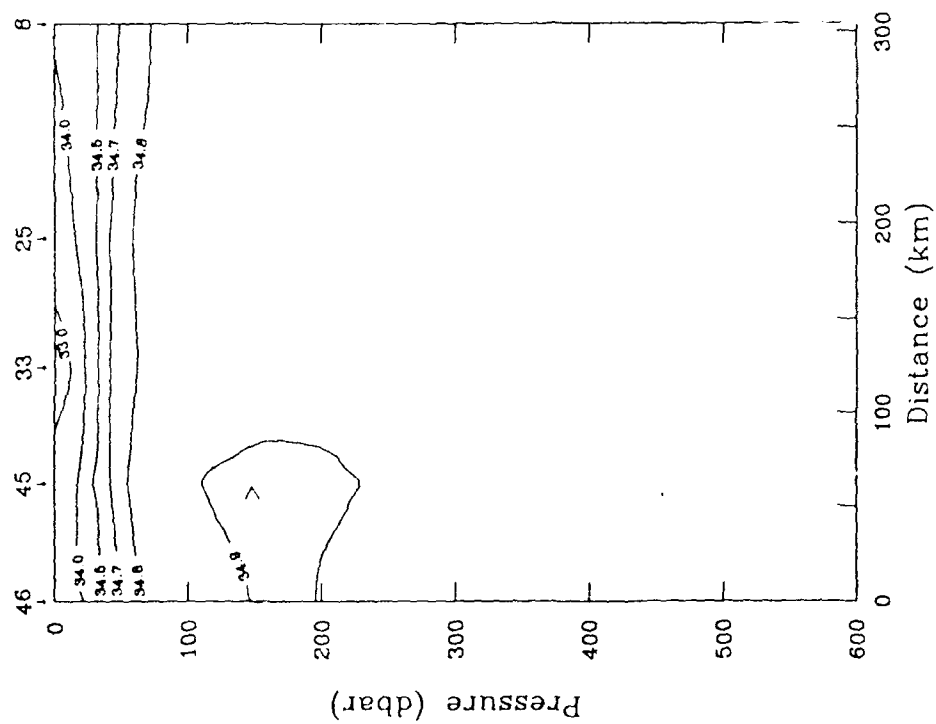


Figure 3.34 BARTLETT 89 salinity Transect E (600 m) (PSU). As with the temperature section, the cross-sectional area of the intermediate salinity maximum is considerably reduced over the 500 km arc from Transect A.

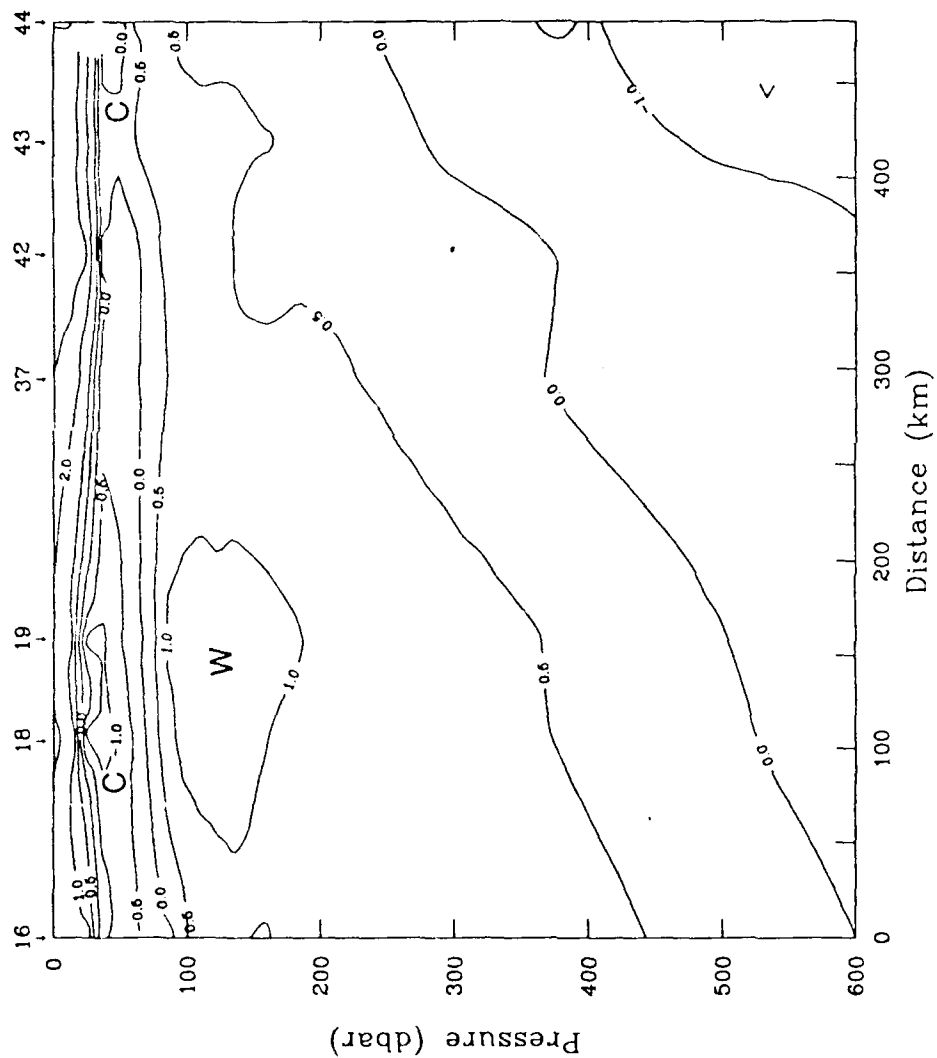


Figure 3.35 BARTLETT 89 temperature Transect F (600 m) ($^{\circ}\text{C}$). Looking northward this and the subsequent section provide a radial (west to east) view of the Jan Mayen Current (JMC) meander. This section slices the cold core and the southern portion of the warm core of the JMC. The cold core is located above the warm core between Stations 18 and 19.

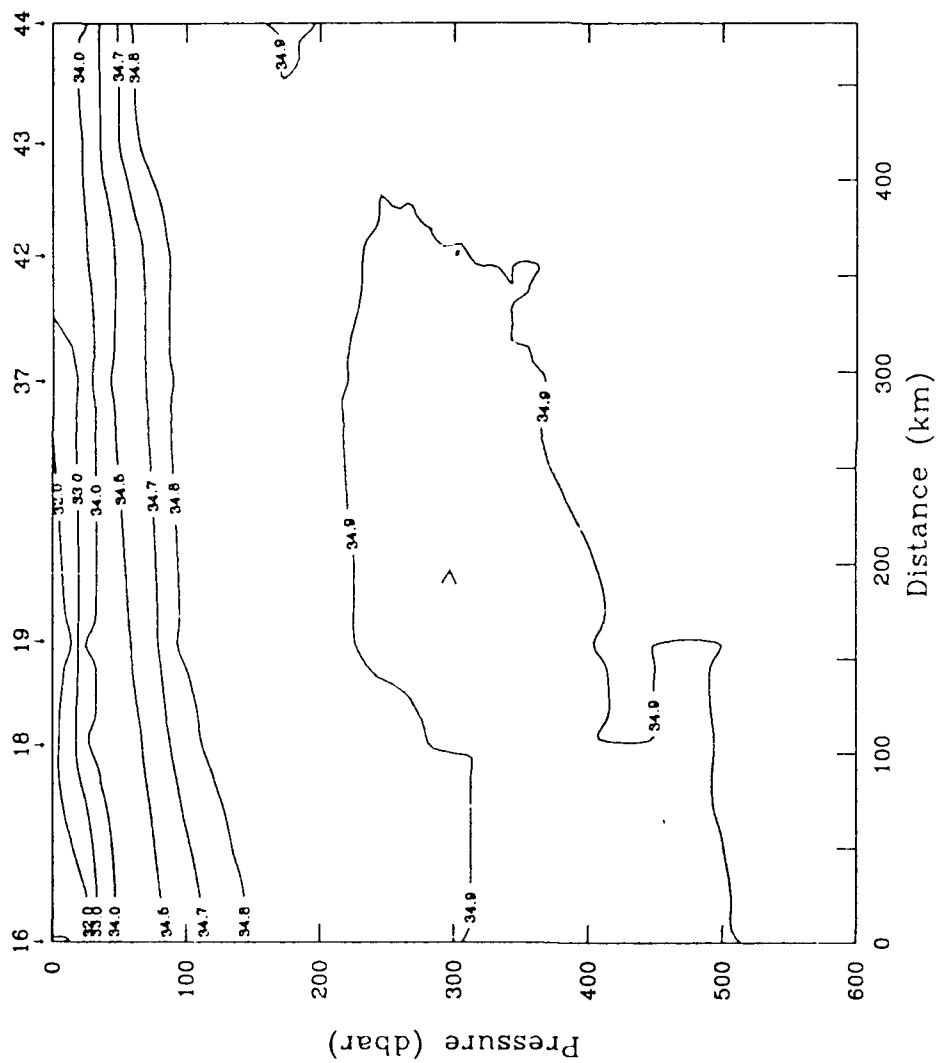


Figure 3.36 BARTLETT 89 salinity Transect F (600 m) (PSU). The characteristic intermediate salinity maximum occurs slightly deeper than the warm core in this section. A tongue of surface Greenland Polar Water extends eastward between Stations 16 and 37.

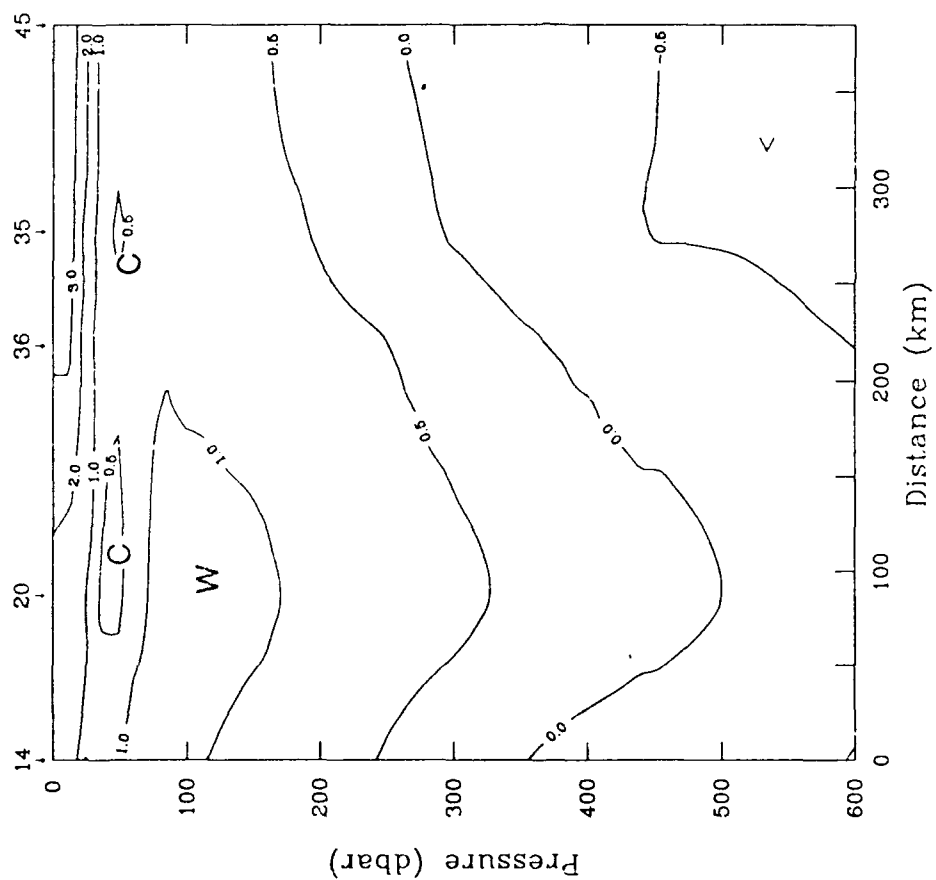


Figure 3.37 BARTLETT 89 temperature Transect G (600 m) ($^{\circ}\text{C}$). Located about 50 km north of Transect F, this section slices the heart of the warm core and the cold core appears more filamental than in Transect F.

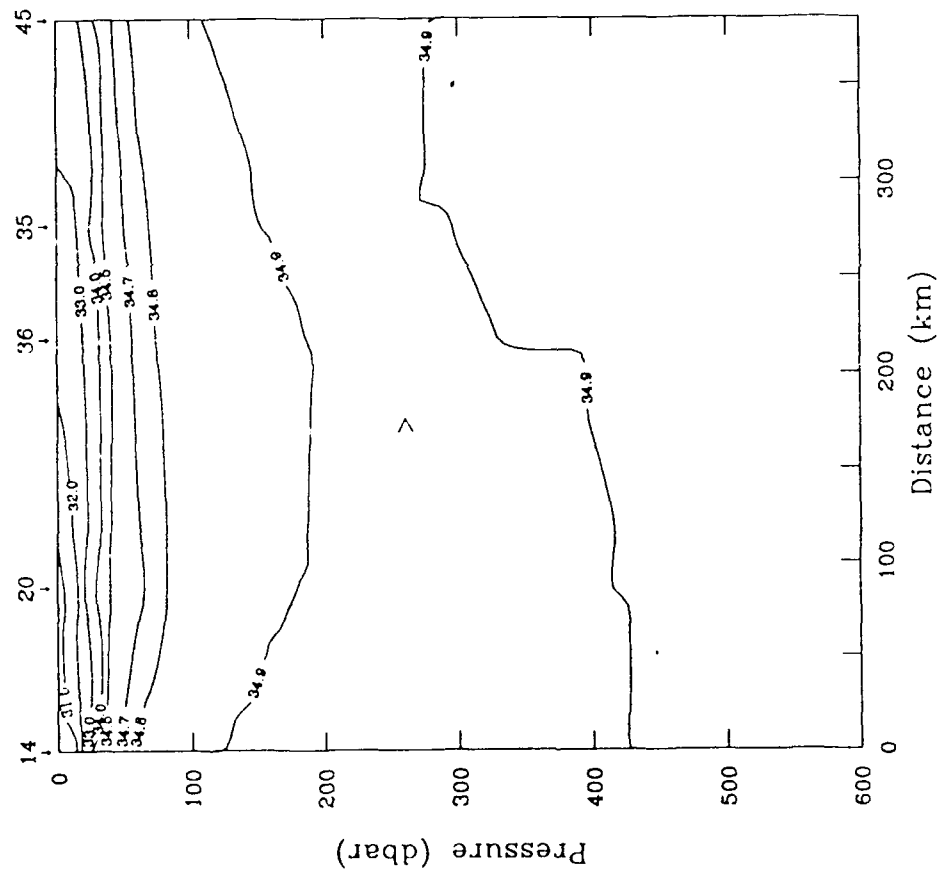


Figure 3.38 BARTLETT 89 salinity Transect G (600 m) (PSU). In this section the salinity maximum is more substantial where the Jan Mayen Current meander first bows eastward from the East Greenland Current. A thin GPW layer remains on the surface.

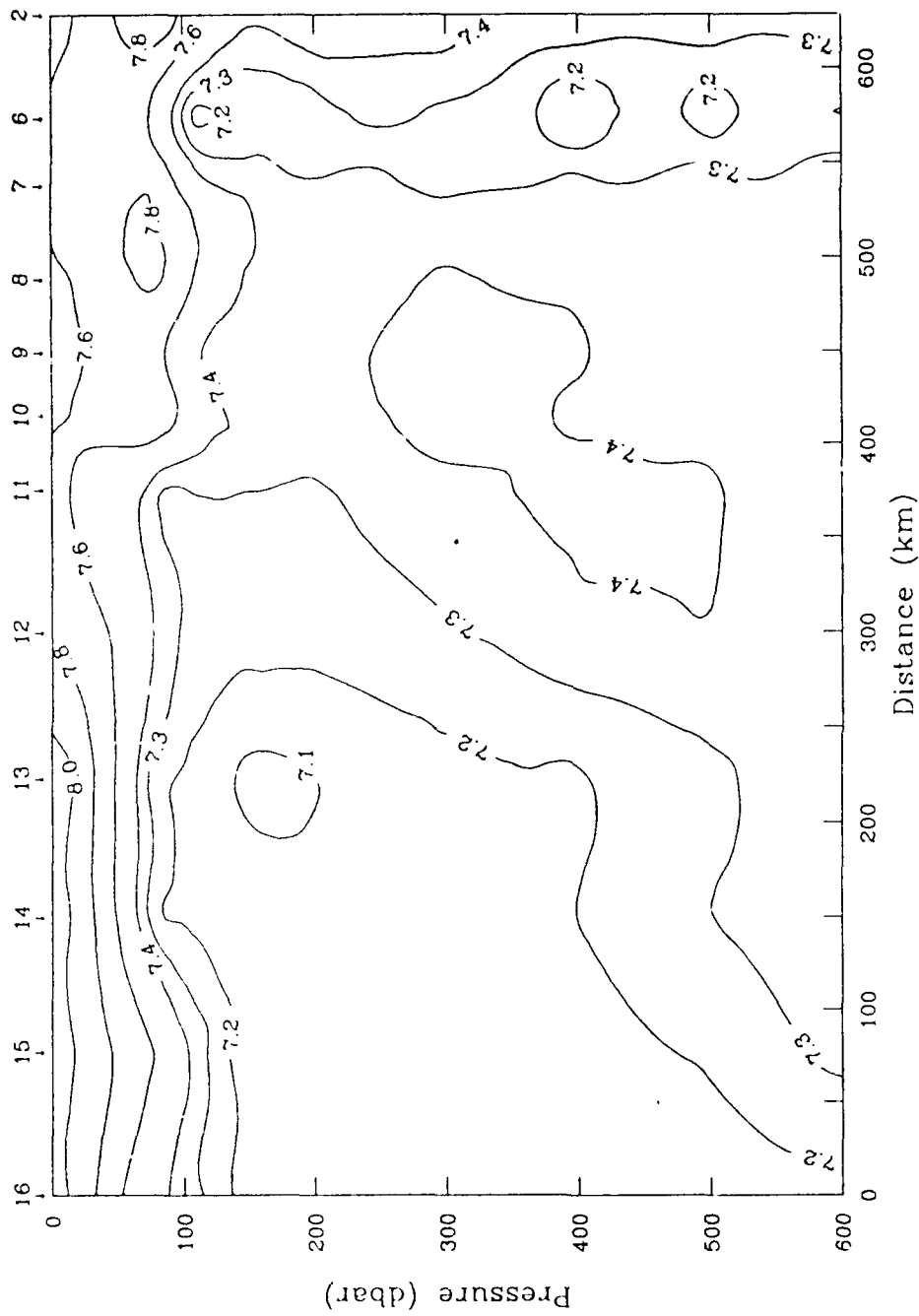


Figure 3.39 BARTLETT 89 dissolved oxygen Transect A (600 m) (ml/l). Vertical sections of dissolved oxygen demonstrate a close relationship to temperature, presumably due to the effect of temperature on the solubility of oxygen in seawater. The concentration of dissolved oxygen ranges from greater than 8.0 ml/l in the cold Greenland and Jan Mayen Polar waters to less than 7.1 ml/l in the warmest Jan Mayen and Return Atlantic intermediate waters. The subsequent sections seem to mirror their respective temperature sections.

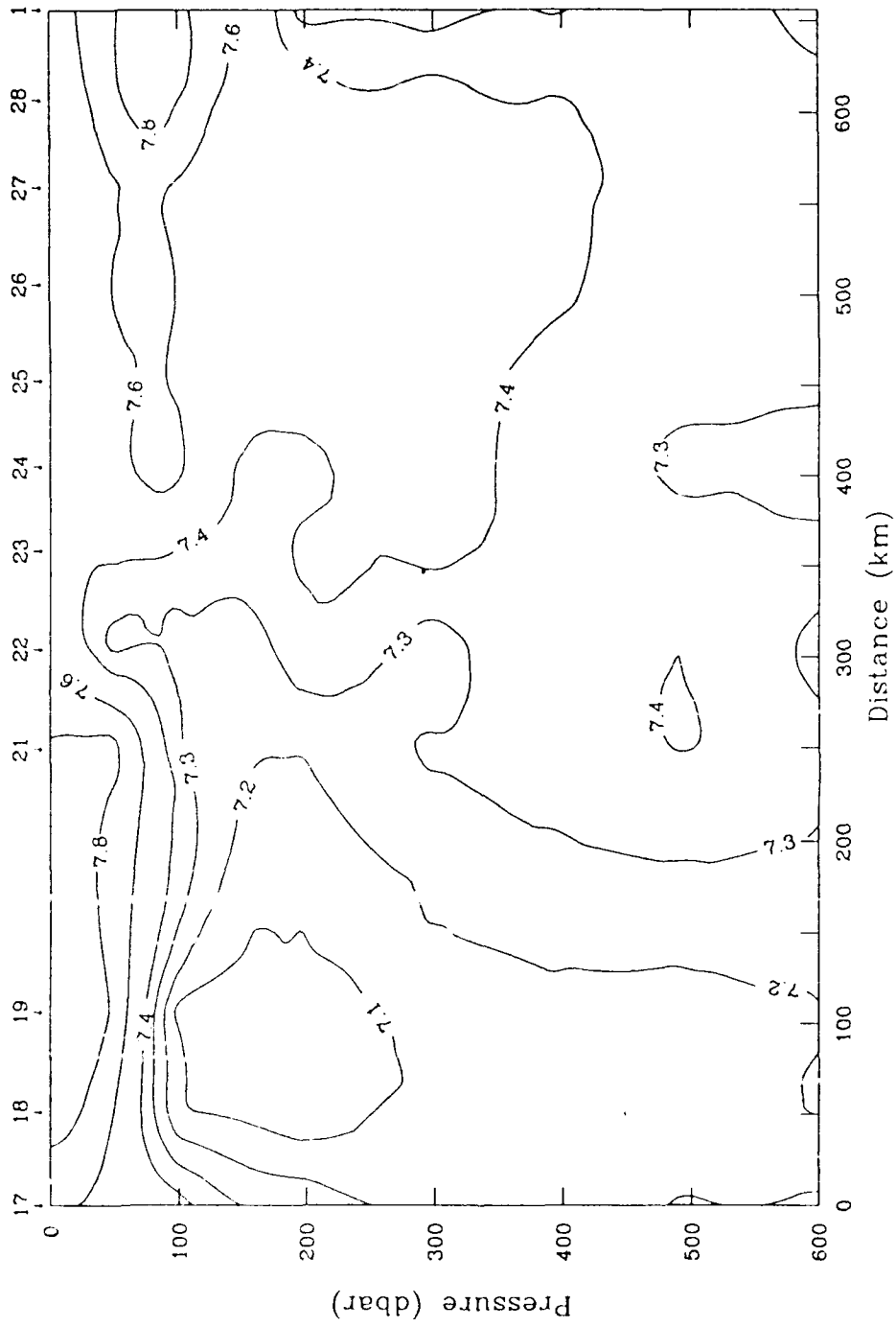


Figure 3.40 BARTLETT 89 dissolved oxygen Transect B (600 m) (ml/l). Refer to Figure 3.39.

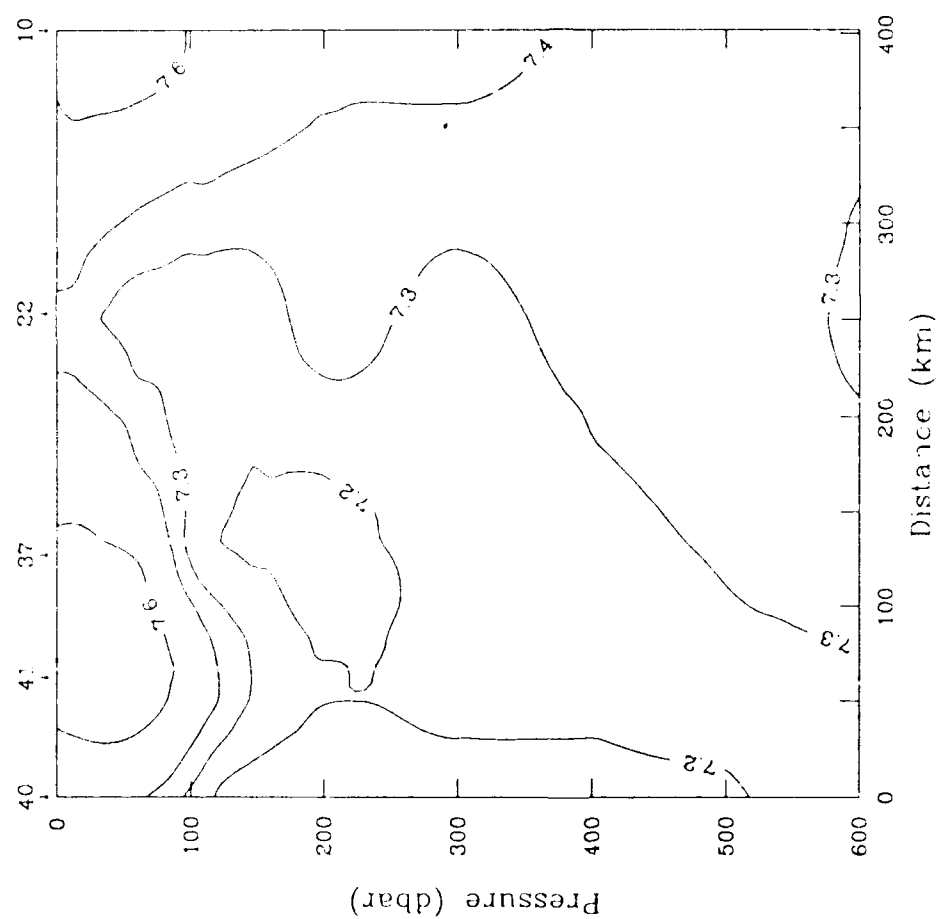


Figure 3.41 BARTLETT 89 dissolved oxygen Transect C (600 m) (ml/l). Refer to Figure 3.39.

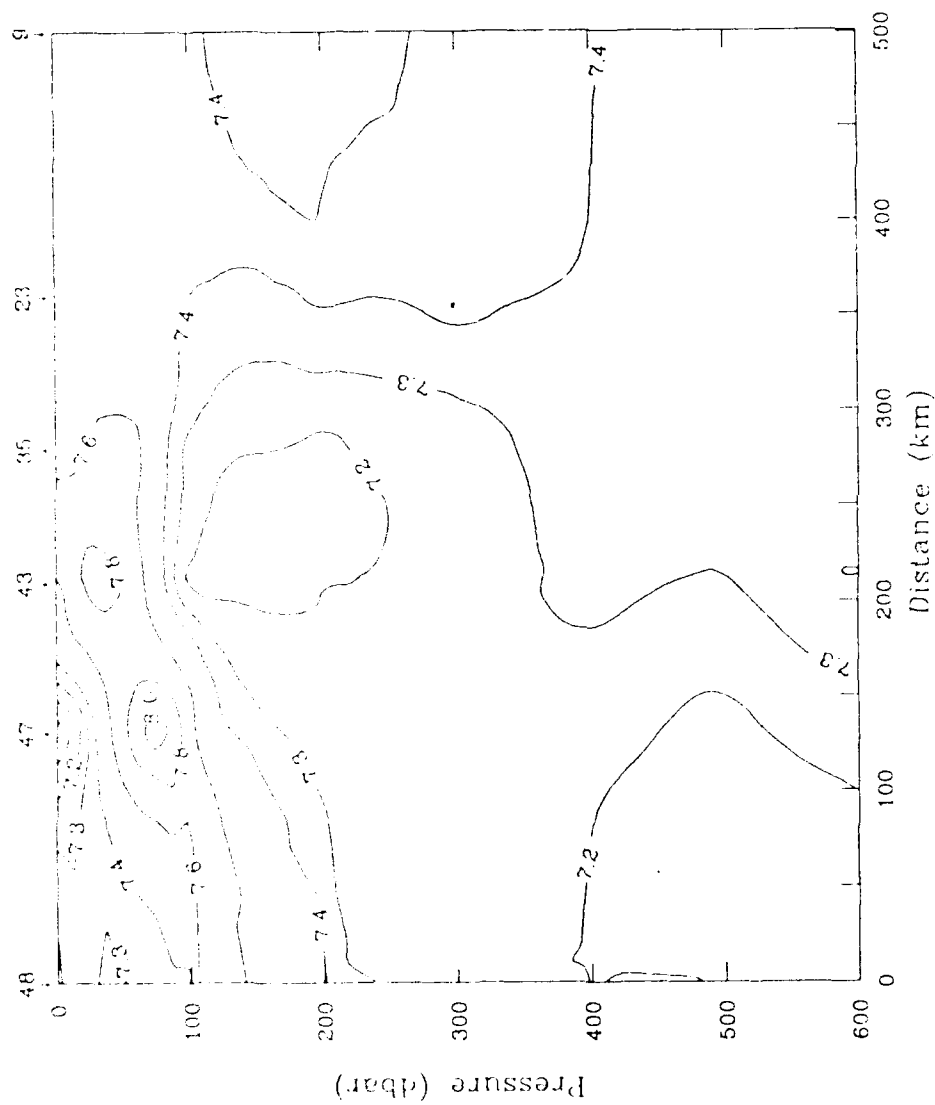


Figure 3.42 BARTLETT 89 dissolved oxygen Transect D (600 m) (ml/l). Refer to Figure 3.39.

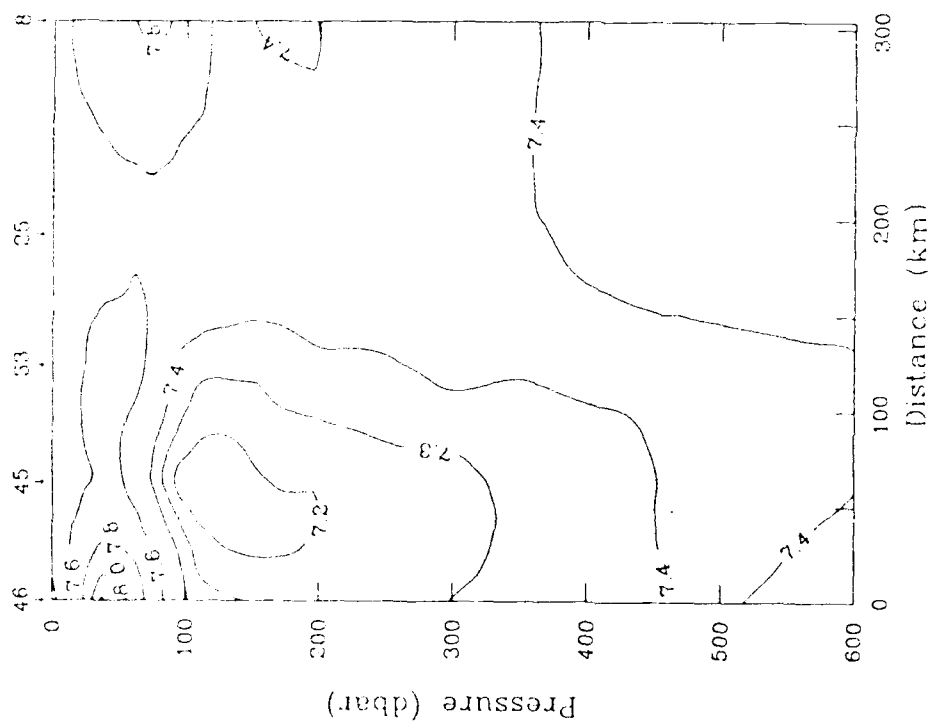


Figure 3.43 BARTLETT 89 dissolved oxygen Transect E (600 m) (ml/l). Refer to Figure 3.39.

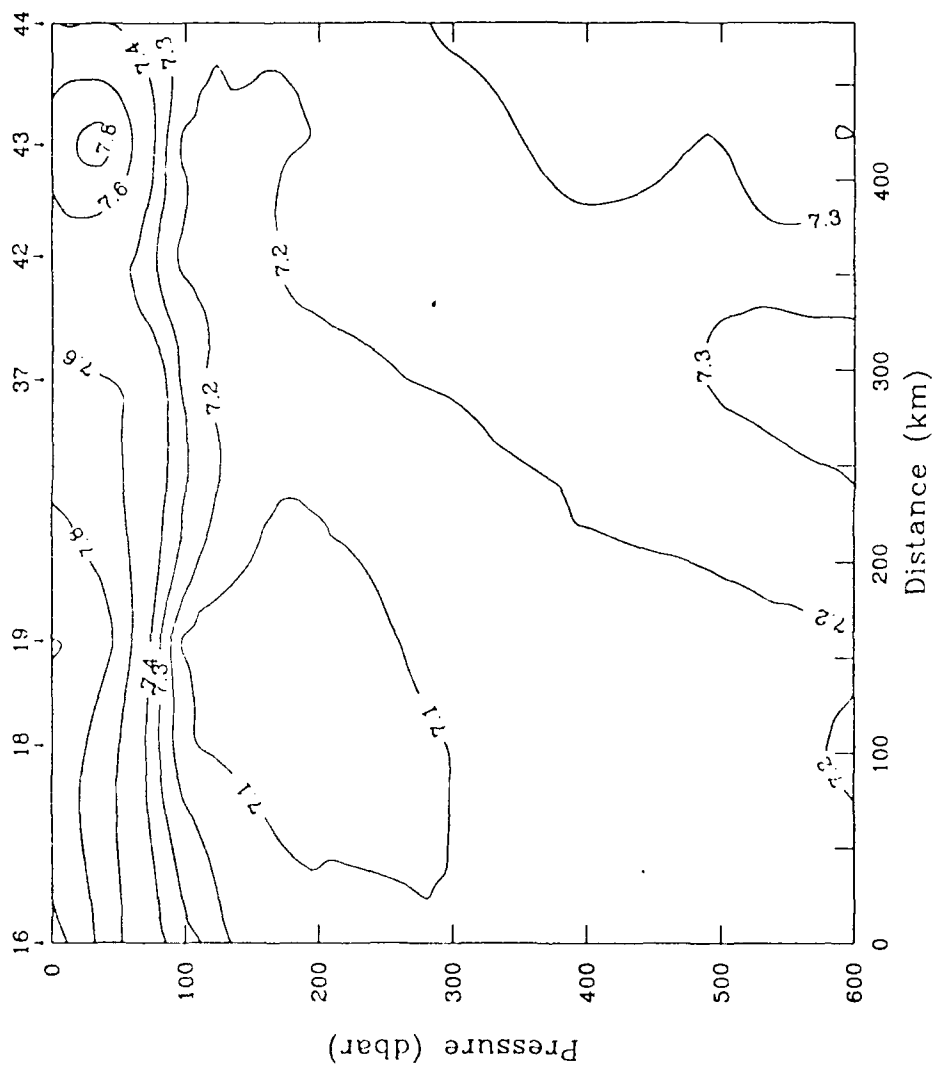


Figure 3.44 BARTLETT 89 dissolved oxygen Transect F (600 m) (mM). Refer to Figure 3.39.

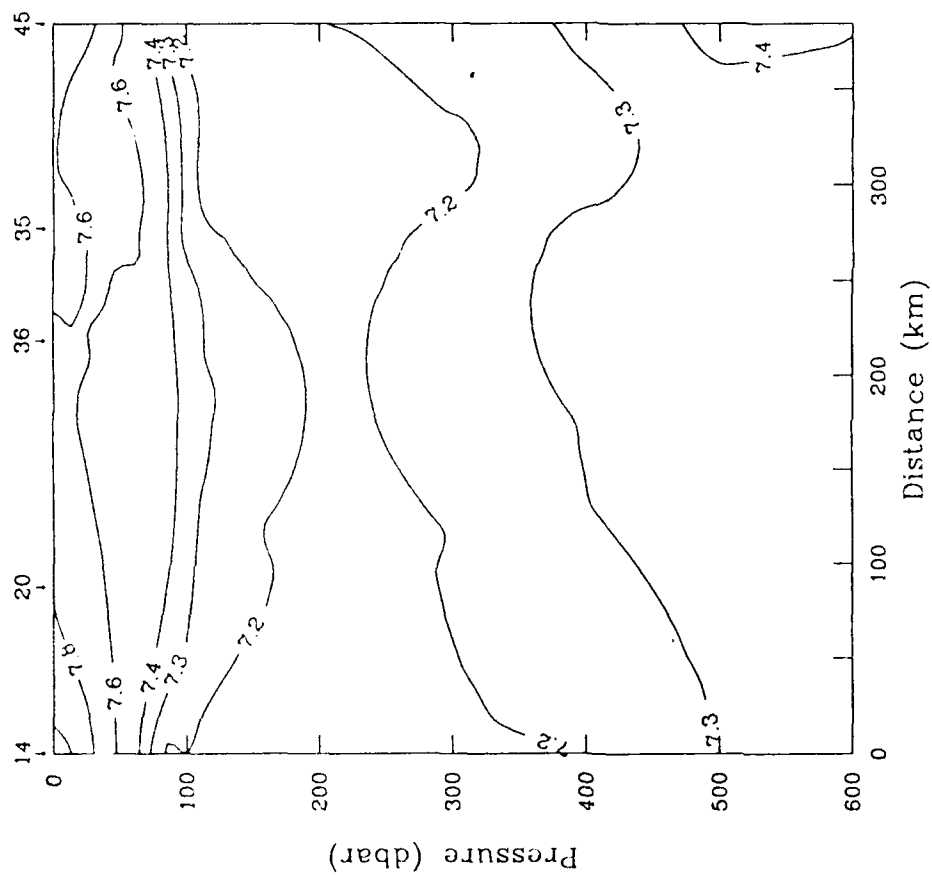
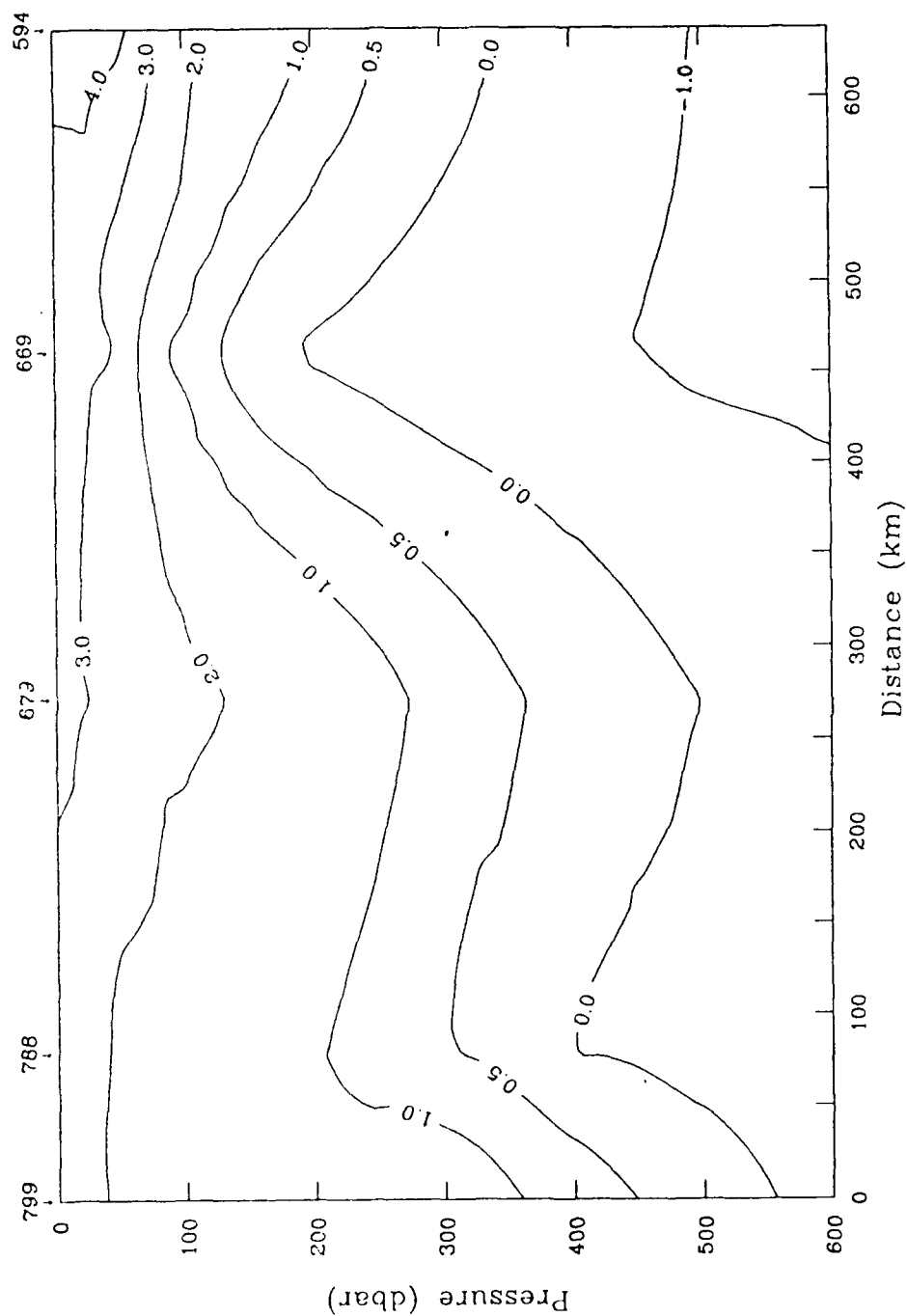


Figure 3.45 BARTLETT 89 dissolved oxygen Transect G (600 m) (ml/l). Refer to Figure 3.39.



JOHAN HJORT/POLJARNIK 58 summer temperature Transect 12 (600 m) ($^{\circ}\text{C}$). This section is constructed to coincide with BARTLETT 89 Transect A. The general arrangement of isotherms is similar to 1989, though no isotherms are closed to delineate a warm or cold current core. The Jan Mayen Current axis appears to be centered at Station 679. Evidence of Greenland Polar Water is absent at the surface.

Figure 3.47

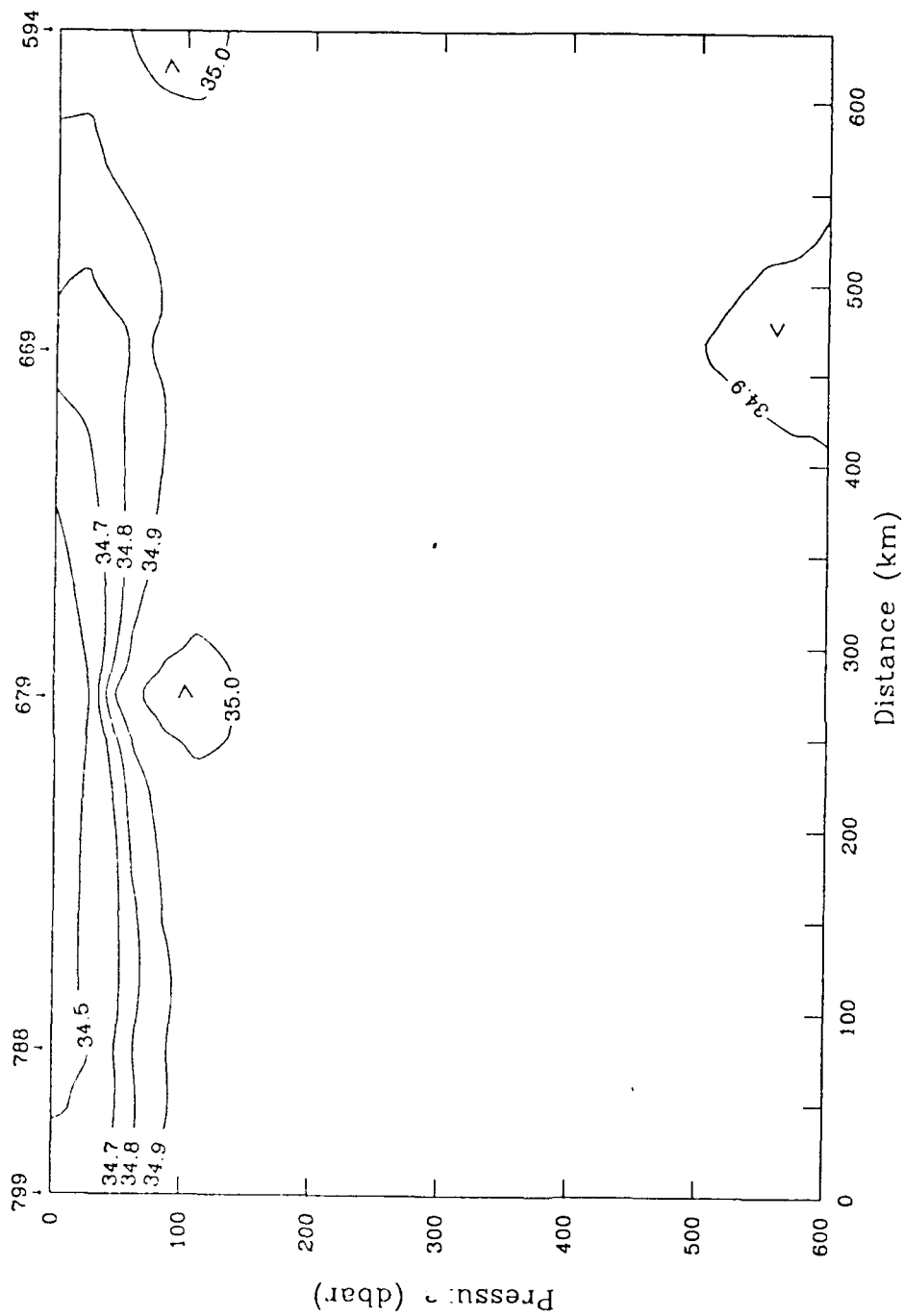
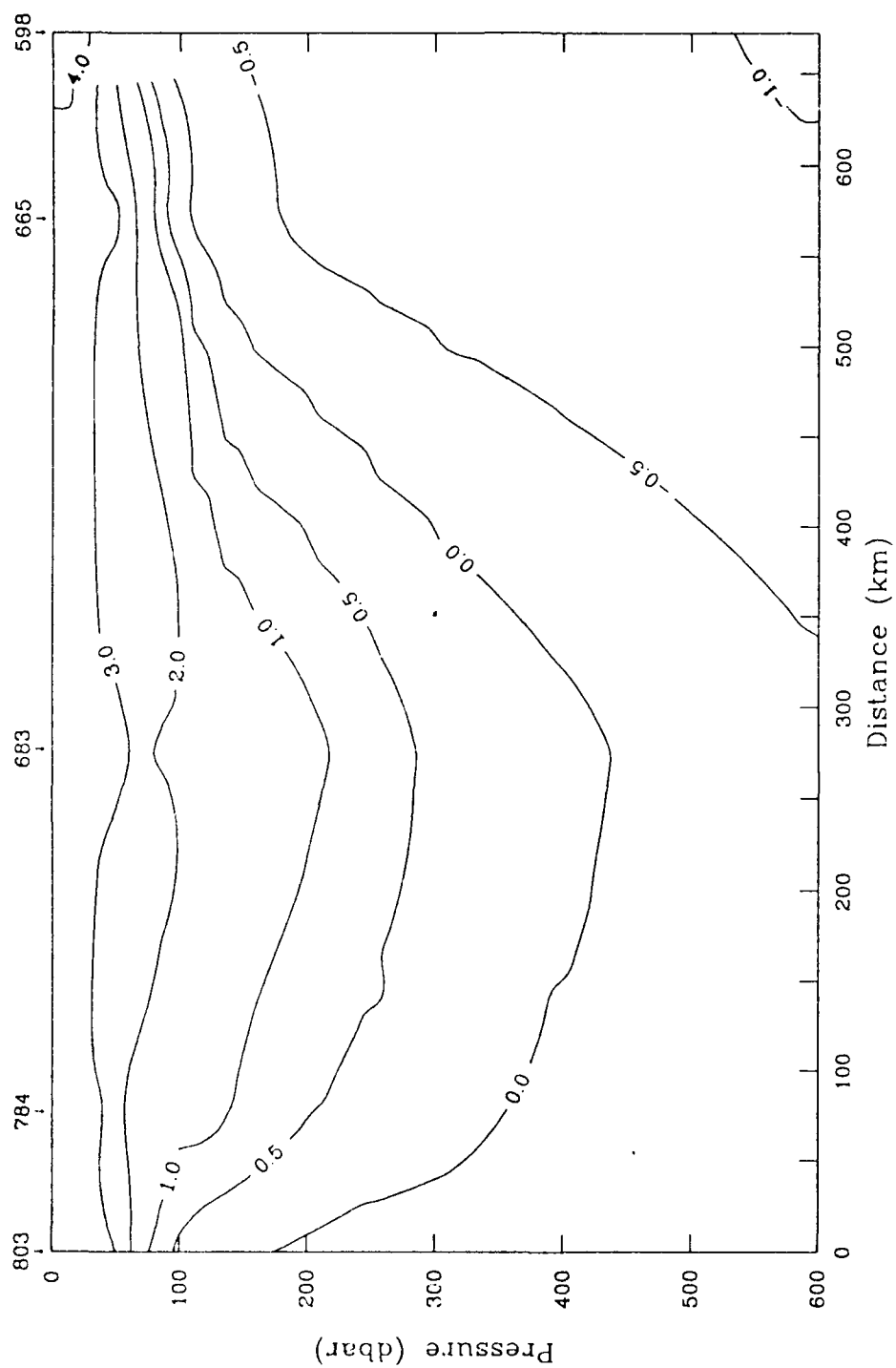


Figure 3.48 JOHAN HJORT/POLJARNIK 58 summer salinity Transect 12 (600 m) (PSU). Similar to the BARTLETT 89 sections, an intermediate salinity maximum at Station 679 is associated with the core of the Jan Mayen Current. There is a lack of low-salinity surface water compared to 1989.



JOHAN HJORT/POLJARNIK 58 summer temperature Transect 14 (600 m) ($^{\circ}\text{C}$). This section which is nearly collocated with BARTLETT 89 Transect B shows the Jan Mayen Current axis is centered near Station 683. Isotherms dome up toward the Greenland Sea Gyre north of Station 665.

Figure 3.49

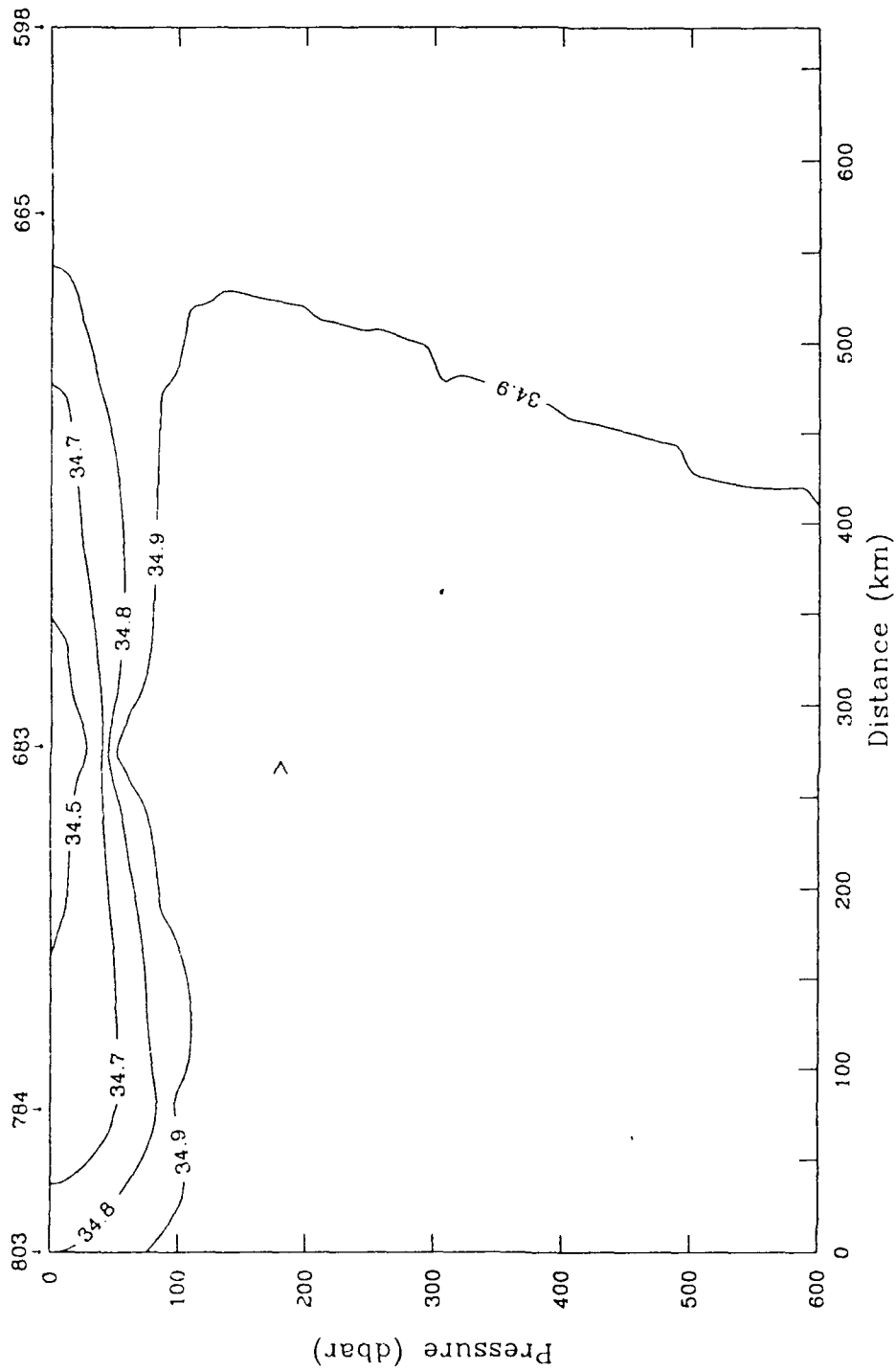


Figure 3.50 JOHAN HJORT/POLJARNIK 58 summer salinity Transect 14 (600 m) (PSU). The Jan Mayen Current is again associated with an intermediate salinity maximum. In contrast, the Greenland Sea Gyre is very weakly stratified including the absence of the usual surface gradient.

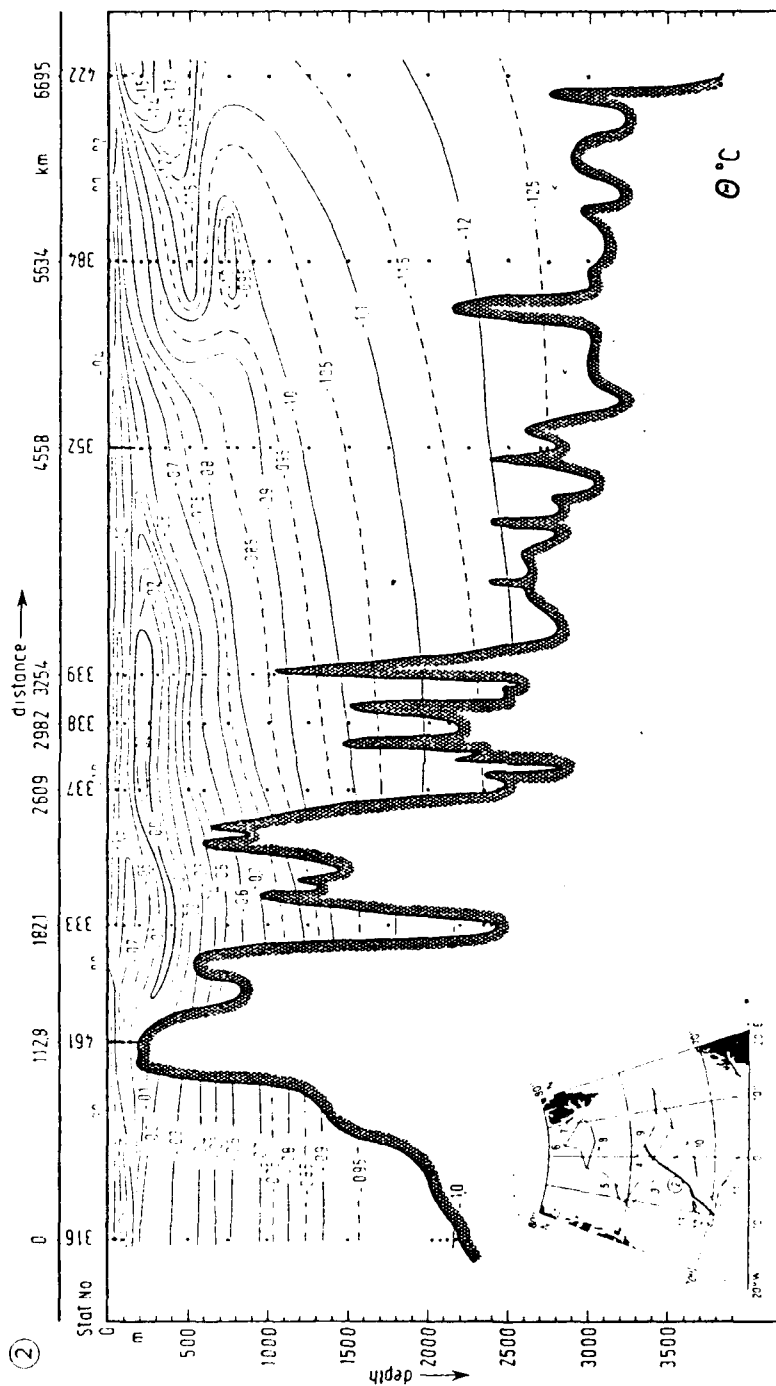


Figure 3.52 METEOR/HUDSON 82 winter temperature Transect 2 (600 m) ($^{\circ}\text{C}$). This section is selected since it shows the manifestation of the Jan Mayen Current as a relatively warm core of waters beneath surface polar waters between Stations 352 and 461 as observed in 1989, though temperatures are seasonally colder (from *Kollermann and Lühje, 1989*).

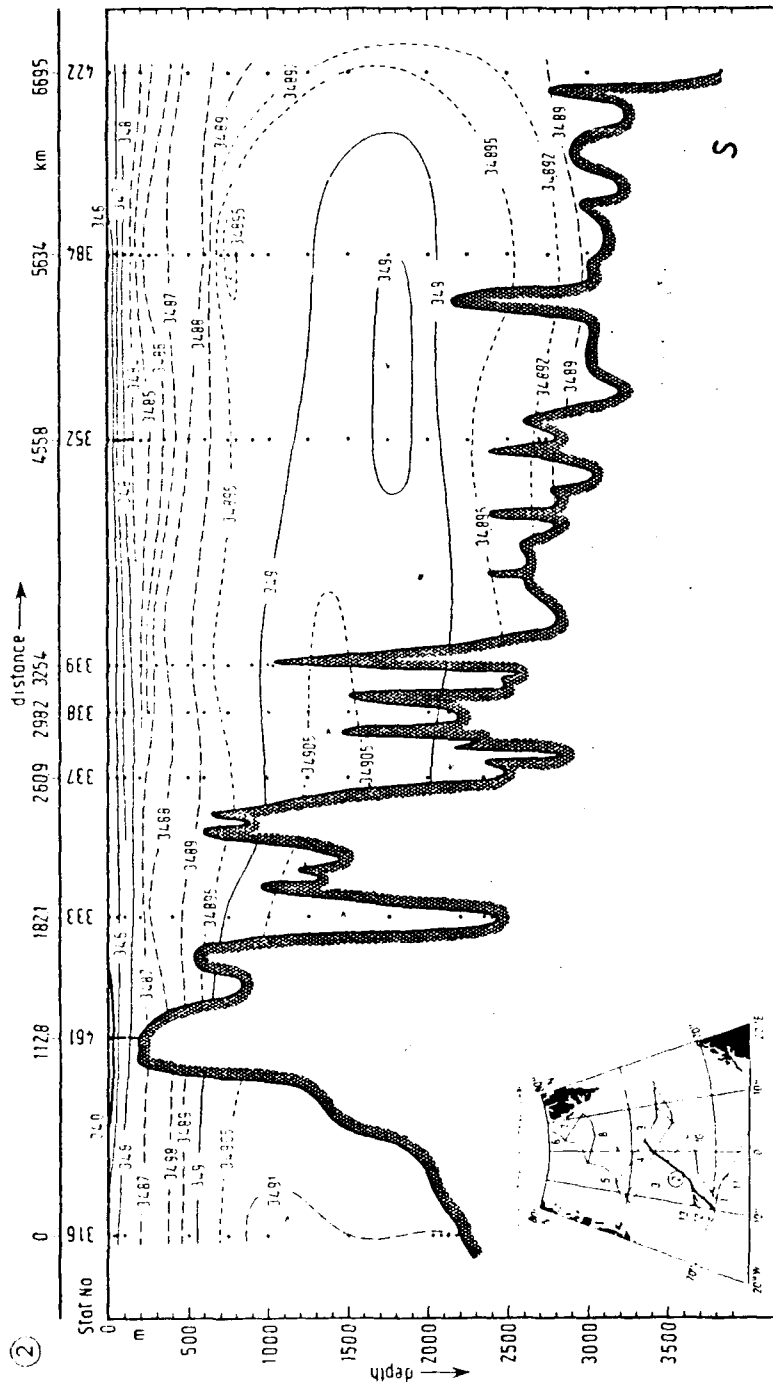


Figure 3.53 METEOR/HUDSON 82 winter salinity Transect 2 (600 m) (1 SU). Lower-salinity surface water is associated with the tip of the Jan Mayen Current meander between Stations 352 and 461. The intermediate salinity maximum seems to occur at greater depth than in 1989 (from Koltermann and Lüthje, 1989).

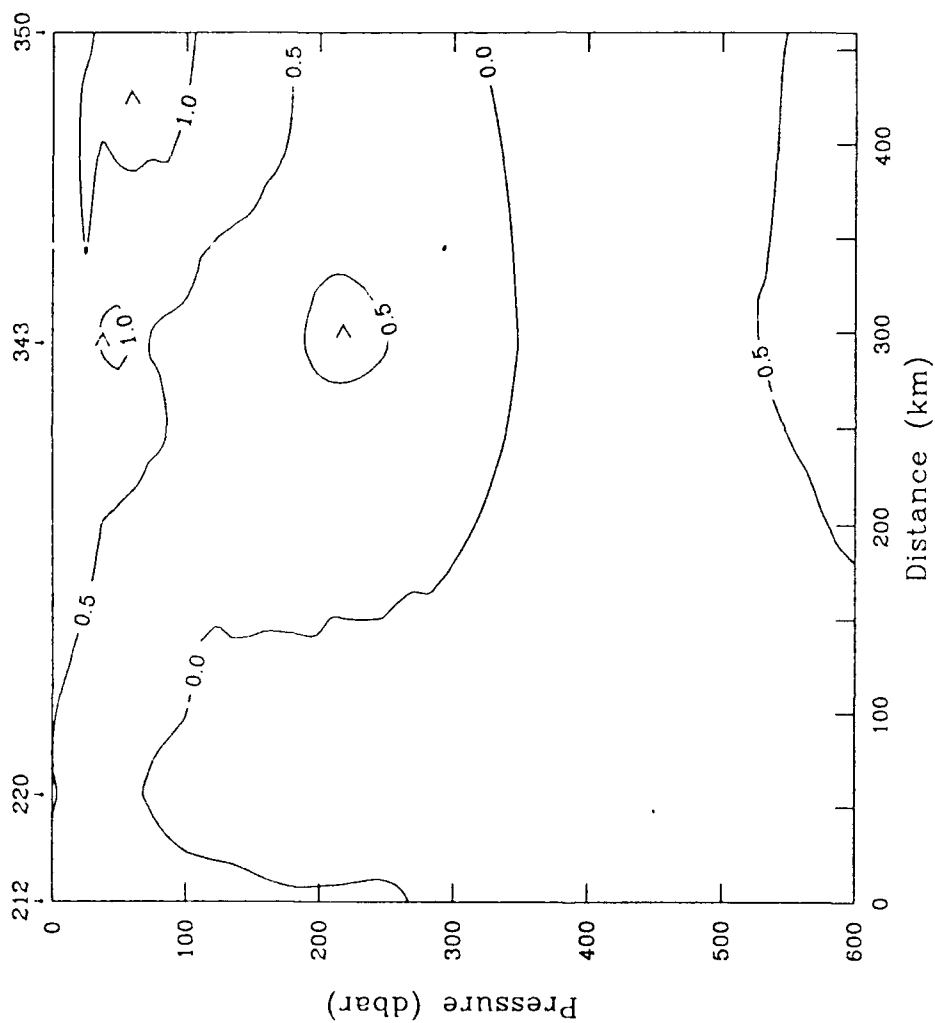


Figure 3.55 JOHAN HJORT/POLJARNIK 58 winter temperature Transect 32 (600 m) ($^{\circ}\text{C}$). This section which is compiled to be nearly collocated with southern portions of BARTLETT 89 Transect A, shows the warm core of a Jan Mayen Current in closed isotherms at Station 343, though there is a lack of low-temperature surface water as in summer 1958.

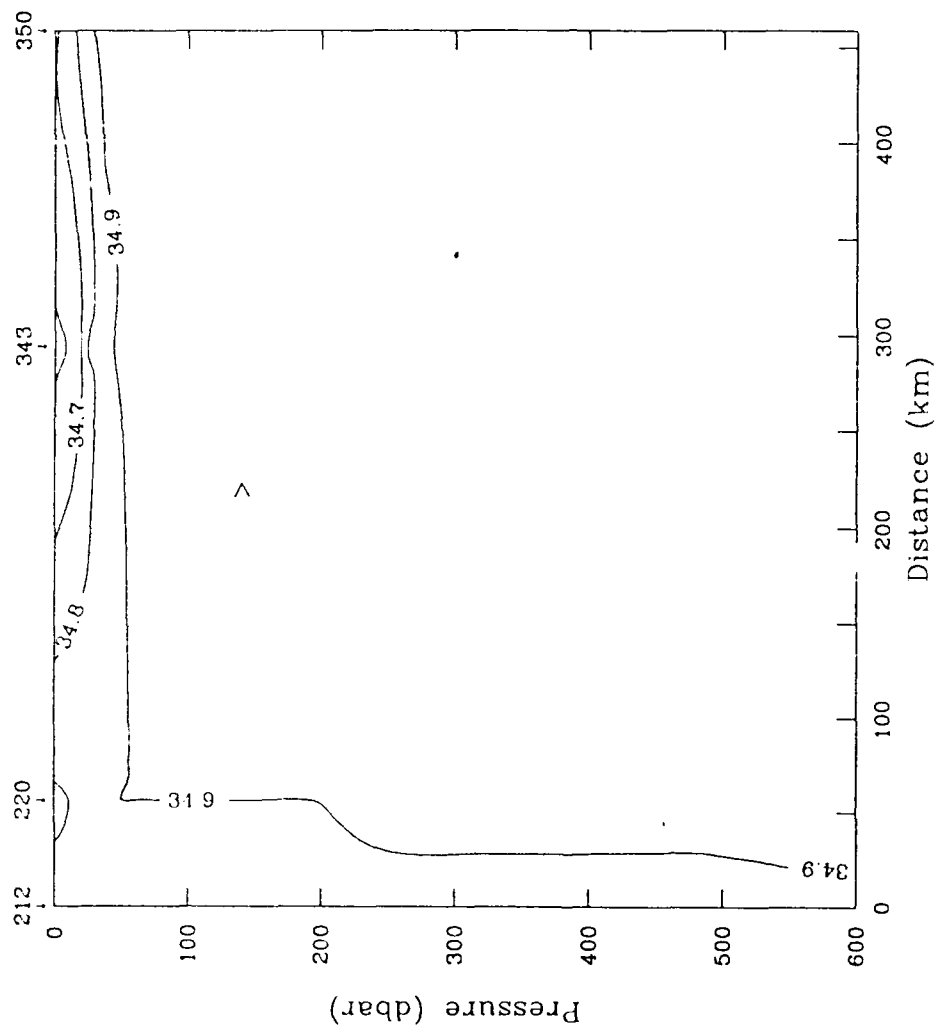


Figure 3.56 JOHAN HJORT/POLJARNIK 58 winter salinity Transect 32 (600 m) (PSU). Though a relative surface salinity minimum at Station 343 is associated with the Jan Mayen Current, actual values are markedly higher than in 1989.

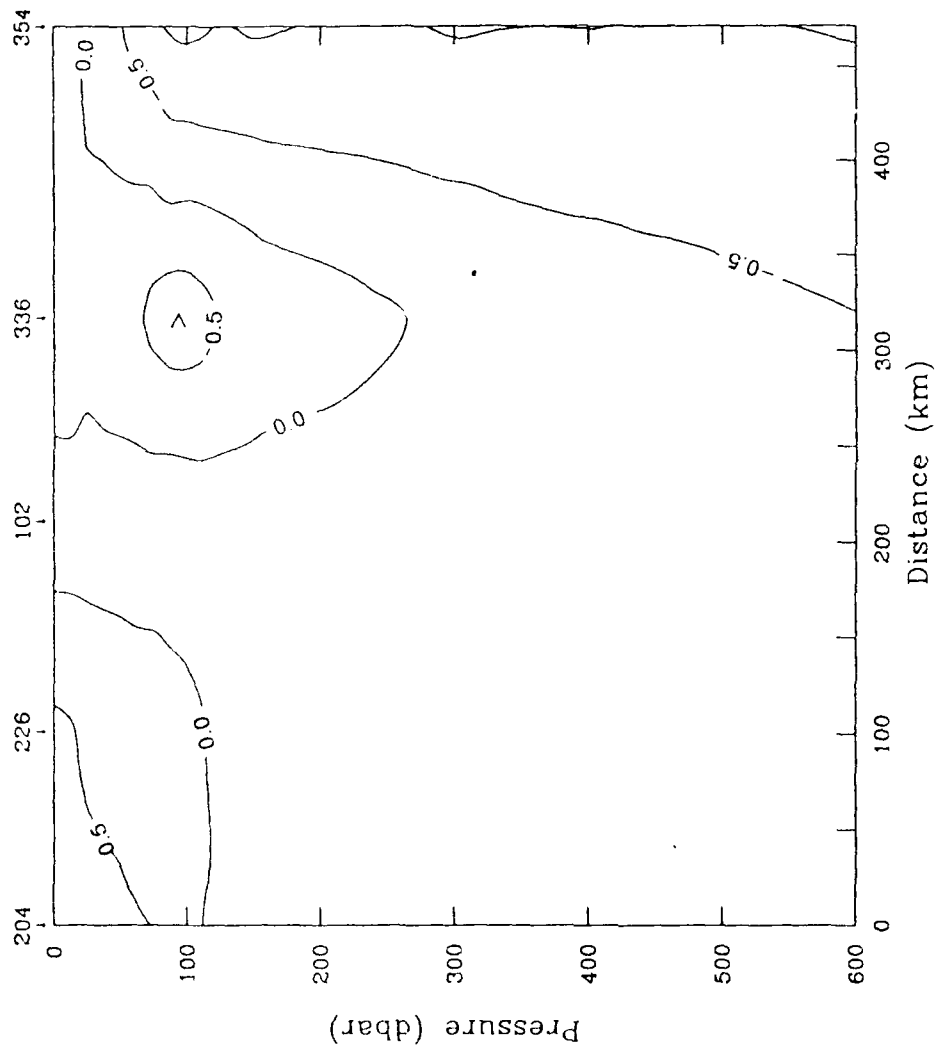


Figure 3.57 JOHANHJORT/POLJARNIK 58 winter temperature Transect 34 (600 m) ($^{\circ}\text{C}$). This section is compiled to be nearly collocated with southern portions of BARTLETT 89 Transect B, though is actually about 50 km farther seaward. The Jan Mayen Current persists from Transect 32 as a core of warm intermediate water warmer than 0.5°C . Isotherms dome upward at Station 354 toward the Greenland Sea Gyre. Surface temperatures are markedly higher than in 1982 or 1989.

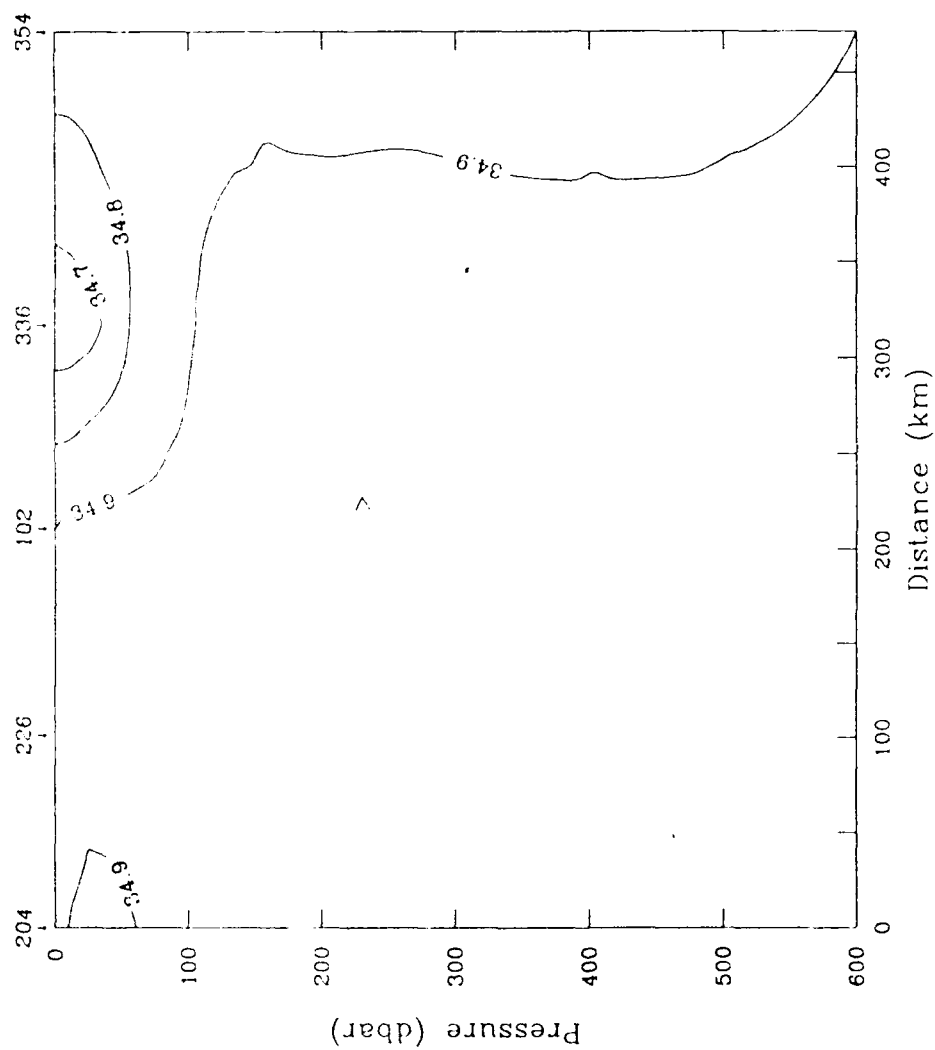


Figure 3.58 JOHAN HUORT/POLJARNIK 58 winter salinity Transect 34 (600 m) (PSU). The Jan Mayen Current continues to be associated with a relative surface salinity minimum and intermediate salinity maximum. Actual surface salinities, however, are markedly higher than in 1982 or 1989.

IV. CIRCULATION AND TRANSPORTS

The water column in the Greenland-Norwegian Sea is generally considered to be weakly stratified except for a shallow seasonal surface gradient that may extend as deep as 100 m. Flow in areas with weak vertical gradients is observed to have a substantial barotropic component. Such structure of the water column is illustrated by the results of the BARTLETT 89 survey. Thus, flows in the Greenland Basin are expected to be significantly barotropic and demonstrate a response to underlying bathymetric features. *Muench (1990b)* indicates that the EGC is significantly barotropic. *Foldvik et al. (1988)*, based on year-long current meter measurements, consider the EGC to be at least half barotropic. In the absence of seasonal fluctuations in this flow, they deduce that the EGC is driven by differences in sea level between the Arctic and Atlantic Oceans rather than the result of a wind-driven gyre system in the Greenland Sea, though *Aagaard (1970)* shows that local wind stress is capable of producing appropriate transports in the basin. In a study of wind stress curl in the region from 1955-87 *Jónsson (1989)* also discounts wind stress as a major driving force of the large scale flow except possibly in the recirculation region south of Fram Strait. Additionally, *Gascard et al. (1988)* describe the EGC as a narrow, baroclinically stable, and largely buoyancy-driven flow.

A. BAROCLINIC FLOW

BARTLETT 89 data are limited to a geostrophic analysis of the baroclinic component of flow in the upper 1000 m. Notable similarities exist, however, between

the BARTLETT 89 dynamic height pattern and the trajectories of Lagrangian drifters as well as the results of a numerical model, both to be discussed in the following section. Thus, the baroclinic velocity field seems to resemble the total flow field in direction.

The surface dynamic height pattern of September 1989 is presented in Figure 4.1. Contours are in dynamic centimeters at the surface referenced to 1000 dbar and the arrows represent frictionless, baroclinic flow. The height gradient is mild in general and is strongest in the EGC and where the JMC branches eastward from the EGC between Stations 10 and 12. The maximum gradient at this point, about 8 dyn cm over 100 km, produces a maximum baroclinic velocity of about 0.07 m s^{-1} . Most interesting in the dynamic height pattern is that the JMC appears partly as an anticyclonic meander in the EGC. About half of the dynamic height contours (hereafter referred to as flow lines) passing eastward through Transect A (Stations 2 to 16) loop back westward to rejoin the EGC as they encounter the JMFZ rise. The other half of the flow lines enter the GSG circulation or cross the Mohn Ridge toward the NAC/WSC.

The dynamic height pattern appears to be heavily correlated with the pattern of the intermediate temperature maximum in Figure 3.10 of the previous chapter. The alignment of these patterns and their relationship with the underlying bathymetry suggests the flow of the JMC meander is significantly barotropic. It is interesting that the baroclinic circulation in the upper water column seems to be well correlated with the barotropic component of flow. *Muench (1990b)* states that baroclinic features are often observed embedded in the largely barotropic, EGC/EGPF system. Furthermore, *Hopkins (1988)* explains that while the dynamic mechanisms are not known, eastward extensions of EGC

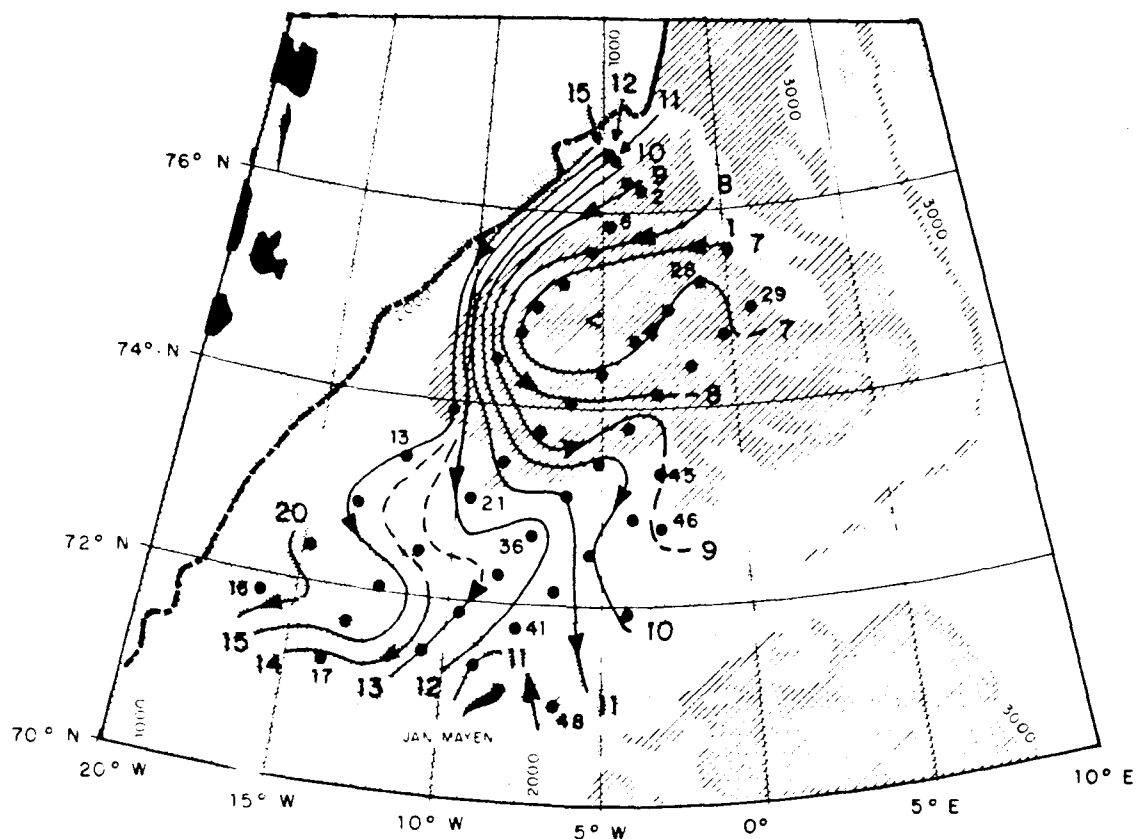


Figure 4.1

BARTLETT 89 dynamic height at the surface referenced to 1000 dbar (dyn cm). The geopotential pattern reveals that the baroclinic component of the Jan Mayen Current is partly an anticyclonic meander in the seaward portion of the East Greenland Current. The remainder of the flow proceeds eastward toward the Norwegian Atlantic Current or becomes incorporated in the Greenland Sea Gyre. Arrows indicate the direction of frictionless baroclinic flow. Mean ice edge shown as a heavy dashed line.

waters such as the JMC meander are assumed to be due to the interaction of the barotropic flow field with the underlying bathymetry.

Historical dynamic height contour patterns share the above features. The METEOR/HUDSON 82 dynamic height pattern in Figure 4.2 shows a closed GSG circulation as well as more detail farther to the east to include the flow in the seaward fringe of the NAC/WSC. The lack of stations in the area of the JMC, however, prevents a depiction of the flow there. The JOHAN HJORT/POLJARNIK 58 summer data in Figure 4.3 also shows a closed GSG circulation, as well as the presence of an anticyclonic meander in the EGC at 72° 30'N which bears strong resemblance to the BARTLETT 89 JMC circulation pattern.

B. TOTAL FLOW

1. Lagrangian Drifters

Three sea ice floe drift trajectories tracked by ARGOS positioning beacons during ARCTEMIZ 89 are utilized in this study to estimate the total flow field in the Greenland Basin (*Gascard and Richez, 1989*). These data were generously made available by *J.-C. Gascard (personal communication)*. It can reasonably be assumed that these ice floes are reasonably unaffected by local winds and thus represent the total flow field, especially since the floes are initially located well within the pack where wind stress and wind drag due to roughness of the floe surface are least (*Muench, 1989*). Internal ice stress is also assumed not to significantly affect the drift of these floes. Figure 4.4 shows

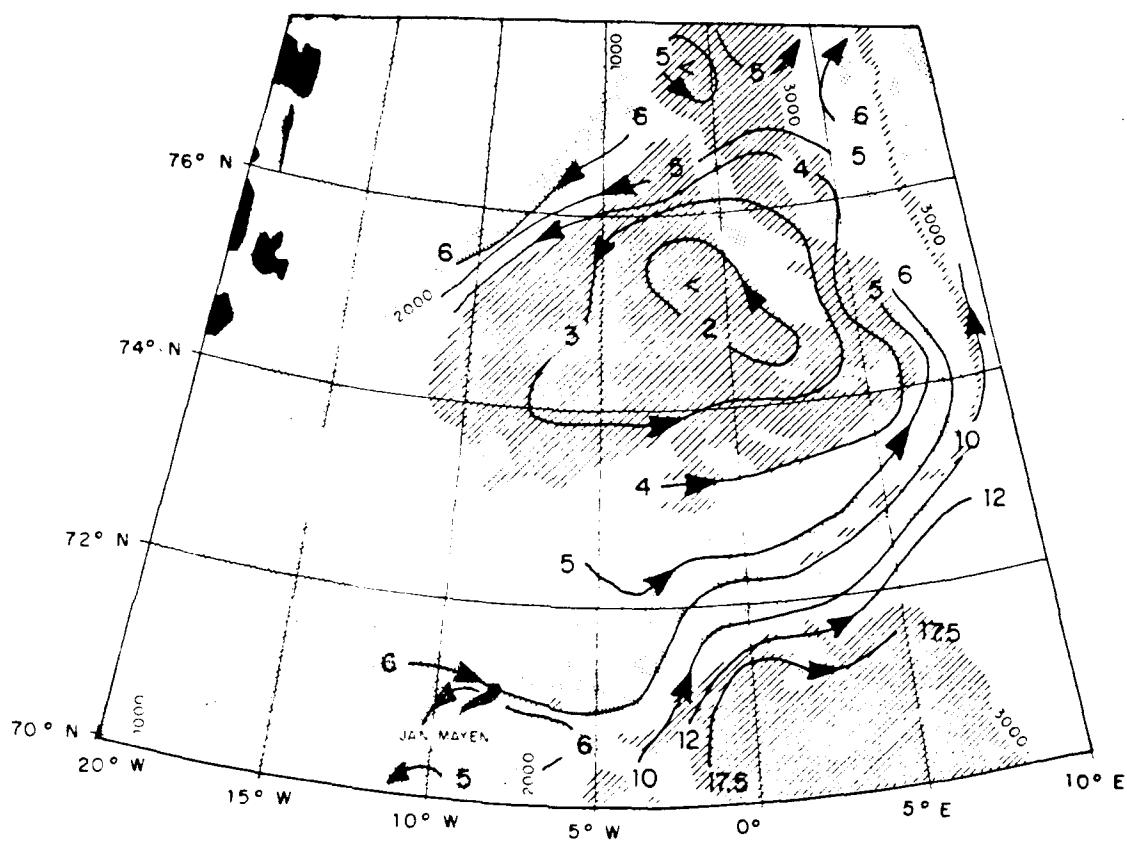


Figure 4.2 METEOR /HUDSON 82 winter dynamic height at 100 dbar referenced to 1000 dbar (dyn cm). The geopotential pattern is similar to that of BARTLETT 89 in so far as they overlap. A lack of stations prevents definition of the Jan Mayen Current, however, stations in the eastern Greenland Basin show a weak gyre circulation and a stronger gradient in the seaward fringe of the NAC. Arrows indicate the direction of frictionless baroclinic flow (from Koltermann and Lüthje, 1989).

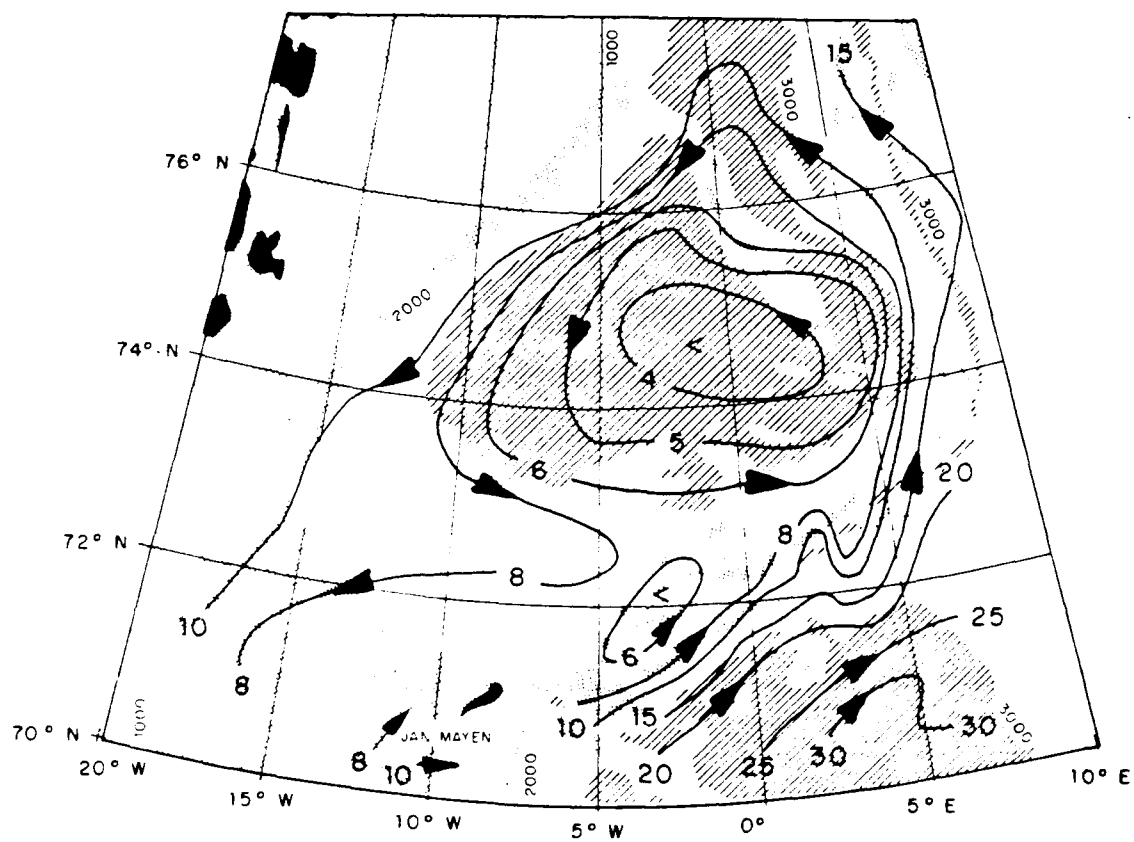


Figure 4.3 JOHAN HJORT/POLJARNIK 58 summer dynamic height at the surface referenced to 1000 dbar (dyn cm). The geopotential pattern is very similar to those in 1982 and 1989. Stations in the western Greenland Basin show the baroclinic component of the Jan Mayen Current is partly an anticyclonic meander in the East Greenland Current. Arrows indicate the direction of frictionless baroclinic flow (from Dietrich, 1969).

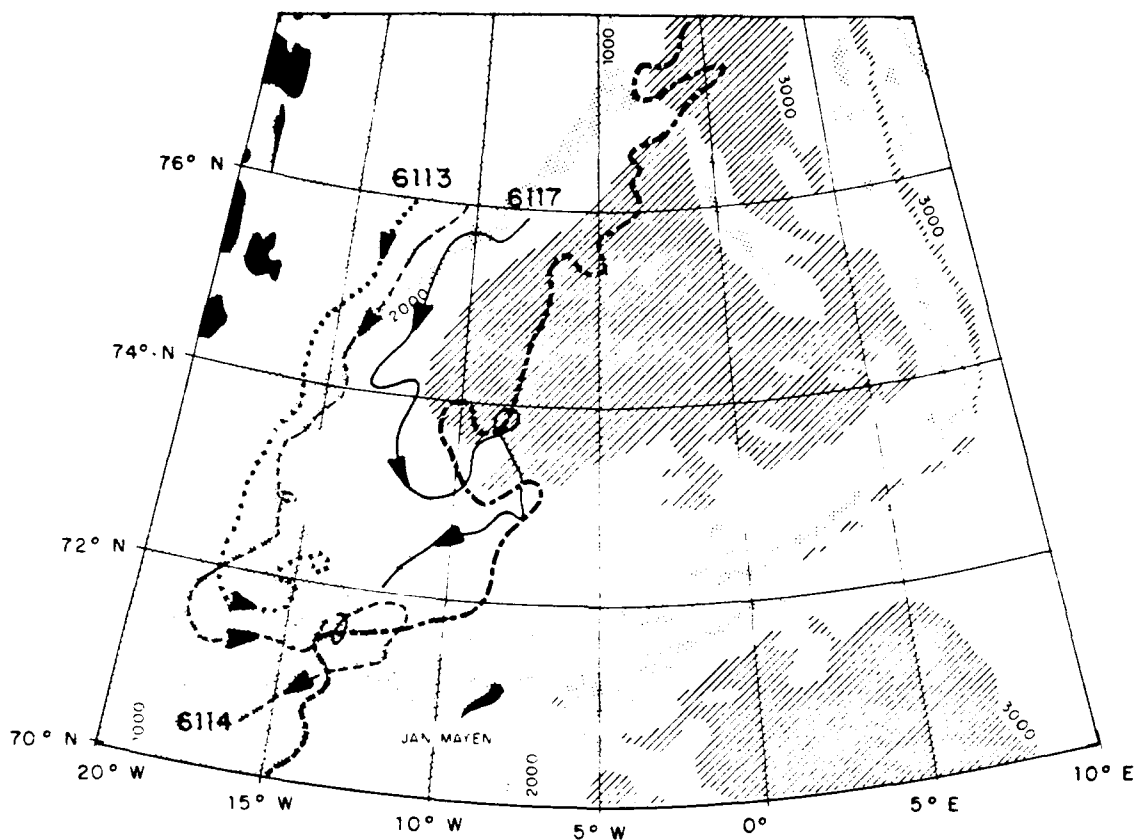


Figure 4.4

ARCTEMIZ 89 ice floe drift trajectories late May to early August (floe numbers 6113, 6114, 6117). Ice floes tracked by ARGOS beacons become involved with the Jan Mayen Current (JMC) circulation. Ice floes are initially located well within the pack away from the wind effects of the marginal ice zone and turn eastward dependent on their initial relative positions in the East Greenland Current (EGC). An analogy can be made to the turning of the warm and cold cores of the JMC. Assuming minimal wind drag and internal ice stress the floes show the total flow of the JMC is as an anticyclonic meander in the EGC in this region. Mean ice edge shown in heavy dashed line (courtesy of J.-C. Gascard, *personal communication*).

portions of three ice floe drift tracks during the time frame of late May to mid-August 1989.

Each of the three floes (numbered 6113, 6114, and 6117) initially turns eastward and then executes an anticyclonic loop to proceed toward the EGC north of the JMFZ rise. Each of the three drift tracks compares remarkably well with the BARTLETT 89 dynamic height flow pattern given a moderate meridional translation of the JMC meander axis of about 75 km over the time period from June to September 1989 (up to a four month gap between observations). The floes propagate at an approximate average speed of $> 0.2 \text{ m s}^{-1}$ in contrast to the maximum BARTLETT 89 baroclinic velocities in the area of 0.7 m s^{-1} , thus a large barotropic component is evident.

A correlation appears to exist between the relative, lateral positioning of the floe in the EGC north of 74°N and the position at which it turns eastward into the JMC. Floe 6117 located nearer the seaward edge of the EGC turned much earlier (around 73°N) than the two floes located farther westward overlying the east Greenland shelf (between $71^{\circ} 30'$ to 72°N). It is interesting to note that as the initial positions of the floes in the EGC are similar to the relative positions of the GPW and RAtIW cores straddling the EGPF. The inboard floes (6113 and 6114) demonstrate an apparent delay in turning eastward as does the JMPW core compared with the JMatIW core of the JMC in the previous chapter (see Figure 3.14). Thus, similar dynamic processes may be responsible in each case.

2. A Numerical Model

A numerical investigation of the circulation of the Greenland and Norwegian seas by *Legutke (1989)* sheds additional light on the total flow field in the JMC region. This general circulation, primitive equation model developed at the University of Hamburg achieves 20 km horizontal resolution in 12 vertical layers and resolves bottom topographic features, though eddies are not resolved since the radius of deformation (R_d) is of order 5 km at this latitude. Initial stratification and forcing functions are derived from climatological annual mean data. Model fields are subsequently forced by historical wind data over a 2.5 year period utilizing a backward time stepping scheme. Total volume exchanges through open boundaries are deduced from observations and are constant in time.

Model results in the JMC region were generously made available by *S. Legutke (personal communication)*. The streamlines in Figure 4.5 are derived from the model results and indicate the direction of the total flow field in the upper 300 m of the water column. Flow speeds vary from 14 to 0.2 m s^{-1} in the EGC to $< 0.1 \text{ m s}^{-1}$ in the JMC. Model velocities in the EGC are reasonably close to observed ice floe velocities of order 0.2 m s^{-1} . The model circulation pattern is also quite similar to the BARTLETT 89 observed baroclinic circulation in Figure 4.1. Of interest in this similarity is the manifestation of the JMC partly as an anticyclonic meander in the seaward portion of the EGC. A set of vertical velocity sections collocated with BARTLETT 89 Transects A and B show little vertical shear in the flow and point to a considerable barotropic component. Analysis of the model results clearly indicates that the axis of the JMC warm

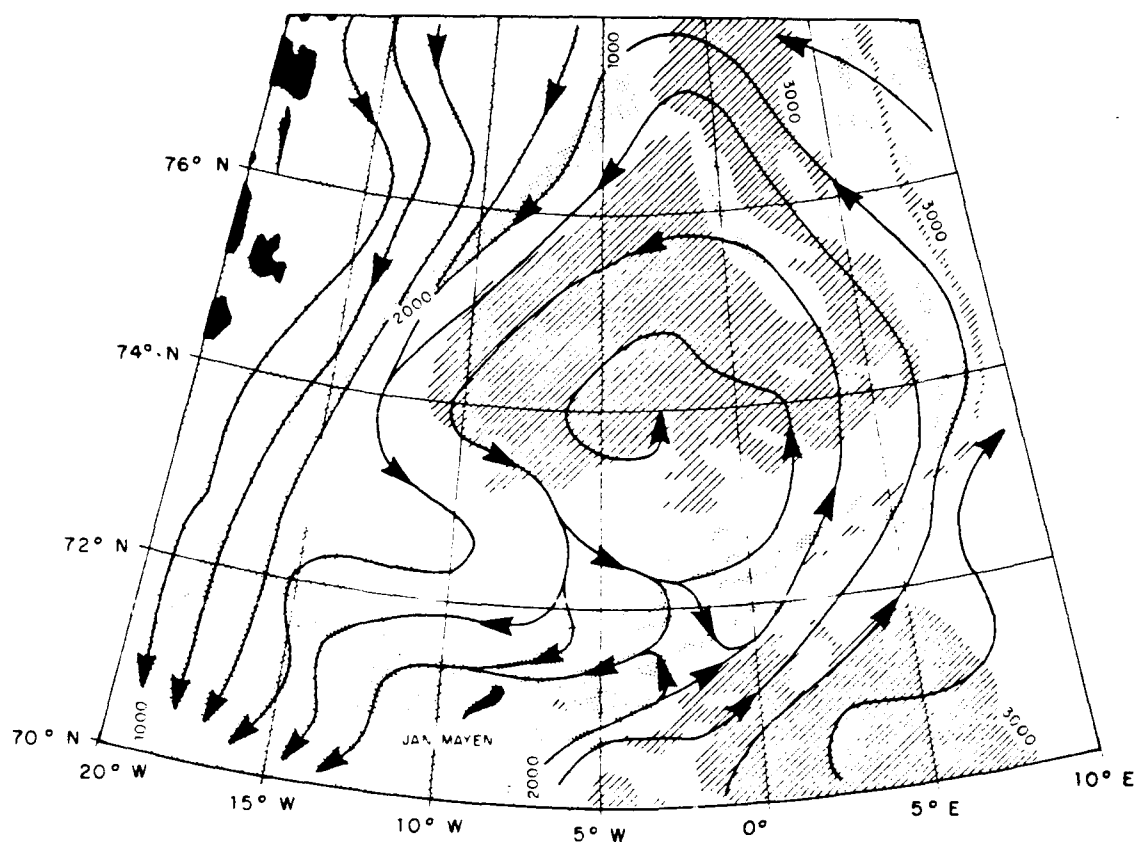


Figure 4.5 Flow streamlines of a general circulation model at the University of Hamburg. The model is initialized with mean climatological data and subsequently run for 2.5 years with 6-hourly winds. Flows through open boundaries are derived from observation and are constant in time. The Jan Mayen Current is shown as an anticyclonic meander in the East Greenland Current with secondary circulations to the Greenland Sea Gyre and Norwegian Atlantic Current (courtesy of S. Legutke, *personal communication*).

and cold cores are laterally separated (warm core to the north) as observed in the BARTLETT 89 data.

C. TRANSPORTS

Transports of fresh water and heat by the JMC and its total volume flow from the surface to 1000 m depth are calculated from BARTLETT 89 data based on the baroclinic velocity field. Baroclinic velocities are computed in vertical sections along each of the five southwest-northeast legs as well as around the perimeter of the BARTLETT 89 survey. Due to the prevalent, weak dynamic height gradient, velocities away from the EGC are typically $< 0.02 \text{ m s}^{-1}$. The core of baroclinic flow appears to be confined to the upper 100 m of the water column.

1. Total Volume Transport

Foldvik et al. (1988) estimate the net southward volume transport by the EGC above 700 m to be 3 Sv with mean speeds of $0.1\text{-}0.3 \text{ m s}^{-1}$ based on year long current meter measurements. *Bourke et al. (1988)* give an estimate of 3.1 Sv for the baroclinic transport of the EGC. Thus the net total southward transport of the EGC is estimated to be of order 3-4 Sv.

BARTLETT 89 data calculations yield an estimated total baroclinic flow of nearly 2 Sv for the JMC as it flows eastward through Transect A. Slightly less than half of the flow exits the Greenland Basin toward the NAC and about 5 % enters the GSG circulation. Approximately 1 Sv constitutes the return flow of the JMC meander which rejoins the EGC as it crosses the JMFZ sill. These flow rates appear to be proportionate

to the model transports of *S. Legutke (personal communication)*, though the flow through Transect A is 3 to 4 Sv greater in the model. The disparity in actual transports is undoubtedly due to an unknown barotropic velocity component in the BARTLETT 89 survey.

2. Transport of Fresh Water and Heat

The fresh water budget is of critical importance to vertical circulation at high latitude centers of convection such as the GSG. According to *Aagaard and Carmack (1989)*, if the surface fresh water excess is too great, a convective region may be capped causing convection to cease. Below a certain salinity, even if surface waters are cooled to the freezing point, they remain too buoyant to penetrate the intermediate waters. *Aagaard and Carmack (1989)* contend, however, that a slight surface salinity gradient is optimum, *i.e.*, a minimum degree of buoyancy must be present, to ensure that cooling at the surface is sufficient to take advantage of the thermobaric effects of compressibility at low temperatures which enhance penetration of the lower water column.

The liquid fresh water transport by the JMC into the BARTLETT 89 survey area is calculated from the baroclinic flow field using a reference salinity for the Nordic Seas of 34.93 (after *Aagaard and Carmack, 1989*). Approximately $29 \times 10^6 \text{ kg s}^{-1}$ of fresh water enters the survey area via the JMC meander while $14 \times 10^6 \text{ kg s}^{-1}$ exits to the south still within the meander, $4 \times 10^6 \text{ kg s}^{-1}$ exits to the east toward the NAC/WSC, and $11 \times 10^6 \text{ kg s}^{-1}$ remain in the survey area (Figure 4.6). Thus, nearly one half of the fresh water that leaves the EGC within the JMC meander also returns to the EGC via the meander while one third is retained in the basin. A fresh water excess of $340 \text{ km}^3 \text{ y}^{-1}$

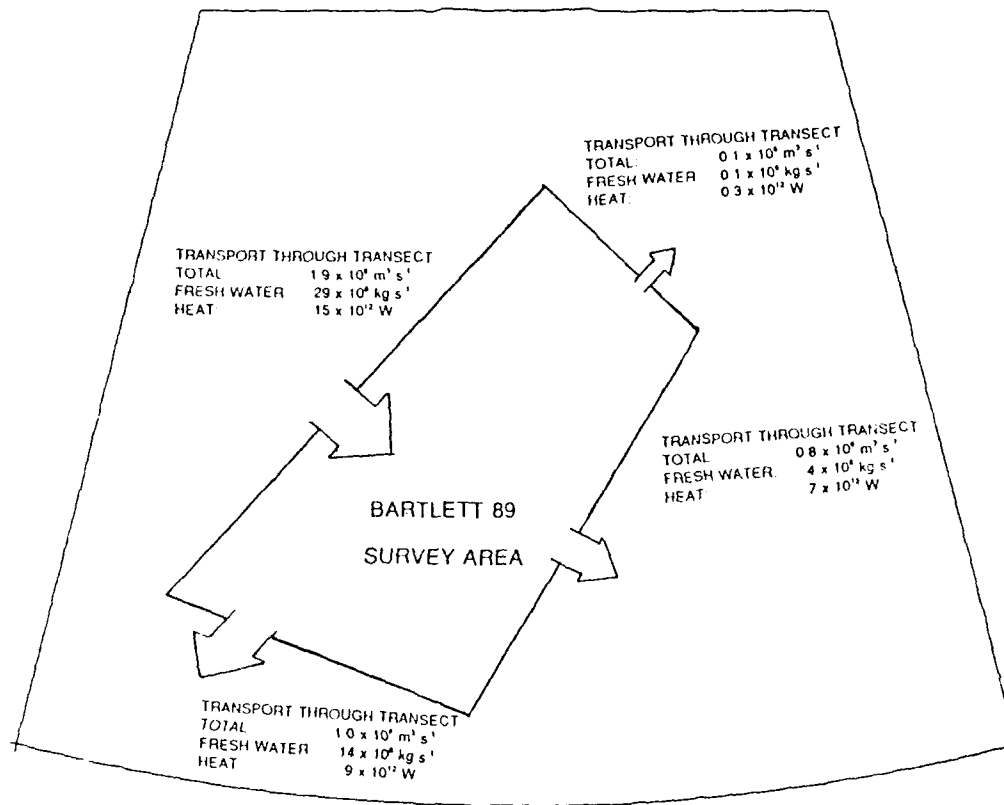


Figure 4.6 Schematic of baroclinic total volume flow rate, volume flow rate of liquid fresh water, and heat advection rate in/out of the BARTLETT 89 survey area. Fresh water volume estimated based on a reference salinity of 34.93 (Aagaard and Carmack, 1988).

results for the 240,000 km² area covered by the BARTLETT 89 survey. This equates to a 1.4 m layer of fresh water per year which must be neutralized by a combination of sea ice formation and convective mixing to maintain a balance in the region. It is assumed that the increased transport of fresh water that would be realized if the uncertain barotropic contribution (expected to be of the order of the baroclinic contribution) were to be considered is roughly balanced by the seasonal fluctuations of both the magnitude of the total flow field and the quantity of available liquid fresh water.

Aagaard and Carmack (1989) estimate the liquid fresh water content of the GSG alone to be 77 km³ over an area of 135,000 km² or 0.57 m of fresh water which is replenished annually. They note that if the effects of extreme winter cooling on surface density stratification are taken into account, only 0.29 m of annual ice formation is required to provide a sufficient increase in surface salinity to cause overturn. In comparison, the BARTLETT 89 estimate of 1.4 m seems reasonable since the estimate of *Aagaard and Carmack (1989)* solely involves the GSG which is considerably more saline in the upper water column than the remainder of the 1989 survey area and thus would store less fresh water. *Aagaard and Carmack (1989)* also estimate that annually, 1160 km³ of fresh water flows southward from the Arctic Ocean in the EGC. Thus by the BARTLETT 89 calculation roughly one third of the total annually available quantity of liquid fresh water in the EGC cycles through the Greenland Basin within the JMC meander. Roughly one fourth of this liquid fresh water volume annually available in the EGC is retained within the survey area.

Calculations of the heat transport through the BARTLETT 89 survey area utilizing a reference temperature of -1.8°C indicate a net loss at a rate of $1 \times 10^9 \text{ W}$ which is essentially indistinguishable from zero considering the size of the survey area. Thus, an advective heat balance seemed to exist at the time of the survey.

V. DEEP WATER

A. INTRODUCTION

Current thinking holds that deep water circulation within the basins of the Greenland and Norwegian seas and the Eurasian Basin of the Arctic Ocean is interconnected and semi-closed. The general deep circulation may be considered to begin with a flow out of the Eurasian Basin on the west side of Fram Strait which continues southward along the east Greenland continental slope and circulates cyclonically around the Boreas and Greenland basin system. Some of this flow branches into the Lofoten and Norwegian basins while the remainder continues in a deep cyclonic gyre eventually returning to the Eurasian Basin via the east side of Fram Strait (*Jónsson, 1989*). The three basic deep water masses within this circulation are Eurasian Basin Deep Water (EBDW) originally referred to as Arctic Ocean Deep Water (AODW), Greenland Sea Deep Water (GSDW), and Norwegian Sea Deep Water (NSDW). The names connote their predominant sea or basins of residence. Important external processes that provide input to this system include brine formation on the shelf regions surrounding the Eurasian Basin and ventilation via convection in the GSG.

Swift et al. (1983) observed AODW to be more saline than either GSDW or NSDW which enter the Eurasian Basin through Fram Strait from the Greenland and Norwegian seas. Based on radionuclide distributions, they deduce that the increase in salinity is due to the addition of brine formed in the northern Barents and other surrounding shelf

regions. AODW is referred to as EBDW by *Aagaard et al. (1985)* since it was observed to be confined to that basin by the Lomonosov Ridge. They also postulate that this EBDW is formed when brine from the peripheral arctic shelves mixes with NSDW which enters the Eurasian Basin via the east side of Fram Strait. They observed that the relatively warm, saline EBDW, in turn, exits the Eurasian Basin along the east Greenland continental slope.

GSDW has been hypothesized to form via several processes, the two principal ones being small-scale convective chimneys first observed in the Weddell Sea and modeled by *Killworth (1979)* who states this process could apply to the GSG; and double diffusive cooling of a subsurface Atlantic Water layer proposed by *Carmack and Aagaard (1973)*. *Rudels et al. (1989)* recently observed a convective event which attained a depth of 1250 m during the 1988 cruise of VALDIVIA. In explanation they present a complex, small-scale process of overturn events which proceed in step-wise fashion to depths dependent on sea ice conditions and the stratification of the upper water column. This process yields GSDW which bears the relatively cold, fresh signature of the surface waters at the time of formation.

Smethie et al. (1988), based on Chlorofluoromethane (CFM) distributions, collate previous findings into a logical scheme of deep water flow between the Eurasian Basin and the Greenland and Norwegian seas and offer an explanation of the process which yields NSDW. CFM, a water mass tracer which is introduced at the surface, has recently been detected in larger amounts than in previous years, thus providing a means of deep water age determination.

Smethie et al. (1988) show that EBDW exits the Eurasian Basin where the pressure compensated density anomaly referenced to 2000 dbar (σ_2) is about 37.46 kg m^{-3} . This density surface is coincident with the sill depth at Fram Strait and is also that occupied by GSDW. The southward isopycnal flow of EBDW along the east Greenland continental slope is unobstructed until it encounters the JMFZ where it is forced eastward to circulate cyclonically around the southern periphery of the Greenland Basin.

During this southward journey in the Greenland Sea they postulate that EBDW and GSDW mix isopycnally in equal parts producing the uniform water mass, new NSDW, distinguishable from old NSDW only by a high concentration of CFM supplied by the GSDW component. Some new NSDW flows eastward through gaps in the southern Mohn Ridge system into the Norwegian and Lofoten basins and some flows northward through the Boreas Basin. Eventually old NSDW, distinguishable from new NSDW only by a lower concentration of CFM, leaves the northern Lofoten Basin to join the northward flow of new NSDW, some of which recirculates southward under the EGC and some of which flows back into the Eurasian Basin with smaller quantities of GSDW via the east side of Fram Strait.

Swift and Koltermann (1988) present evidence in the form of hydrographic and current meter data that the inflow of new NSDW to the Norwegian and Lofoten basins occurs through the trough associated with the JMFZ. Deep water properties in the Greenland and Lofoten basins during the BARTLETT 89 survey seem to support the contention of *Swift and Koltermann (1988)*.

B. ANALYSIS OF BARTLETT 89 DEEP WATER DATA

The three deep water masses which are present in the Greenland Basin are listed in Table 5.1. Potential temperatures and salinities for these waters are presented from various data sources for comparison. With the exception of values from *Hopkins (1988)*, which are summarized from recent literature, values derived from actual data sets are an arithmetic mean of measurements at or below 2500 m depth, a regime where the deep waters are relatively homogeneous (look ahead to Figure 5.3). The population size and standard deviation are also included.

The BARTLETT 89 data are extracted from the final data report of the Ocean Data Facility (ODF) at Scripps Institution of Oceanography (SIO). Temperatures are from calibrated CTD measurements and salinities are determined from bottle samples analyzed on an Autosol. Data from Stations 2, 11, and 21 are used to determine values for GSDW (see Figure 2.1 for station locations). Data from HAAKON MOSBY 89 Station 32, which is collocated with the Greenland Sea Project inter-calibration site, is used to determine values for NSDW (see Figure 2.1). BARTLETT 89 Stations 40 and 48 are not used in this determination of NSDW since at these locations NSDW occurs in areas where the vertical density gradient is too great for an accurate assessment of deep water core properties. The HAAKON MOSBY Station 32 data are extracted from the ODF preliminary data report though is considered comparable to BARTLETT 89 data in that both CTD instruments were calibrated in the same time frame at SIO. These data were graciously made available by A. Foldvik (*personal communication*). JOHAN HJORT 58 values are discussed in the following section.

Table 5.1 Deep Water Masses of the Greenland Basin. The potential temperatures and salinities represent mean values at or below 2500 m \pm standard deviation from the indicated data set. Population size is in parens. Values from *Hopkins (1988)* represent values summarized from recent literature.

Data Source	Water Mass		
	Greenland Sea Deep Water (GSDW)	Norwegian Sea Deep Water (NSDW)	Eurasian Basin Deep Water (EBDW)
BARTLETT 89	-1.200 \pm .014 34.896 \pm .001 (12)		
HAAKON MOSBY 89		-1.045 \pm .004 34.907 \pm .001 (18)	
JOHAN HJORT 58 Summer	-1.21 \pm .03 (7)	-1.05 \pm .01 (3)	
JOHAN HJORT 58 Winter	-1.18 \pm .02 (3)	-1.04 \pm .01 (2)	
<i>Hopkins (1988)</i>	-1.25 34.89	-1.05 34.91	-0.80 34.93

The Θ -S curves for each of the five BARTLETT 89 stations deeper than 1000 m plus HAAKON MOSBY 89 Station 32 are shown in Figure 5.1. Stations 2, 11, and 21 in the northern and central Greenland Basin are relatively cold and fresh compared to Station 48 and H. MOSBY Station 32 located within the Lofoten Basin which are slightly warmer (by $> 0.1^{\circ}\text{C}$) and saltier (by > 0.05 PSU). Station 40 is located in 2200 m of water on the west side of the JMFZ trough which leads to the Lofoten Basin. This station shares characteristics of both basins starting warm and salty at 1000 m then becoming cold and fresh near the bottom.

Smethie et al. (1988) observe EBDW to occupy a level where $\sigma_2 = 37.46 \text{ kg m}^{-3}$ which corresponds to a depth in the Eurasian Basin of 2400-2500 m or approximately the 2600 m sill depth at Fram Strait. In the Greenland Basin this density surface occurs at a depth of 1500-2000 m, above the denser GSDW. Figure 5.2 shows Θ -S characteristics of station data within the band where $\sigma_2 = 37.45$ to 37.46 kg m^{-3} . A steady progression of properties occurs along this isopycnal band from Stations 2 and 11 in the northwestern Greenland Basin to Station 21 in the central basin to Stations 40 and 48 separated by the JMFZ trough and H. MOSBY Station 32 in the central Lofoten Basin. The steady increase in temperature and salinity across these stations is assumed to be due to the isopycnal influx of EBDW circulating with GSDW initially southward along the east Greenland continental slope, thence cyclonically along the JMFZ, and eventually northward along the west side of the Mohn Ridge back to the Boreas Basin. Thus, the mixing of EBDW and GSDW seems to occur along the western and southern periphery of the deep cyclonic circulation in the Greenland-Boreas basin system.

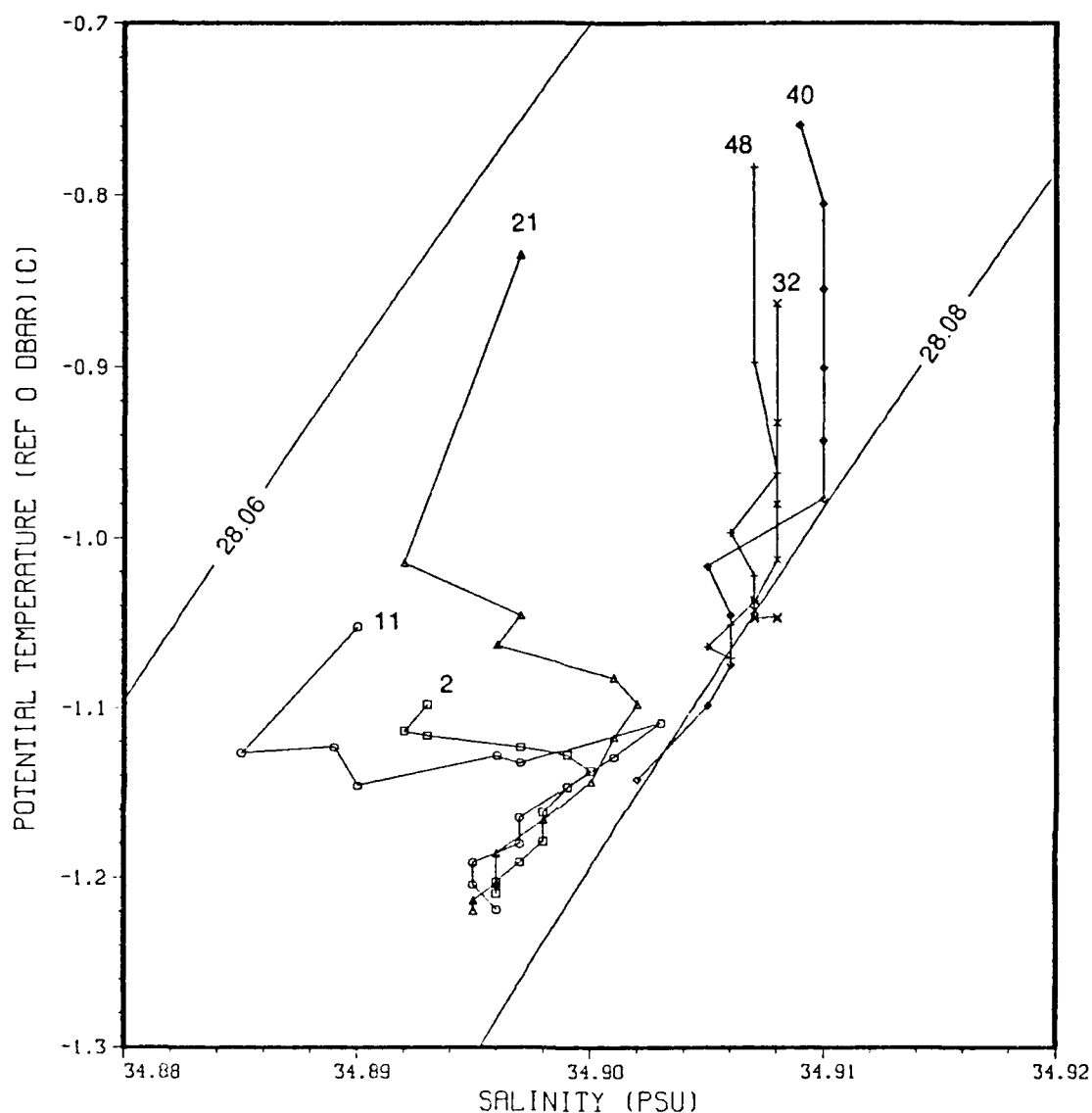


Figure 5.1

Θ -S diagram of BARTLETT 89 (plus H. MOSBY 89 Station 32) deep station bottle data (1000-3500 m) on contours of σ_{θ} (ref. pressure 0 dbar). Θ -S curves of Stations 2, 11, and 21 in the Greenland Sea Deep Water of the north and central Greenland Basin are characteristically colder, and fresher than those of Stations 48 and H. MOSBY Station 32 in the Norwegian Sea Deep Water of the Lofoten Basin. Station 40 located in the Greenland Basin at the mouth of the Jan Mayen Fracture Zone trough shares characteristics of both water masses. These curves enable comparison of potential temperatures and salinities between water masses and visualization of the differences in vertical gradients between the basins, however, density comparison of the deep waters is inaccurate with pressure referenced to the surface. See Table 5.1 for water mass descriptions (H. MOSBY data courtesy of A. Foldvik, *personal communication*).

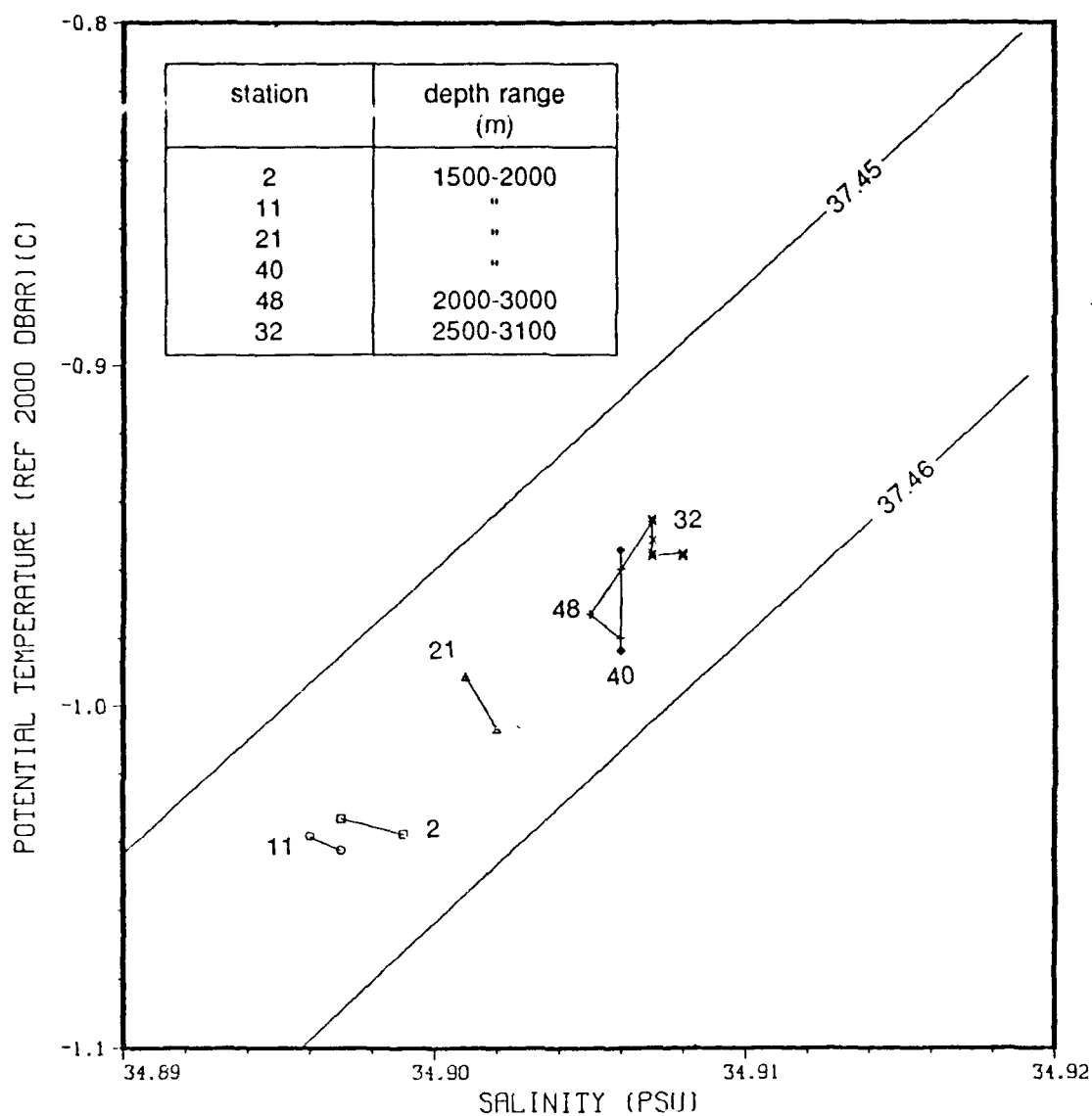


Figure 5.2

Θ -S diagram of BARTLETT 89 (plus H. MOSBY 89 Station 32) deep station bottle data ($\sigma_2 = 37.45$ to 37.46 kg m^{-3}) (ref. pressure 2000 dbar). On this pressure-compensated density surface is seen the progressive isopycnal mixing southeastward across the Greenland Basin of warm, saline Eurasian Basin Deep Water and cold, fresh Greenland Sea Deep Water to form Norwegian Sea Deep Water. The process is complete at Station 40 located within the Greenland Basin. This progression corroborates the theory of Swift and Koltermann (1988). Depth range of this density surface is given for each station. Refer to Table 5.1 for water mass descriptions (H. MOSBY data courtesy of A. Foldvik, personal communication).

The progression of properties between these stations illustrated in Figure 5.2 shows that isopycnal mixing of EBDW and GSDW to form NSDW is already complete at Station 40 located on the west side of the Mohn Ridge at the mouth of the JMFZ trough. Beginning at Stations 2 and 11, properties are characteristic of GSDW and occur at 1500-2000 m depth. At Station 21 properties (still at 1500-2000 m) are mid-way between those at Stations 2 and 11 and those at Stations 40, 48 and H. MOSBY Station 32. Finally, properties at the latter group of stations share the characteristics of NSDW. In this region the depth of the density surface cascades from 1500-2000 m at Station 40 to 2000-2500 m at Station 48 to 2500-3500 m at H. MOSBY Station 32. The theory of *Swift and Koltermann (1988)* seems to be demonstrated by these limited observations.

On a σ_3 plane, Figure 5.3 shows that properties are relatively homogeneous at Stations 2, 11, 21, 48, and H. MOSBY Station 32 in the near-bottom or core deep waters which lie beneath the isopycnal mixing described above. Station 40 terminates at the bottom at about 2100 m and is not shown. In the Greenland Basin at Stations 2, 11, and 21 core GSDW occurs in the band where $\sigma_3 = 41.99$ to 42.00 kg m^{-3} . At Station 48 and H. MOSBY Station 32 in the Lofoten Basin core NSDW is less dense and occurs in the band where $\sigma_3 = 41.98$ to 41.99 kg m^{-3} . The homogeneous waters at Station 48 lie in a deep depression and are slightly denser than at the same depth at H. MOSBY Station 32 indicating GSDW influence. NSDW lies above this depth at Station 48, still in the final stages of mixing.

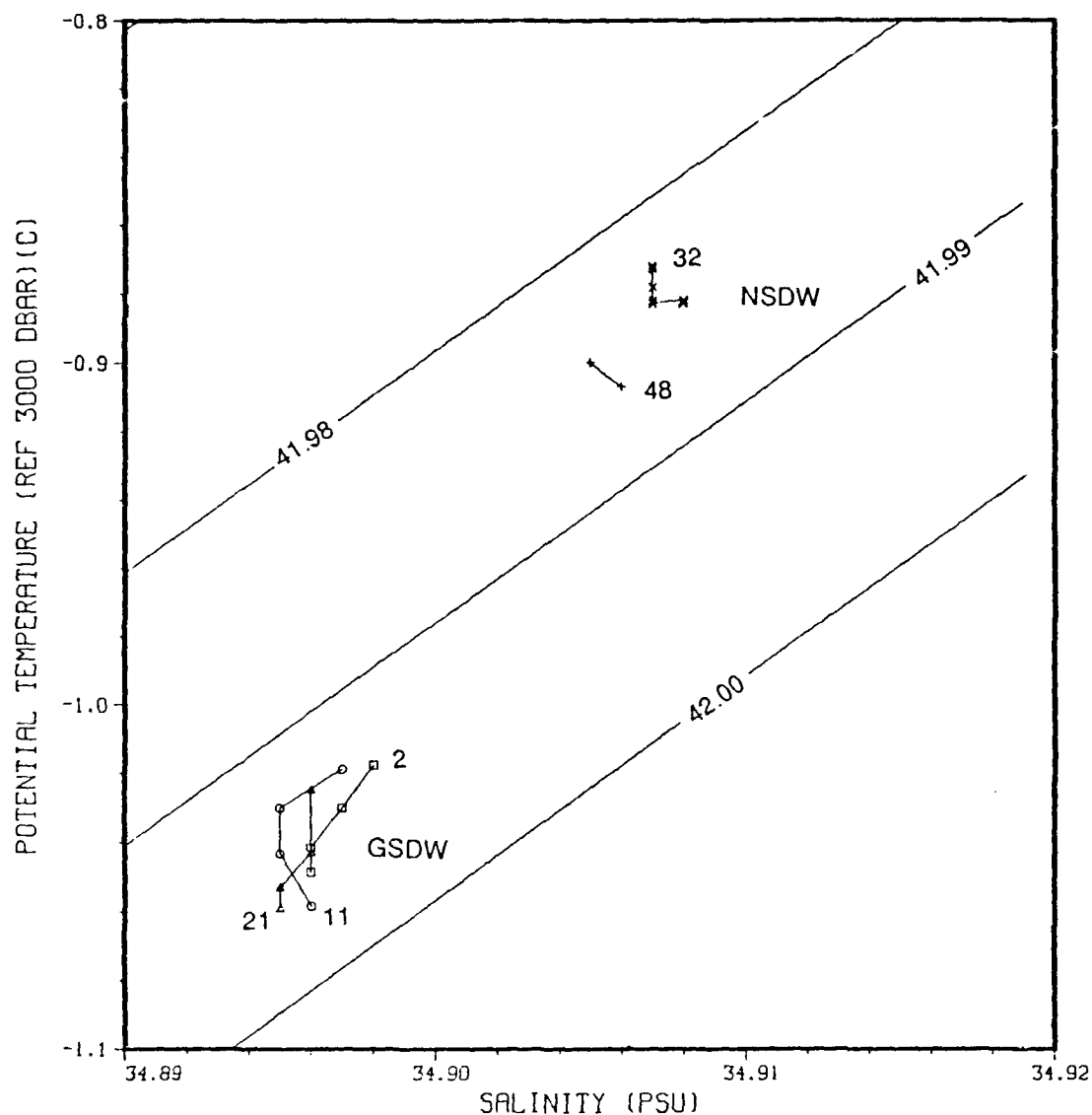


Figure 5.3

Θ -S diagram of BARTLETT 89 (plus H. MÖSBY 89 Station 32) deep station bottle data below 2500 m ($\sigma_t = 41.98$ to 42.00 kg m^{-3}) (ref. pressure 3000 dbar). The near-bottom waters are most comparable on this pressure-compensated density surface. The vertical density gradient at each station is minimal at this level. The core Greenland Sea Deep Water of the Greenland Basin is significantly denser than the core Norwegian Sea Deep Water of the Lofoten Basin. Refer to Table 5.1 for water mass descriptions (H. MÖSBY data courtesy of A. Foldvik, *personal communication*).

Concerning the concept of a bottom water, since the vertical density gradient is smooth in the deep waters which overlie the core NSDW in the Lofoten Basin, there are no grounds to delineate a bottom water (compare Figures 5.1 and 5.3). In the Greenland Basin, however, relatively sharp vertical temperature and salinity gradients occur above the core GSDW where isopycnal mixing is taking place. Thus, in the sense that the deepest waters in the Greenland Basin are isolated by an overlying intrusion of EBDW at these BARTLETT 89 stations, they could be considered bottom waters in much the same manner that *Smethie et al. (1988)* define Eurasian Basin Bottom Water. *Kottermann and Lüthje (1989)* do not recognize a bottom water in the Greenland Basin, but simply define the density level where $\sigma_3 = 41.005$ as the upper limit of core GSDW. Alas, the existence of such a separation of bottom waters across the entire basin cannot be assessed with the limited number of deep stations in this study.

C. HISTORICAL COMPARISON

The only digital historical deep water data conveniently usable for this study are those of the JOHAN HJORT 58 survey from which summer and winter data have been selected from locations similar to the BARTLETT 89 deep stations. A quantitative comparison of salinity is not possible since the presumed margin of error of the Mohr titration is of the order of 0.03 PSU which is greater than the entire salinity range of the BARTLETT 89 deep water data set. In both winter and summer 1958, however, there appears to be a progressive increase in salinity southeastward across the Greenland Basin

of about 0.02 PSU as is observed in 1989. The progressive increase in salinity results in salinities becoming similar on both sides of the JMFZ trough.

The range of potential temperatures derived from reversing thermometer measurements, having a presumed accuracy of $\pm 0.01^\circ\text{C}$, compare well with temperatures at collocated BARTLETT 89 stations. In both seasons of 1958, a progressive warming trend southeastward across the basin occurs as in 1989. Most interesting is the close agreement in potential temperatures among data sets seen in Table 5.1. In all cases potential temperatures could be considered nearly identical taking into account the standard deviation. The plots found in *Koltermann and Lüthje (1989)* of potential temperature and salinity on the density surface where $\sigma_2 = 37.457 \text{ kg m}^{-3}$ also show warm, saline waters circuiting the western and southern limbs of the deep gyre in the Greenland Basin toward the Mohn Ridge. The temperature and salinity range of these waters seem to be in very good agreement with BARTLETT 89 deep data though statistical comparison is not possible. Thus, there appears to be no appreciable inter-annual variation in temperature in either basin though slight cooling following the winter season is indicated in both basins in 1958. Conclusions must be tempered, however, since the statistical population is small and deep station spacing is sparse.

VI. CONCLUSIONS

A thorough analysis of data obtained during the September 1989 cruise of the USNS BARTLETT to the southern Greenland Sea, together with available supplemental and historical data, leads to several conclusions.

Hydrographic analyses show the Jan Mayen Current (JMC) is manifested in the eastward bowing of East Greenland Current (EGC) waters in the region of 74°N which are confined to the Greenland Basin in their eastward extent. Historical data *Dietrich, 1969; Koltermann and Lüthje, 1989*) show the axis of the JMC extension may vary of order 100 km north or south of this position.

The surface signature of the JMC consists of a tongue of cold, fresh Greenland Polar Water (GPW) which forms a shallow frontal boundary with the warmer, more saline surface arctic waters of the Greenland Sea Gyre (GSG) to the north and the considerably warmer, saline Atlantic surface waters of the Norwegian Atlantic and West Spitsbergen Currents (NAC/WSC). At intermediate depths the JMC consists of a system of two cores, one of cold, moderately saline Jan Mayen Polar Water (JMPW) at ~50 m and one of warm, saline Jan Mayen Atlantic Intermediate Water (JMA_{At}IW) at ~100 m. The cold core of JMPW (modified GPW) is displaced about 100 km southward of the warm core of JMA_{At}IW (modified Return Atlantic Intermediate Water (RA_{At}IW)). The warm core forms a frontal boundary with the cooler, more weakly stratified intermediate arctic waters of the GSG to the north. To the south a weak front is observed between the warm core

and the more homogeneous intermediate waters of the NAC at the southeast corner of the Greenland Basin. Horizontal sections of various surface and intermediate properties consistently portray a response to underlying bathymetric features indicative of the predominantly barotropic circulation of the JMC system.

A comparison with historical data (*Dietrich, 1969; Koltermann and Lüthje, 1989*) is highlighted by a significant cooling and freshening of the upper few hundred meters of the water column in 1982 and 1989, most likely resulting from above normal GPW influx. Little if any GPW influence is indicated in 1958. Also, a perturbation with a RATIW core in the seaward fringe of the EGC just south of the Greenland Fracture Zone occurs in both 1982 and 1989 suggesting a possible semi-permanent eddy or meander at this location which corroborates the observations of *Gascard et al. (1988)* and *Muench (1990b)*.

Strong similarities between the dynamic height field (0-1000 dbar) and the Lagrangian trajectories of drifting ice floes (*Gascard and Richez, 1989*) as well as the results of a general circulation model (*Legutke, 1989*) lead to the major finding of this study. The JMC is revealed to be partly an anticyclonic meander in the seaward fringe of the EGC, triggered by the bathymetric influence of the JMFZ, contrary to the classical view of a continuous eastward flow solely constituting the southern limb of the GSG. Baroclinic calculations show a total eastward meander flow of 2 Sv with half of that flow remaining within the meander to rejoin the EGC and half being distributed between the GSG and NAC/WSC. Baroclinic estimates of the annual liquid fresh water excess as a result of the transport of the JMC equate to a 1.4 m layer over the survey area. This

volume represents roughly one quarter of the total annually available volume of fresh water in the EGC estimated by *Aagaard and Carmack (1989)*.

Analyses of the deep data indicate isopycnal mixing of warm, saline Eurasian Basin Deep Water (EBDW) and cold, fresh Greenland Sea Deep Water (GSDW) to yield Norwegian Sea Deep Water (NSDW). The mixing ratios reveal that NSDW is increasingly prevalent toward the southern limb of the deep cyclonic gyre along the JMFZ such that mixing is complete on the Greenland Basin side of the Mohn Ridge, corroborative of the NSDW formation process hypothesized by *Smethie et al. (1988)* and *Swift and Koltermann (1988)*. Comparison with deep data from the 1982 cruises of the METEOR and HUDSON and the 1958 cruises of the JOHAN HJORT indicates no appreciable inter-annual fluctuation in temperature or salinity.

LIST OF REFERENCES

- Aagaard, K., Wind-driven transports in the Greenland and Norwegian seas, *Deep-Sea Research*, 17, 281-291, 1970.
- Aagaard, K. and E.C. Carmack, The role of sea ice and other fresh water in the Arctic circulation, *Journal of Geophysical Research*, 94, 14,485-14,498, 1989.
- Aagaard, K., J.H. Swift, and E.C. Carmack, Thermohaline circulation in the arctic mediterranean seas, *Journal of Geophysical Research*, 90, 4833-4846, 1985.
- Bourke, R.H., R.F. Blythe, and R.G. Paquette, Preliminary cruise report of USNS BARTLETT to the Greenland Sea in September 1989, *Technical Report NPS 68-90-001*, Naval Postgraduate School, Monterey, California, 1989.
- Bourke, R.H., R.F. Blythe, and R.G. Paquette, Data report, USNS BARTLETT cruise to the Greenland Sea in September 1989, *Technical Report NPS 68-90-006*, Naval Postgraduate School, Monterey, California, 1990.
- Bourke, R.H., J.L. Newton, R.G. Paquette, and M.D. Tunnicliffe, Circulation and water masses of the east Greenland shelf, *Journal of Geophysical Research*, 92, 6729-6740, 1987.
- Bourke, R.H., A.M. Weigel, and R.G. Paquette, The westward turning branch of the West Spitsbergen Current, *Journal of Geophysical Research*, 93, 14,065-14,077, 1988.

- Carmack, E.C. and K. Aagaard, On the deep water of the Greenland Sea, *Deep-Sea Research*, 20, 687-715, 1973.
- Dickson, R.R., J. Meincke, S.-A. Malmberg, and A.J. Lee, The "great salinity anomaly" in the northern North Atlantic 1968-1982, *Progress in Oceanography*, 20, 103-151, 1988.
- Dietrich, G., *Atlas of the Hydrography of the Northern North Atlantic*, Conseil International Pour L'Exploration de la Mer, Service Hydrographique, Copenhagen, 1969.
- Foldvik, A., K. Aagaard, and T. Tørresen, On the velocity field of the East Greenland Current, *Deep-Sea Research*, 35, 1335-1354, 1988.
- Gascard, J.-C., C. Kergomard, P.-F. Jeannin, and M. Fily, Diagnostic study of the Fram Strait marginal ice zone during summer from 1983 and 1984 Marginal Ice Zone Experiment Lagrangian observations, *Journal of Geophysical Research*, 93, 3613-3641, 1988.
- Gascard, J.-C. and C. Richez, ARCTEMIZ 89 17 Aout au 26 Septembre 1989 rapport de mission, *Rapport interne LODYC 89/05*, Laboratoire D'Océanographie Dynamique et de Climatologie, Université Pierre and Marie Curie, Paris, 1989.
- Hopkins, T.S., THE GIN SEA Review of Physical Oceanography and Literature from 1972, *SACLANTCEN Report SR-124*, Undersea Research Centre, Supreme Allied Command Atlantic, 1988.

- Jónsson, S., The structure and forcing of the large- and mesoscale circulation in the Nordic Seas, with special reference to the Fram Strait, Ph.D. thesis, Department of Oceanography, University of Bergen, Bergen, 1989.
- Killworth, P.D., On "chimney" formations in the ocean, *Journal of Physical Oceanography*, 9, 531-534, 1979.
- Koltermann, K.P. and H. Lüthje, *Hydrographic Atlas of the Greenland and Northern Norwegian Seas (1979-1987)*, Deutsches Hydrographisches Institut Nr. 2328, Hamburg, 1989.
- Lazier, J.R.N., Oceanographic conditions at Ocean Weather Ship BRAVO 1964-1974, *Atmosphere-Ocean*, 18, 227-238, 1980.
- Legutke, S., A numerical investigation of the circulation in the Greenland and Norwegian seas, Ph.D. thesis, Institut für Meereskunde, Universität Hamburg, Hamburg, 1989.
- Muench, R.D., The Sea Ice Margins: A Summary of Physical Phenomena, *NOAA Technical Memorandum ERL PMEL-88*, Environmental Research Laboratories, National Oceanic and Atmospheric Administration, Department of Commerce, Washington, D.C., 1989.
- Muench, R.D., The oceanography report, *EOS, Transactions, American Geophysical Union*, 71, 750-755, 1990a.
- Muench, R.D., Mesoscale phenomena in the polar oceans, in *Polar Oceanography, Part A: Physical Science*, pp. 223-285, Academic Press, Inc., New York, 1990b.
- Paquette, R.G., R.H. Bourke, J.F. Newton, and W.F. Perdue, The East Greenland Polar Front in autumn, *Journal of Geophysical Research*, 90, 4866-4882, 1985.

- Parkinson, C.L., J.C. Comiso, H.J. Zwally, D.J. Cavalieri, P. Gloersen, and W.J. Campbell, Arctic Sea Ice, 1973-1976: Satellite passive-microwave observations, *NASA Report SP-489*, pp. 193-195, Scientific and Technical Information Branch, National Aeronautics and Space Administration, Washington, D.C., 1987.
- Perry, R.K., H.S. Fleming, N.Z. Cherkis, R.H. Feden, and P.R. Vogt, *Bathymetry of the Norwegian-Greenland and Western Barents Seas*, chart, Environmental Sciences Branch, Acoustics Division, Naval Research Laboratory, Washington, D.C., revised, 1984.
- Rudels, B., D. Quadfasel, H. Friedrich, and M.-N. Houssais, Greenland Sea convection in the winter of 1987-1988, *Journal of Geophysical Research*, 94, 3223-3227, 1989.
- Smethie, W.M., Jr., D.W. Chipman, J.H. Swift, and K.P. Koltermann, Chloro-fluoromethanes in the arctic mediterranean seas: evidence for formation of bottom water in the Eurasian Basin and deep-water exchange through Fram Strait, *Deep-Sea Research*, 35, 347-369, 1988.
- Swift, J.H. and K.P. Koltermann, The origin of Norwegian Sea Deep Water, *Journal of Geophysical Research*, 93, 3563-3569, 1988.
- Swift, J.H., T. Takahashi, and H.D. Livingston, The contribution of the Greenland and Barents seas to the deep water of the Arctic Ocean, *Journal of Geophysical Research*, 88, 5981-5986, 1983.

INITIAL DISTRIBUTION LIST

1.	Defense Technical Information Center Cameron Station Alexandria, Virginia 22304-6145	2
2.	Library (Code 52) Naval Postgraduate School Monterey, California 93943-5000	2
3.	Chairman (Code Oc) Department of Oceanography Naval Postgraduate School Monterey, California 93943-5000	1
4.	Chairman (Code Mr) Department of Meteorology Naval Postgraduate School Monterey, California 93943-5000	1
5.	Superintendent Attn: Dr. R.H. Bourke (Code Oc/Bf) Dr. R.G. Paquette (Code Oc/Pa) Dr. K.L. Davidson (Code Mr/Ds) Naval Postgraduate School Monterey, California 93943-5000	7 1 1
6.	Research Administration (Code RI) Naval Postgraduate School Monterey, California 93943-5000	1
7.	Chairman Department of Oceanography U.S. Naval Academy Annapolis, Maryland 21402	1
8.	Chief of Naval Operations Attn: NOP-02 NOP-22 Department of the Navy Washington, D. C. 20350	1 1

- | | | |
|-----|--|---|
| 9. | Chief of Naval Research
Attn: Arctic (Code 1125)
800 N. Quincy Street
Arlington, Virginia 22217 | 1 |
| 10. | Commander
Naval Oceanography Command
Stennis Space Center
Bay St. Louis, Mississippi 39522-5000 | 1 |
| 11. | Commanding Officer
Naval Oceanographic and Atmospheric
Research Laboratory
Stennis Space Center
Bay St. Louis, Mississippi 39522 | 1 |
| 12. | Commanding Officer
Naval Oceanographic Office
Stennis Space Center
Bay St. Louis, Mississippi 39522-5001 | 1 |
| 13. | Commanding Officer
Naval Polar Oceanography Center,
Suitland
Washington, D.C. 20373 | 1 |
| 14. | Director (Code 19)
Arctic Submarine Laboratory
Building 371
Naval Ocean Systems Center
San Diego, California 92152 | 2 |
| 15. | Director
Attn: Technical Information Division
Naval Research Laboratory
Washington, D. C. 20375 | 1 |
| 16. | Director Naval Oceanography Division
Naval Observatory
34th and Massachusetts Avenue NW
Washington, D.C 20390 | 1 |

- | | | |
|-----|---|-------------|
| 17. | Director
Naval Oceanographic and Atmospheric
Research Laboratory
Monterey, California 93943-5006 | 1 |
| 18. | Commanding Officer
Submarine Development Squadron TWELVE
Naval Submarine Base
New London
Groton, Connecticut 06349 | 1 |
| 19. | Cold Regions Research and Engineering Laboratory
Attn: Library
U.S. Army Corps of Engineers
Hanover, New Hampshire 03755-1290 | 1 |
| 20. | Applied Physics Laboratory
Attn: Mr. R.E. Francois
Dr. J. Morison
Library
University of Washington
1013 Northeast 40th Street
Seattle, Washington 98105 | 1
1
1 |
| 21. | Woods Hole Oceanographic Institute
Attn: Dr. N. Fofonoff
Library
Woods Hole, Massachusetts 02543 | 1
1 |
| 22. | Scripps Institution of Oceanography
Attn: Dr. B.D. Cornuelle (A-030)
Dr. P.F. Worcester (A-030)
Dr. J.H. Swift (A-014)
La Jolla, California 92093 | 1
1
1 |
| 23. | Graduate School of Oceanography
Attn: Library
Narragansett Bay Campus
University of Rhode Island
Narragansett, Rhode Island 02882 | 1 |

- | | | |
|-----|--|-------------|
| 24. | School of Oceanography
Attn: Dr. L.K. Coachman
Dr. S. Martin
Library
University of Washington
Seattle, Washington 98195 | 1
1
1 |
| 25. | School of Oceanography
Attn: Library
Oregon State University
Corvallis, Oregon 97331 | 1 |
| 26. | Scott Polar Research Institute
Attn: Sea Ice Group
Library
University of Cambridge
Cambridge, England
CB2 1ER | 1
1 |
| 27. | Institute of Polar Studies
Attn: Library
103 Mendenhall
125 South Oval Mall
Columbus, Ohio 43210 | 1 |
| 28. | Institute of Marine Science
Attn: Library
University of Alaska
Fairbanks, Alaska 99701 | 1 |
| 29. | Department of Oceanography
Attn: Library
University of British Columbia
Vancouver, British Columbia
Canada
B2Y 4A2 | 1 |

- | | | |
|-----|--|-------------|
| 30. | Bedford Institute of Oceanography
Attn: Dr. P. Jones
Dr. A. Clarke
Library
P.O. Box 1006
Dartmouth, Nova Scotia
Canada
B2Y 4A2 | 1
1
1 |
| 31. | Department of Oceanography
Attn: Library
Dalhousie University
Halifax, Nova Scotia
Canada
B3H 4J1 | 1 |
| 32. | National Snow and Ice Data Center
Attn: MIZEX Data Manager,
Dr. R. Armstrong
Cooperative Institute for Research
in Environmental Sciences
Boulder, Colorado 80309 | 2 |
| 33. | Institute of Ocean Sciences
Attn: Dr. E. Carmack
Dr. E.L. Lewis
P.O. Box 6000
Sidney, British Columbia
Canada
V8L 4B2 | 1
1 |
| 34. | Institut fur Meereskunde
Attn: Dr. D. Quadfasel
Dr. J. Meincke
Dr. S. Legutke
Universitat Hamburg
Troplowitzstrasse 7
D-2000 Hamburg 54
Federal Republic of Germany | 1
1
1 |

- | | | |
|-----|---|--------|
| 35. | Pacific Marine Environmental Laboratory
Attn: Dr. K. Aagaard
Dr. C. Pease
National Oceanic and Atmospheric
Administration
7600 Sand Point Way NE
Seattle, Washington 98115-0070 | 1
1 |
| 36. | Department of Geology
Attn: Dr. T.O. Manley
Middlebury College
Middlebury, Vermont 05753 | 1 |
| 37. | Geophysical Institute
Attn: Dr. A. Foldvik
Dr. S. Jónsson
University of Bergen
Allegaten 70
5007 Bergen
Norway | 1
1 |
| 38. | Applied Oceanography Group
Attn: Dr. T.S. Hopkins
Undersea Research Centre
Supreme Allied Command Atlantic
APO New York, 09019-5000 | 1 |
| 39. | Alfred Wegener Institute
for Polar and Marine Research
Attn: Dr. E. Fahrbach
Am Handelshafen 12
D-2850 Bremerhaven
Federal Republic of Germany | 1 |
| 40. | Norsk Polar Institute
Attn: Dr. T. Vinje
Dr. B. Rudels
P.O. Box 158
N-1330 Oslo Lufthavn
Norway | 1
1 |

41. Laboratoire d'Océanographie Dynamique
 et de Climatologie
 Attn: Dr. J.-C. Gascard
 Universite Pierre et Marie Curie
 Paris 6, Paris
 France
1

42. Institute for Marine Research
 Attn: Dr. S.-A. Malmberg
 P.O. Box 1390
 Skulagata 4
 121 Reykjavik
 Iceland
i

43. Science Applications, Inc.
 Attn: Dr. R. Muench
 13400B Northup Way Suite 36
 Bellevue, Washington 98005
1

44. Dr. Tom A. McClimans
 NHL
 N-7034 Trondheim
 Norway
1

45. Dr. John L. Newton
 10211 Rookwood Drive
 San Diego, California 92131
1

46. LT Robert F. Blythe
 11027 Glencreek Circle
 San Diego, California 92131
1